KFKI 1/2008

Z. Hózer
P. Windberg
I. Nagy
L. Matus
N. Vér
M. Kunstár
A. Vimi
M. Horváth
T. Novotny
E. Perez-Feró
A. Pintér
M. Balaskó

CODEX-CT-1 EXPERIMENT: QUENCHING OF FUEL BUNDLE AFTER LONG TERM OXIDATION IN HYDROGEN RICH STEAM

CENTRAL
RESEARCH
INSTITUTE FOR
PHYSICS

BUDAPEST

CODEX-CT-1 EXPERIMENT: QUENCHING OF FUEL BUNDLE AFTER LONG TERM OXIDATION IN HYDROGEN RICH STEAM

Z. Hózer, P. Windberg, I. Nagy, L. Matus, N. Vér,
M. Kunstár, A. Vimi, M. Horváth, T. Novotny, E. Perez-Feró, A. Pintér, M. Balaskó
Hungarian Academy of Sciences
KFKI Atomic Energy Research Institute
H-1525 Budapest, P.O.Box.49, Hungary

Abstract

Z. Hózer, P. Windberg, I. Nagy, L. Matus,
N. Vér, M. Kunstár, A. Vimi, T. Novotny, E. Perez-Feró, M. Horváth, A. Pintér, M. Balaskó:
CODEX-CT-1 EXPERIMENT: QUENCHING OF FUEL BUNDLE AFTER LONG TERM OXIDATION IN HYDROGEN RICH STEAM

The cleaning tank incident at the unit 2 of Paks NPP in 2003 resulted in severe fuel damage of 30 assemblies. The fuel rods heated up due to insufficient cooling and the zirconium components suffered heavy oxidation. Opening of the tank and quenching of the assemblies by cold water led to fragmentation of brittle zirconium components. Due to the poor instrumentation there were many open questions concerning the course of the incident and the behaviour of fuel assemblies. In order to improve the understanding of the phenomena that took place during the Paks-2 incident integral tests have been carried out in the CODEX (Core Degradation Experiment) facility. The tests simulated the whole scenario of the incident using electrically heated fuel rods. The final state of the fuel rods showed many similarities with the conditions observed after the incident at the NPP and for this reason it is very probable that the thermal conditions and chemical reactions were also similar in the tests and in the incident. The post-test examination of CODEX-CT-1 bundle indicated that the high degree of embrittlement was a common result of oxidation and hydrogen uptake by the Zr components.

Kivonat

Hózer Z., Windberg P., Nagy I., Matus L.,
Vér N., Kunstár M., Vimi A., Novotny T, Perez-Feró E.,Horváth M., Pintér A., Balaskó M.:
A CODEX-CT-1 KÍSÉRLET: FŰTŐELEMEK ELÁRASZTÁSA HOSSZÚ IDEJŰ, HIDROGÉNDÚS GŐZBEN TÖRTÉNT OXIDÁLÁS UTÁN

A Paksi Atomerőmű 2-es blokkján 2003-ban üzemzavar következett be, amely során a tisztítótartályban kezelt 30 darab kazetta súlyos sérüléseket szenvedett. A fűtőelemek a nem kielégítő hűtés következtében felhevültek és a cirkónium részegységek jelentős mértékben oxidálódtak. A tisztítótartály felnyitásakor beáramló hideg víz a kazetták széttöredezéséhez vezetett. A tartályban nem voltak mérőműszerek, ezért sok nyitott kérdés maradt az üzemzavart követően a fűtőelemek sérülésének részleteiről. Az üzemzavar lefolyásának jobb megértése érdekében integrális kísérletekre került sor a CODEX (Core Degradation Experiment) berendezésen. A kísérlet elektromosan fűtött fűtőelem rudakkal szimulálta az üzemzavar teljes történetét. A fűtőelemek végállapota sok tekintetben hasonlított a paksi üzemzavarban megsérült kazettákra, ezért nagyon valószínű, hogy hasonló hőtechnikai és kémiai folyamatok játszódtak le a kísérleti berendezésben és a tisztítótartályban. A CODEX-CT-1 köteg vizsgálata jelezte, hogy a cirkónium részegységek nagymértékű elridegedésben egyaránt fontos szerepe volt az oxidációnak és a hidrogén felvételnek.

Contents

List of tables

List of figures

1. INTRODUCTION

The cleaning tank incident at the unit 2 of Paks NPP on 10th April 2003 resulted in severe fuel damage of 30 assemblies. The fuel rods heated up due to insufficient cooling. The zirconium components suffered heavy oxidation. The final quenching of the assemblies lead to fragmentation of brittle zirconium components. Due to the poor instrumentation there were many open questions concerning the course of the incident and the behaviour of fuel assemblies. In 2005 a new experimental programme was launched with the following objectives:

- Better understanding of the phenomena that took place during the Paks-2 incident.
- Improving knowledge on the behaviour of NPP fuel under accident conditions.
- Supporting model development with paying special attention to the effect of hydrogen uptake on cladding embrittlement.

The test programme included small scale tests (the COHYRA programme [1]) and large scale tests with electrically heated 7-rod bundles in the CODEX facility. The results of the first test (CODEX-CT-1) are described in the present report.

2. THE CODEX FACILITY

The CODEX (COre Degradation EXperiment) facility was originally built for severe accident studies. Several experiments have been carried out with VVER and PWR bundles. Behaviour of fuel rods in high temperature steam, quenching at high temperature, phenomena related to air ingress scenarios and the role of control rods were addressed in the earlier tests [2, 3].

In the CODEX-CT (Cleaning Test) test series the original arrangements have been significantly changed. It was a basic requirement to the facility to withstand high temperature conditions for several hours. Due to the small size of the facility it was clear that only part of the cleaning tank can be simulated. Since the thermal hydraulic events were well understood from numerical analysis, the main purpose of the CODEX-CT tests was the simulation of fuel behaviour during the Paks-2 incident. The main conditions of the incident had to be reproduced in the facility and the full scenario of the Paks-2 incident was simulated. It was a great challenge to reach ≈1200-1300 °C in upper part of the facility, while the bottom of the bundle was cooled by water.

	Paks-2 cleaning tank	CODEX-CT facility
Number of fuel rods	3870	7
Total flow rate	21 t/h	106 l/h
Total volume of coolant	6 m^3	9.2 l
Volume of steam	4 m^3	6 l
Total surface of Zr	300 m^2	0.44 m^2
Ratio of total Zr surface / total volume of coolant	50 m^{-1}	48 m^{-1}
Total power	241 kW	2.3 kW

Table 1. Main parameters of the Paks cleaning tank and the CODEX-CT facility

In the design of the facility the ratio of Zr surface to the total volume was kept as a main parameter providing the similarity for fuel oxidation process (see Table 1). The relative power of the facility was much more than the decay heat of the original assemblies, since the heat losses are much higher in the case of a small scale facility.

The facility was equipped with sophisticated instrumentation including the measurement of temperatures, flowrates, pressures and power. Two special devices were applied for the monitoring of hydrogen: one measured the concentration in the cleaning tank, while the other recorded the integral volume of release hydrogen from the system. The scheme and the main components of the CODEX-CT facility are shown in Fig. 1. The main parameters of the Paks-2 cleaning tank and of the CODEX-CT facility are compared in Table 1.

There were no internal heaters applied inside of the fuel rods in the reconstructed facility. External heaters were used to reach high temperature in the test section. The fuel

bundle was longer than in the previous tests and several technological systems were connected to the test section.

The test section with the electrically heated VVER type bundle represented the cleaning tank. Inlet and outlet junction were connected to the bottom section and perforation were used to facilitate the formation of by-pass flow. The external heater rods surrounded the bundle.

The spent fuel storage pool was simulated with an expansion tank that was connected to the test section. Special condenser unit was applied to receive coolant from the test section during the quenching phase.

2.1. FUEL ASSEMBLY

In the CODEX-CT experiments the fuel rods were filled with alumina pellets and pressurised inside. The bundle included seven rods and it was covered by hexagonal shroud made of Zr2.5%Nb alloy. Original E110 (Zr1%Nb) type VVER cladding material was used in the fuel rods. The spacer grids were manufactured from E110 (Zr1%Nb) alloy as well. The fuel rods were arranged on a hexagonal lattice with the typical parameters of the VVER-440 bundle using five spacer grids (Fig. 2). The main parameters of the bundle are summarised in Table 2 and the scheme and the cross-section of the bundle are shown in Figures 2 and 3.

Number of fuel rods in the bundle	7
Cladding material	Zr1%Nb
Length of fuel rods	1000 mm
External cladding diameter	9.1 m
Internal cladding diameter	7.8 mm
Material of pellets	Al_2O_3
External diameter of pellets	7.7 mm
Diameter of internal hole in the pellets	3 mm
Height of pellets	10 mm
Number of spacer grids	5
Material of spacer grids	Zr1%Nb
Height of spacer grids	10 mm
Thickness of spacer grids	0.4 mm
Pitch size	12.2 mm
Material of shroud	Zr2.5%Nb
Thickness of shroud	2 mm
Material of header	SS

Table 2. Main characteristics of fuel rod bundle

The original UO_2 pellets were replaced by Al_2O_3 pellets in the tests, for the interaction between UO_2 and other core materials was not foreseen in the planned temperature range.

Similarly to VVER-440 type pellets the Al_2O_3 pellets had internal holes, which were used for the thermocouples in the tests.

The internal pressurisation of the fuel rods was important feature in these experiments, since ballooning and burst played significant role in the degradation of fuel bundle. The fuel rods were pressurised individually and this solution made possible the pressurisation of each rods to different initial value. The fuel rods were filled up by argon and were closed in cold state of the bundle.

The upper part of the bundle included a small stainless steel header that simulated the top nozzle of the fuel assembly.

The fuel bundle had perforations on each side of the hexagonal shroud at elevation 15 mm. The diameter of perforations was 6 mm, their total number was 6. It made possible the by-pass flow from the bundle.

2.2. HEATERS

There were no internal heaters applied inside of the fuel rods, but external heaters were used. It made possible the establishment of a more uniform temperature distribution along the fuel rods that characterises the long term radiation heat transfer conditions. Furthermore the internal heaters could have stabilised the structure of the fuel rods and so could have prevented fragmentation of fuel rods.

Twelve heaters were placed around the bundle. Their active length was 1 m. The heater wire was made of 3 mm diameter Kanthal APM material. It was covered by stainless steel cladding. There was Al_2O_3 insulation between the central wire and the cladding. The heater wires and the cladding were parallel connected. A special flange was used for the connection to the electric supply system, which could provide ≈3 kW maximum power in the facility.

Number of heaters	12
Length of heaters	1000 mm
Cladding material	stainless steel
External/internal diameter of cladding	10 mm / 8 mm
Material of heater wire	Kanthal APM
Diameter of heater wire	3 mm
Material of insulation	Al_2O_3
External/internal diameter of insulation	8 mm / 3 mm
Max. total power of all heaters	3 kW
Voltage	0-10 V
Current	0-300A
Electrical resistance at 20 °C	17.08 mOhm
Electrical resistance at 1300 °C	17.76 mOhm

Table 3. Main characteristics of heaters

The heaters were welded into the bottom plate of the test section. The other ends of the heaters were not fixed. This solution eliminated the formation of stresses associated with the

thermal expansion of the heaters. The schematic view of the heaters and a picture of the flange are shown in Fig. 4 and the main parameters are summarised in Table 3.

2.3. CLEANING TANK MODEL

In the cleaning tank the coolant entered the fuel assemblies from the bottom, flowed up inside of the VVER-440 type assemblies that are covered by shroud and turned back in the upper plenum. Then flowed down between the assemblies and left the volume through a junction that was placed just above the bottom plate. This flow path was simulated in the CODEX-CT facility with the help of a stainless steel tube around the fuel bundle and heaters (Fig. 5). The water flowed up inside of the tube, turned back at the top of the tube and flowed down to the outlet junction in the annular space between this tube and the wall of the test section.

There were six perforations with 6.4 mm diameter on the tube at the elevation of 25 mm. The by-pass flow was established through these perforations in the test. There were six perforations with 6 mm diameter on the shroud at 15 mm elevation.

There were two possibilities for the formation of by-pass flows in the cleaning tank:

a) Through the perforations of the shroud. This flow was simulated with the holes in the shroud of the bundle.
b) Through the gap between fuel assembly bottom nozzle and the bottom plate of the cleaning tank due to the imperfect seating of the assemblies. In the tests this path was simulated so that part of the coolant was injected directly outside of the bundle and flowed out through the perforations of the steel tube.

The coolant in the cleaning tank was circulated with the help of a pump. The coolant was injected into the lower chamber of the cleaning tank model. The bottom plate of the test section had several perforations. There were 12 perforations inside of the assembly shroud with 5 mm diameter. 12 perforations with 5 mm diameter were between the heaters and the shroud. The plate had 12 perforations with 7 mm diameter between the heaters and the steel tube (see left side picture in Fig. 6).

The cleaning tank model with the bundle was connected to another vessel that simulated the water volume of the spent fuel storage pool. The outlet junction of the cleaning tank model was located at 15 mm elevation (Fig. 6). The zero level corresponded to the elevation of bottom plate in the test section.

The temperature of the inlet flow was maintained using a heat exchanger that was cooled on the secondary side by tap water. There was an air let-down (gas off) valve located on the top of the tank that made possible the release of gas-steam mixture from the tank.

2.4. EXPANSION TANK

In the Paks incident the cleaning tank was surrounded by the water of the spent fuel storage pool and the water of the pool was circulated in an open loop through the tank. In the CODEX-CT tests the spent fuel pool was simulated with a special expansion tank. The

volume of the tank was 28.9 l, the internal diameter of the cylindrical vessel was 320 mm (Fig. 7.)

The expansion tank was pressurised inside by argon and the internal pressure was established so that it was close to the hydrostatic pressure of a ≈13 m high water column. The expansion tank was equipped with relief and safety valves as well. The pressure in the facility was regulated through this gas system.

The expansion tank was connected to the outlet junction of the cleaning tank model through a tube. This connection line was opened during the tests and made possible the evacuation of water from the cleaning tank to the expansion tank. In the quench phase of the tests this line provided water injection to the bottom of the tank. Another line was connected to the top of the cleaning tank model. During the tests it was closed by a valve that was opened only in the quench phase for the injection of water to the top of the bundle.

2.5. CONDENSER TANK

The elements of the CODEX-CT facility accumulated about ≈8 MJ energy during the long time experiments. Since the final phase of the tests included water quench of this system, it was necessary to take care of the released steam. For this reason a 100 l volume condenser tank was connected to the cleaning tank model (Fig. 8). It contained ≈20^{o}C water and it was connected to the top of the cleaning tank model (Fig. 1). The tank was made of Plexiglas. It was designed so that the water in condenser warmed up to ≈60^{o}C during the expected test conditions.

When the quench phase started this connection was opened and the steam-hydrogen mixture was released through a ceramic filter into the condenser tank. The non-condensable gas (hydrogen) from the mixture was collected in a 40 l gas tank. The volume of the released hydrogen through the condenser tank was determined using the pressure measurements of this gas tank.

2.6. INSTRUMENTATION

In order to understand the main processes in the tests rich instrumentation was applied in the CODEX-CT tests. Large part of the preparatory work was devoted to the collection of instrumentation equipment, their calibration and testing. The temperature, pressure, water level, flowrate and electric power measurement are described here (Tables 4, 5 and 6), while the hydrogen measurements are summarised in the next two chapters.

Temperature measurements were taken in the following places:

- in each fuel rod in two different elevations (two thermocouples failed and they are not listed in Table 4) ,
- on the shroud in different positions,
- on the heaters,
- in the gap between the steel tube and the vessel wall of the cleaning tank model,
- inlet and outlet of coolant,
- pyrometer was positioned on the top of the cleaning tank and indicated the temperature of the top of the bundle.

Pressure was measured in the following places:

- in each fuel rod,
- in the expansion tank.

Water level was measured as pressure difference in two places:

- expansion tank,
- cleaning tank model (test section with fuel bundle).

Temperature measurement	Thermocouple type	Placement	Position (mm)
TFR136	K	Rod No. 1	360
TFR183	R	Rod No. 1	830
TFR229	K	Rod No. 2	290
TFR276	R	Rod No. 2	760
TFR322	K	Rod No. 3	220
TFR355	R	Rod No. 3	550
TFR415	K	Rod No. 4	150
TFR462	R	Rod No. 4	620
TFR550	K	Rod No. 5	500
TFR596	R	Rod No. 5	960
TFR690	R	Rod No. 6	900
TFR755	R	Rod No. 7	550
TSH27	K	Shroud	270
TSH70	R	Shroud	700
THR70	R	Heater	700
TG5	K	Gap	50
TG27	K	Gap	270
TG50	K	Gap	500
TG74	K	Gap	740
TG97	K	Gap	970
TCIN	K	Inlet	
TCOUT	K	Outlet	

Table 4. Temperature measurements

Electric power was measured with a power-meter connected to the transformer unit. There was a video camera connected to the top of the cleaning tank model. It provided useful visual information on the heat up of the bundle during the experiments.

Thermocouple type	K	R
material	Ni-CrNi	Pt-Pt13%Rh
insulation	MgO	MgO
sheath material	Inconel	Inconel
external diameter (mm)	0.8	1.6

Table 5. Thermocouple characteristics

Parameter	Device	Placement	Comment
system pressure	pressure transducer	expansion tank	0-6 bar (ABS) 4-20 mA
test section level	DP transducer	test section	0-75 mbar 4-20 mA
quench tank level	DP transducer	quench tank	0-75 mbar 4-20 mA
coolant flowrate	calibrated flowmeter	coolant inlet junction	resolution: 1 impulse / 1 liter
fuel rod pressure	pressure transducer	fuel rods	0-100 bar (ABS) 4-20 mA
hydrogen flowrate	gas measuring system with "U"-pipe	gas off junction (1)	charging volume: ≈0,8 liter / cycle
hydrogen concentration	system with TCD	gas off junction (2)	
power	choppered transformator		output: 0-3000 W
	video camera	top of test section	

Table 6. Measurement of system parameters

2.7. HYDROGEN FLOWRATE MEASUREMENT

The hydrogen production was a key factor in the Paks incident and for this reason two independent systems were applied in the CODEX-CT tests to collect data on hydrogen production and release from the tank.

The hydrogen produced during the oxidation of Zr in high temperature steam accumulated in the upper volume of the cleaning tank. In the first tests the operation of the air letdown (gas off) valve was simulated and part of the produced hydrogen was released

from the tank. The flowrate of release was manually regulated so that the system pressure remained constant.

The released hydrogen-steam mixture first entered a condenser unit, where the steam was condensed. The remaining noncondensable gas (only hydrogen) was collected in a large U tube. Initially the U tube was filled with water. The hydrogen was injected into one leg of the U tube and the water level in the other leg moved up. The accumulated gas was released when its volume reached 0.8 l. It took place before the water level reached the bottom of the U tube. After the release the hydrogen accumulation started again in one leg of the tube in the next cycle. During the most intense period of the test the U tube was opened almost every minute (Fig. 9).

The volume of released hydrogen was calculated using the number of cycles and the water level in the U tube.

2.8. HYDROGEN CONCENTRATION MEASUREMENT

The concentration of hydrogen gas in steam was a substantial factor during the processes; it reflected the extent of zirconium-steam reaction, the amount of formed and released hydrogen during the pressure reduction, moreover was necessary for assessment of rate of steam-zirconium reaction and embrittlement of cladding. Thermal conductivity method was used for the measurements.

Pressure in the cleaning tank was 2.6 bars in the CODEX-CT-1 test. Steam-hydrogen mixture containing 0-100 vol% H_2 was expected, the detector facility was planned to work in this range. Because only steam and hydrogen were in the atmosphere to be investigated a thermal conductivity detector (TCD) of a gas chromatograph seemed to be satisfactory as basic sensor. The scheme of analyser unit can be seen in Fig. 10.

Previous experiences with the same detector proved, that an argon stream with ca 1 cm^3/sec with about 20-30 vol% hydrogen added to this stream is a range, where good reproducible results can be achieved after a proper calibration. The intensity of gas stream from the bundle had to be adjusted to this concentration range.

The TCD detector had a pure argon stream on the reference side and that was added to the steam-hydrogen mixture coming from the bundle area. The measuring side of TCD had an argon or argon-hydrogen mixture flow with constant water vapour content (saturated at 0 ^oC), determined by ice-water bath. This solution had some advantages: at deep cooling the vessels should be tightened by ice, absorbers would need to large volume and the time resolution would be poor. The present solution gave a time constant not more than some seconds.

The TCD was involved into a Wheatstone bridge. The data collection was performed by computer equipped with analog-digital conversion. H_2 concentrations, the time, temperature of TCD, temperature of capillary tube were also registered. The TCD temperature was adjusted to about 140 ^oC to avoid water condensation and reduce the amount of adsorbed water. Calibration of TCD was performed by argon-H_2 mixture by exact

modelling of the conditions at the experiment. It means that on reference cell streamed through pure argon, on detector cell argon-hydrogen mixture saturated with water vapour at 0 ^{o}C (ice bath).

As inlet device between the bundle and TCD a capillary tube has been used and it determined the intensity of steam-hydrogen mixture. It has the advantage compared to a needle valve that it resulted in a well reproducible flow. The capillary was an 8.5 m long stainless steel tube originally intended to be a liquid chromatograph column. Its inner diameter was 0.236 mm. The tube was also heated to 140 °C for avoiding steam condensation. The streaming intensity of gas in capillary tube has been calculated by the Poiseuille's law.

$$p_1^2 - p_2^2 = \frac{16 \cdot \eta \cdot G}{r^4 \cdot \pi} \cdot \frac{k \cdot T}{m} \cdot l \qquad (1)$$

or

$$p_1^2 - p_{21}^2 = \frac{16 \cdot \eta}{r^4 \cdot \pi} \cdot \frac{V}{T_F} \cdot \frac{273.16}{22410} \cdot R \cdot T \cdot l$$

where G mass of gas streamed through during time unit,
p_1 and p_2; pressure at inlet and outlet of capillary, respectively,
η dynamic viscosity,
k Boltzmann constant,
T temperature of capillary in K,
T_F temperature of gas measuring unit in K,
R gas constant,
l length of capillary tube,
r inner radius of capillary,
m mass of gas atoms,
V gas streaming rate measured at temperature T_F.

This formula has been used for determination of capillary diameter, when argon was applied for the measurement. TCD calibration was performed with argon-hydrogen mixture. On TCD reference side pure dry argon was applied. Like at real experiment hydrogen was mixed in between the reference and measuring side and also saturated with water vapour at 0 ^{o}C. Streaming of Ar was constant (1 ml/s) and the hydrogen was added at different rate. The results of calibration can be seen in Fig. 11. In the figure an equation is presented to calculate hydrogen concentration in gas streaming through the TCD measuring cell from the voltage signal of Wheatstone bridge. The formula resulted from fitting

$$C(H_2\ v/v\%) = 0.287 \cdot (mV) - 3.098 \cdot 10^{-4} \cdot (mV)^2 + 7.86 \cdot 10^{-5} \cdot (mV)^3 \qquad (2)$$

where mV - TCD bridge signal in mV at our experimental arrangement.

The evaluation of results demanded the flow intensity of hydrogen component leaving the capillary tube. It is

$$\frac{dV_{H_2}}{dt} = \frac{dV_{Ar}}{dt} \cdot \frac{c_{H_2}}{1 - c_{H_2}} \qquad (3)$$

where $\frac{dV_{H_2}}{dt}$ the intensity of hydrogen flow from the capillary,

$\frac{dV_{Ar}}{dt}$ intensity of argon flow in the reference side and mixing,

c_{H_2} hydrogen concentration from TCD signal.

To estimate the hydrogen concentration in bundle area hydrogen component from capillary was compared with the total amount of gas streaming through the capillary. The latter was calculated by using equation (1) and the appropriate parameters as follows:

P_1	pressure in bundle;	2.6	bar
P_2	outer pressure;	1.0	bar
r	inner radius of capillary,	0.118	mm
l	length of capillary	8.5	m
T	temperature of capillary	400	K
η	dynamic viscosity of gas	$13.5 \cdot 10^{-6}$	Pa·s
T_F	ambient temperature.	300	K

The viscosity of steam - hydrogen mixture had been calculated according to the method published by C.R. Wilke [4]. Results are plotted in Fig. 12. The original method of calculation would be too complicated for evaluation of results with some thousands values, therefore a polynomial formula had been fitted for the values calculated according to Wilke method. It resulted for the dynamic viscosity

$$\eta = 13.385 - 1.4668 \cdot c(H_2) + 9.4329 \cdot c(H_2)^2 - 10.321 \cdot c(H_2)^3$$

The capillary temperature was 400 K on the main part of its 8.5 m length. Up to about 70 vol% H_2 component the η is constant with an error not larger than accuracy of other parameters and TCD measurements.

As was mentioned earlier the concentration of hydrogen in the bundle can be achieved by comparing of escaping hydrogen and the total escaping gas volume rate. Because of the total escaping gas volume rate leaving the bundle is depending on hydrogen concentration and pressure at the evaluation can be made only by iterative calculation method. According to our experience the evaluation of every single measured point needed up to 0.1 vol% accuracy was achieved after 19 iteration steps.

3. THE CODEX EXPERIMENTAL PROGRAMME

In the AEKI an experimental programme was initiated focusing on the high temperature behaviour of VVER fuel and core materials. The interactions of Zr1%Nb cladding with UO_2 pellet, stainless steel spacer and boron steel absorber were studied in small scale separate effect tests [5]. On the basis of the experience gained in these tests the CODEX integral test facility was constructed to continue this work under more prototypic conditions.

First the capabilities of the facility were demonstrated carrying out the CODEX-1 experiment with Al_2O_3 pellets. The test section was heated up with argon, and then the electric power was increased. When the rod bundle degradation was indicated by temperature measurements, the power was switched off and the section was cooled down by argon. The post-test examination showed that the rod bundle was partially damaged, the further melting was stopped in time. So the facility proved to be applicable to the experimental analysis of controlled core degradation processes. In the second experiment similar procedures were taken, but the Al_2O_3 pellets were replaced with UO_2 [2]. The CODEX-3/1 and CODEX-3/2 experiments were performed with quick water cooling [2]. Air ingress conditions were simulated in the AIT-1 and AIT-2 tests with PWR fuel rods [3, 6]. The B4C test was devoted to the examination of control rod degradation and gas production during a severe reactor accident [2]. Some of the CODEX tests are listed in the OECD/CSNI In-Vessel Core Degradation Code Validation Matrix [7]. The main parameters of the test matrix are given in Table 7.

After significant reconstruction of the CODEX facility special tests have been carried out with the main conditions of the Paks-2 cleaning tank incident. First a preliminary test was performed with empty cladding tubes and sheets of assembly shroud. The CODEX-CT-1 test was carried out with 1 m long seven-rod bundle and simulated the whole scenario of the incident.

Test	Bundle type	Pellet	Year	Test type
CODEX-1	7-rod VVER	Al_2O_3	1995	scoping test
CODEX-2	7-rod VVER	UO_2	1995	escalation and slow cooling down
CODEX-3/1	7-rod VVER	UO_2	1996	water quench at 1150 ^oC
CODEX-3/2	7-rod VVER	UO_2	1997	water quench at 1500 ^oC
CODEX-AIT-1	9-rod PWR	UO_2	1998	air ingress
CODEX-AIT-2	9-rod PWR	UO_2	1999	steam oxidation and air ingress
CODEX-B4C	7-rod VVER	UO_2,B_4C	2001	control rod degradation
CODEX-CT-1	7-rod VVER	Al_2O_3	2006	long term oxidation and quench

Table 7. Main parameters of CODEX test matrix

4. PRELIMINARY TEST

The original purpose of the preliminary test was the testing of different components and measurement systems of the facility. In order to have information on the kinetics of zirconium oxidation and on the dynamical behaviour of the system with hydrogen production pieces of fuel rod cladding and plate of zirconium shroud were placed in the test section. The total amount of zirconium alloy was equal to the mass of zirconium in the 7 rod bundle that was used in the later tests. The CODEX-CT preliminary test was carried out on 20th June 2006. The main events and actions are summarised in Table 8.

At the beginning of the test the facility was filled up with water and 2.6 bar system pressure was established (Fig. 23) with the help of an argon system connected to the expansion tank. After an initial trial the electrical power was increased to 2.3 kW between 900-1100 s (Fig. 29). The power was kept constant until the end of the test. The pump was started up at 950 s with about 130 g/s flowrate (Fig. 26). Secondary side cooling of the heat exchanger was activated at 3120 s (Fig. 21).

After the decrease of flowrate to 30 g/s at 5000 s (Fig. 26) the coolant temperature in the top of the test section started to increase and the boiling of water led to formation of steam volume in the tank. The water level was stabilised at 7000 s above the elevation of by-pass holes. The temperature monotonously increased and reached 1200 ^{o}C at 25000 s (Figs. 19 and 20). The cladding tube and shroud plates were oxidised for several hours in high temperature steam. The first indication of hydrogen production was detected at 11000 s.

The gas off valve was opened for hydrogen release at 12120 s and the release rate was increased at 16300 s by further opening. The valve was closed between 21411-22217 s and that period there was no hydrogen release from the tank (Fig. 27). This action led to some oscillations in the system and some gas bubbling took place from the cleaning tank model to the expansion tank. The level measurement in the expansion tank showed strong oscillations (Fig. 25) that were related to the gas content in the connecting line.

The main units of the facility were tested to check their functionality. The preliminary test made possible the tuning of air letdown valve that was used for the controlled release of produced hydrogen. The test was terminated with switching off the electric power of the heaters at 25000 s (Fig. 29). After a short period steam + gas mixture was released from the tank at the top of the vessel and the bundle was quenched by water and technological cooled-down was performed (the condenser tank was not connected to the test section during the preliminary test).

The total volume of released hydrogen was 180 l at 25000 s and additional 16 l was produced during the cool-down period (Fig. 27). The volume of condensed water was 56 ml in the condenser of the U tube system at 25000 s.

The hydrogen concentration measurement and data collection equipment was also in operation during the preliminary test. Substantial trouble with the capillary was found during the experiment. At the beginning of the test the bundle area was filled with water. Solid particle impurities in water with sizes comparable to the capillary inner diameter were

collected at the starting end of tube forming a bottleneck and reduced the flow rate. At the end of experiment the extent of flow diminution has been checked by 2.6 bar argon. The flow rate appeared 9.5 times lower, than at open capillary. It was taken into account at the evaluation. The hydrogen concentration results are presented in Fig 28. The hydrogen concentration curve showed higher and lower values in time. It was connected with release of hydrogen-steam gas mixture from the bundle from time to time. To avoid the reduction of capillary diameter in the further experiments a tiny filter was placed up to its bundle end. The filter unit was an all metal construction to withstand the high temperature. This solution proved to be satisfactory, the flow diminution did not appear.

Time (s)	Event
900	Start of power increase
950	Pump start up, coolant flowrate 130 g/s
1100	2300 W power reached
5000	Flowrate decrease to 30 g/s
7000	Low water level stabilised
12120	Start of hydrogen release through gas off valve
25000	1200 ºC temperature reached
25000	Power switched off, cool-down initiated

Table 8. Main events and actions of the CODEX-CT preliminary test

5. THE CODEX-CT-1 EXPERIMENT

In order to simulate the Paks-2 incident special conditions were applied in the CODEX facility. The pressurised fuel bundle included seven rods with pellets inside surrounded by E110 cladding tubes. The CODEX-CT-1 experiment was carried out on the 5th July 2006. The main events and actions are summarised in Table 9.

The test started with several technological actions. The test section was filled with water and the initial water level was established in the expansion tank. The cleaning tank model and the expansion tank were connected through the outlet junction of the cleaning tank located at 15 mm above the bottom plate by opening the valve. The upper connection between the top of cleaning tank and the expansion tank was closed. Water circulation with ≈80 g/s flowrate was established (Fig. 63) and the secondary side heat exchanger was put into operation. The electrical power of the heaters was set to 2.3 kW (Fig. 66). The fuel rods were pressurised in the beginning of the test to different values between 6 and 30 bars in cold state (Figs. 53-59). Under these conditions most the power of the heaters was removed by the coolant. The external surface temperature of the facility was measured regularly with a manual equipment during the test (Table 11).

The CODEX-CT-1 experiment was performed in three main phases:

0-2580 s, formation of steam volume

- During the first phase of the test water was evaporated from the upper part of the volume and a water level was established at the elevation of by-pass. The flowrate was reduced from ≈80 g/s to ≈45 g/s between 1400 and 2000 s (Fig. 63).

- The decrease of coolant flowrate led to heat up of the water and formation of steam volume as a result of by-pass flow. The water level in the test section dropped from the original 110 cm to 10 cm between 2400-2580 s (Fig. 61). The water released from the cleaning tank model resulted in the increase of coolant level in the expansion tank the same time (Fig. 62).

2570-27820 s, high temperature oxidation in hydrogen rich steam

- The low water level was kept for seven hours with constant coolant flow and electric power. The temperatures monotonously increased and the maximum temperature reached ≈1250 ^{o}C. Figures 30-41 show fuel rod temperatures in the seven rods at different elevations. Temperature profiles in different moments of the test are shown in Fig. 67. The hottest part of the rods was in the central-upper section at about 500-700 mm elevation (Figs. 37, 41 and 67). The bottom part of the rods was cooled by water and the temperatures remained low in that section (Fig. 36).
- The heat-up of the bundle led to oxidation of Zr components. The hydrogen content in the atmosphere started to increase after 5000 s and it indicated the beginning of the oxidation process (Fig. 65). The first release of hydrogen took place at 6800 s (Fig. 64) after manual opening of the gas off valve on the top of the cleaning tank model. The regular operation of the U tube system started at about 15000 s (Fig. 64). After this time the gas off valve was mainly open and it provided stable hydrogen release with almost constant system pressure in the facility. The steam part of the released hydrogen + steam mixture was condensed in the condenser unit and the condensate was collected and its mass was measured several times during the test (Table 10).
- At the end of this phase about 60 % H_2 concentration appeared to be as base value, at peaking it raised up to 80 % (Fig. 65). Because the steam was flowing through not only on bundle part with zirconium alloy part, but on stainless steel heaters as well, a full steam starvation could not appear. Inlet of capillary was at top of the test section, where hydrogen was diluted with steam. The total hydrogen release before quench was 270 l.
- Six out of the seven rods lost their integrity due to burst between 800-900 ^{o}C. (Rod No. 1 failed at 9075 s, rod No. 6 at 9174 s, rod No. 5 at 9410 s, rod No. 4 at 9496 s, rod No. 3 at 10239 s and rod No. 2 at 10554 s.) The pressure increase reached a maximum during the test and before burst their value slightly decreased (Fig. 53-58). It was a result of plastic deformation that increased the internal gas volume and had larger effect on the pressure change, than the temperature increase. Rod No. 7 (the central rod) had the lowest initial pressure and failed only at the quenching phase (Fig. 59).
- At the beginning of this phase the coolant removed about 20% of the electrical power and at the end about 35% .

27820-28710 s, water quench

- Finally the bundle was quenched from the bottom and the top simulating the opening of the cover of cleaning tank. The quench process included several steps.
- The gas off valve on the top of the tank was closed and that prevented the further release from the cleaning tank at 27730 s.
- The connecting line between the cleaning tank model and the condenser tank was opened at 27820 s. The release of steam + hydrogen mixture lead to pressure decrease in the system (Fig. 62) and that initiated water injection from the expansion tank into the cleaning tank model.

- The upper connection between the expansion tank and the cleaning tank model was opened at 27884 s.
- The water level in the condenser tank increased by 10 cm. The volume of gas in the tank was 8 l that was about the volume of the gas in the cleaning tank model. It meant that there was no significant hydrogen production during the quench phase.
- Electrical power was switched off at 28067 s (Fig. 66). The cool down of the facility took relatively long time because of the large thermal inertia of the structural materials and insulation.

Time (s)	Event
0	Initial conditions established (2300 W power, 80 g/s flowrate)
2000	Flowrate reduction to 45 g/s
2400	Start of water level decrease
2580	Low water level established
5000	Beginning of Zr oxidation (indicated by hydrogen measurement)
6800	Start of hydrogen release through gas off valve
9075	Burst of fuel rod No. 1
9174	Burst of fuel rod No. 6
9410	Burst of fuel rod No. 5
9496	Burst of fuel rod No. 4
10239	Burst of fuel rod No. 3
10554	Burst of fuel rod No. 2
27370	1245 ºC temperature reached
27730	Closing gas off valve
27820	Opening of gas release to condenser tank
27820	Beginning of quench from the bottom
27884	Start of quench from the top
27900	Burst of fuel rod No. 7
28067	Power switched off

Table 9. Main events and actions of the CODEX-CT-1 test

Time (s)	Total mass of condensate (g)
10440	82
16380	126
21060	157
27180	181

Table 10. Measured mass of condensate in the gas release system

Time (s)	Inlet temp. (ºC)	Outlet temp. (ºC)	Temperature on the thermal insulation (ºC)				
			bottom		centre		top
1440	36	40	28	27	28	29	29
2400	40	43	28	28	28	29	29
4140	28	30	28	29	29	29	29
5520	27	28	27	28	30	32	31
7440	28	30	30	34	36	41	36
9780	30	32	33	44	50	55	45
10920	28	30	33	50	60	66	51
13140	28	30	35	58	82	99	64
15480	28	30	38	78	114	130	80
18660	31	33	44	104	162	166	102
21600	30	32	51	119	175	185	122
23820	29	31	53	128	193	213	131
26640	30	35	58	178	214	242	147
27600	30	33	55	141	230	256	156
28920	30	62	53	135	196	228	164

Table 11. Measured temperatures on the external surface of the facility

6. EXPERIMENTAL RESULTS

The CODEX-CT preliminary test and the CODEX-CT-1 test well illustrated the probable scenario of the Paks-2 cleaning tank incident.

The operation with high flowrate led to stable conditions, since the electrical power and heat removal with the coolant were in balance. The flowrate decrease (simulating the operation of the small pump in the incident) quickly led to the stratification of water in the cleaning tank model and rapid formation of steam volume in the vessel. The water level was established according to the elevation of by-pass holes in the facility.

The dry period of the tests lasted about seven hours, like in the incident in 2003. This period was characterized by monotone temperature increase in the dry section of the fuel rods. Plastic deformation of cladding tubes took place and the high pressure rods suffered burst at about 800 ºC. Only one fuel rod survived the period of plastic deformation without burst, but its internal pressure was very low. The oxidation of zirconium produced high amount of hydrogen. In the preliminary test 196 l and in the CODEX-CT-1 277 l was released from the tank under controlled conditions.

The maximum temperature reached 1245 ºC in the test. The temperature profile (Fig. 68) showed that the bottom of the bundle was intensively cooled by water, while the upper part heated up to very high temperatures. The top of the bundle was not as high as the central part because of radiation heat losses to the top of the test section.

The quench of fuel was initiated after the long term oxidation in hydrogen rich steam. The scenario included both quench from the bottom and the top, similarly to the cleaning

tank incident. The fragmentation and failure of the brittle fuel took place obviously during this period. In the preliminary test and in the CODEX-CT-1 test the quench process did not lead to significant temperature excursion or hydrogen production peak, since the Zr surfaces were already heavily oxidized.

The oxidized cladding and shroud in both cases were very brittle. The fragmentation of the fuel continued during the handling and post-test examination procedures. The fragmentation during this action was similar to the behaviour of damaged fuel assemblies during their removal from the cleaning tank.

7. POST-TEST EXAMINATIONS AFTER THE PRELIMINARY TEST

7.1. VISUAL EXAMINATION AFTER THE PRELIMINARY TEST

The cladding tubes suffered heavy fragmentation during the test. The fuel rods were heavily oxidised and broken into several pieces and during the handling of the tubes further fragmentation took place (Figures 68-69). The shroud plates were mainly intact, but they were so brittle that the 2 mm thick plates could be broken by hands (Fig. 70). Heavy oxidation was seen on the Zr surfaces. Some fragments of the tubes and plates were used for post-test examination without fixing them in epoxy.

7.2. HYDROGEN ABSORPTION IN THE ZIRCONIUM COMPONENTS

The amount of absorbed hydrogen was determined by high temperature hot extraction gas chromatographic method using CHROMPACK MODEL 438A Gas Chromatograph with thermal conductivity detector (TCD). Small pieces of shroud plates and cladding tubes were investigated after the preliminary test.

The hydrogen content was measured for selected samples from different axial positions. The axial profile of hydrogen concentration was built using the measured data points (Fig. 71). Significant difference was found between the profiles of hydrogen contents in shroud and cladding.

- The amount of absorbed hydrogen in the shroud was monotonously increasing up to 900 mm elevation. The maximum value of hydrogen concentration was above 12000 weight ppm.
- In case of cladding there were two maximums in the profile at 200 mm and 1000 mm elevations. The maximum values of hydrogen concentration were above 10000 ppm. In the central section of the cladding tubes the hydrogen content was much lower, its value was about 2000 ppm.

The main cause of the different hydrogen contents was the different thickness of cladding and shroud. The original shroud thickness was 2 mm, while the cladding was only 0,65 mm thick. During the long term high temperature transient much less β layer remained in the cladding than in the shroud. The β phase can pick up much more hydrogen than the α layer or the oxide scale. That is why there was much more hydrogen in the central (hottest) part of the shroud than in the cladding.

The bottom and top section of the cladding was less oxidized than the central part and so there was much thicker β phase in the bottom and top. This explains the profile of the hydrogen content with two maximums at the bottom and the top.

Using the hydrogen distributions along the length of cladding and shroud the average value of hydrogen content in the two elements was determined. The total masses of cladding tubes and shroud before oxidation were 861 g and 1439 g, respectively. The average hydrogen content in the shroud was 4212 ppm and in the cladding 3701 ppm. The total mass of hydrogen was 9.25 g (3.19 g in the cladding and 6.06 g in the shroud). It was equal to 113 l gas at room temperature.

The total mass of hydrogen produced during the oxidation of Zr can be determined as the sum of hydrogen released from the cleaning tank and absorbed in the metallic Zr. It gives 113+196=309 l hydrogen at room temperature (25.2 g H_2).

7.3. MECHANICAL TESTING OF PRELIMINARY TEST TUBES

The bottom intact section of the cladding tubes was used for mechanical testing. 8-9 mm long rings were cut from the tube and ring compression type testing was carried out to determine the change of cladding ductility and to characterize the embrittlement process. The main objective of these tests was to provide information on the mechanical properties of the cladding close to the place of fuel rod failure.

The ring specimens were examined in radial compression tests using an Instron 1195 universal test machine. The velocity of the crosshead movement was fixed at 2 mm/min. All tests were performed at room temperature. The load versus crosshead displacement curves were recorded and the crushing force and deformation were determined. Generally 2-3 cracks were detected but always the first crack was considered as the sign of failure. The rings were compressed until total plastic deformation had occurred or at least until the first indication of cracking. The load-displacement curves were evaluated to characterize the mechanical behaviour of the samples.

It was obvious that there must have been a transition zone between the bottom of the fuel cladding that was cooled by water and the fragmented section that suffered heavy oxidation and picked up significant amount of hydrogen.

The mechanical behaviour of the ring samples showed significant differences and indicated very well the transition between the bottom ductile part and the oxidised and brittle upper part of the examined segment. The specific energy at failure was determined as the total deformation energy at failure divided by the length of the ring. With this last parameter specimens with different ring lengths can be easily compared. In the bottom part of the tube the cladding was very ductile. The specific energy at failure for those samples was above 400 J/m. The decrease of energy at failure was observed at about 10 centimetres above the water level (Figures 72 and 73) for both examined tubes. (The numbering of tubes corresponds to Fig. 68, where rod No. 1 is the first tube from the left side in the left side picture.) In the upper section of the tubes, where significant oxidation could be observed visually, the

specific energy at failure was much less than 50 J/m. It indicated the high degree of cladding embrittlement. The transition from ductile to brittle behaviour can be seen in the load-displacement curves recorded during the ring compressions tests, too. Fig. 74 shows seven curves from rod No. 6. The bottom part was completely ductile (108 mm elevation). Ductility can be observed for samples between 209-237 mm elevations, but the ductile plateau is shorter and shorter as the elevation increases. Sample cut at 246 mm shows brittle behaviour without any ductile section. The further embrittlement is indicated by the decreasing maximum load for samples 256 and 265 mm. The top section of the tubes could not be tested, for the rings were broken during the cutting procedure and no intact ring could be manufactured. Obviously the cladding in the top section was even more brittle than below.

7.4. METALLOGRAPHIC EXAMINATIONS AFTER THE PRELIMINARY TEST

Cross sections were prepared from some samples that were used for the measurements of hydrogen content. The surfaces were polished and ground after fixing the structure with epoxy. Metallographic examinations were carried out and the thicknesses of remaining metal layer were determined. The following three samples were examined in details:

- Cladding tube from the central section. The measured remaining metal layer thickness of this tube varied between 172-325 μm. Photographs of the cross section from this tube are shown in Fig. 75.
- Shroud from 650 mm elevation. The hydrogen content of this sample was 7500 ppm. The typical structure of Zr metal with high hydrogen content is shown in Fig. 76.
- Cladding from the upper section. The metal layer was between 450-536 μm and the sample was much less oxidised than the cladding tube from the central section. The sample contained 12300 ppm hydrogen. Photographs of the cross section from this tube are shown in Fig. 77.

8. POST-TEST EXAMINATIONS OF THE CODEX-CT-1 BUNDLE

8.1. VISUAL EXAMINATION OF THE CODEX-CT-1 BUNDLE

The fuel rods inside of the bundle suffered severe damage during the tests. The final state was characterised by fragmentation, formation of cracks and brittle failure of the Zr cladding. The bottom part of the fuel that was cooled by water, remained intact. The experience of handling the fuel rod after the test showed that the material was very brittle: even a small mechanical load lead to further fragmentation of the cladding. The upper spacer grids disappeared due to heavy oxidation and it facilitated the relocation of broken fuel rods.

The shroud seemed to be intact after the test and for this reason the bundle inside of the hexagonal shroud was filled up with epoxy. During the handling of the bundle full cross section break took place in the upper part: all fuel rods and the shroud were broken at a given elevation (Fig. 78). For further examinations the bundle was placed in a plastic tube and fixed by epoxy.

8.2. COMPLEX RADIOGRAPHY INSPECTIONS FOR THE CODEX-CT-1 BUNDLE

The complex radiography inspections were produced on the radiography station of the Budapest research reactor. Gamma- and X-ray radiography were used to study the inner structure of the inspected, damaged CODEX-CT-1 bundle. It was packed in a polyvinyl chloride (PVC) tube, its diameter was 62 mm and its length was 1050 mm. The inside of the tube was filled up by epoxy to fix the position of the sample. The radiography pictures were exposed in horizontal position of the PVC tube. A lead marker system was used for the easier identification of the errors. Every five centimetres was marked by lead numbers from zero to 105 cm. The PVC tube is shown in the Fig. 79 with the marker system in the beam position. A step wedge etalon (from 5 to 50 mm, in 10 steps, made from iron) and FE1 type wire picture quality indicator were used to estimate the dimensions of the errors as it is visible in the middle in Fig. 79.

BAS 20 X 40 MS type imaging plate was used as detector both for gamma- and X-ray radiography. BAS 2500 type scanner was used to read the plates. The evaluation work was contributed by AIDA software. The sample was divided in three (A,B and C) bands. The "A" band was from 0 to 350 mm-, "B" band was from 350 to 700 mm and "C" band was from 700 to 1020 mm. Every band was exposed in 0^o, 45^o and 90^o rotations.

The energy of the gamma radiation was 8,2 MeV from the reactor and its dose rate was 8,3 Gy/h, 10 sec was the exposure time with 50 mm lead filter. The weak contrast of the gamma radiography pictures was not available for the high level evaluation work.

The source of the X-ray radiation was MXR 300 type portable, industrial generator. The applied power was 275 kV and 3 mA. The focus distance was 1250 mm. The exposure time was 60 sec. On the high resolution X-ray radiography pictures the cracks of the artificial resin in the PVC tube and the collapses of the fuel elements were very well visible.

The high resolution X-ray radiography pictures showed the fragmentation of the fuel elements and the relocation of some rod segments (Fig. 80 a-g). The Fig.80 a shows the X-ray radiography picture of the whole CODEX-CT-1 bundle in PVC tube. On the left side of the figure is visible the arrangement of the "A", "B" and "C" bands. The longitudinal dimensions of the tube are given by the numbers in centimetre on the right side of Figure 80 a for the coordination of the error places.

At the 8cm, 40cm and 80cm from the bottom of the bundle are found the FE 1 type wire picture quality indicators. The Fig. 80 b-g show the typical errors. A crack of the artificial resin is visible in Fig. 80 b. The full cross section break can be seen in Fig. 80 c and 80 d, where the collapsed fields were found. Some easier damaged details are observed in Fig. 72 e and 72 f, where in the central section indicated that long ballooned areas were formed in the fuel rods. The bottom part of the bundle remained almost intact but the accumulated debris material was found in the Fig. 80 g from the upper parts.

8.3. HYDROGEN ABSORPTION IN THE CODEX-CT-1 BUNDLE

Several pieces of shroud, claddings and spacer grids were investigated after CODEX-CT-1 test in order to determine the amount of hydrogen absorbed in the Zr components.

The hydrogen distribution along the fuel length was similar to the profile observed in the preliminary test: the cladding had a profile with two maximums at the bottom and top, and the hydrogen content of the shroud was higher in the central section than that of cladding (Fig. 81). The hydrogen content in the Zr spacer at elevation 710 mm was 2700 ppm that was between the measured values for cladding (1201 ppm) and shroud (4975 ppm).

Using the hydrogen distributions along the length of cladding and shroud the average value of hydrogen content in the two elements was determined. The total masses of cladding tubes and shroud before the test were 861 g and 1508 g, respectively. The average hydrogen content was 4274 ppm in the shroud and 4435 ppm in the cladding. The total mass of hydrogen was 10.27 g (3.82 g in the cladding and 6.45 g in the shroud). It was equal to 126 l gas at room temperature.

The total mass of five Zr spacers in the bundle was 17 g. Their hydrogen content was not measured at each elevation and so their total hydrogen content was not calculated. Considering that the mass of spacers was less than 1 % of the total Zr mass and the hydrogen content in the measured position was between the values of shroud and cladding, the mass of hydrogen absorbed in the cladding can be estimated as 0.1 g (1 l).

The total mass of hydrogen produced during CODEX-CT-1 test can be determined as the sum of hydrogen released from the cleaning tank and absorbed in the metallic Zr. It gives 126+1+277= 404 l hydrogen at room temperature (33 g H_2).

8.4. METALLOGRAPHIC EXAMINATIONS OF CODEX-CT-1 BUNDLE

17 cross sections were cut from the bundle. The surfaces were polished and ground for metallographic examinations. The positions of cross sections are shown in Table 12. The first cross section was cut from the bottom and the last from the top of the bundle.

No. of cross section	Elevation (mm)	No. of cross section	Elevation (mm)
1	160	10	610
2	210	11	660
3	260	12	710
4	310	13	760
5	360	14	810
6	410	15	860
7	460	16	910
8	510	17	960
9	560		

Table 12. Positions of cross sections

Cross sections of the CODEX-CT-1 bundle are shown in Fig. 82. The fuel rods were numbered counter-clockwise from the rod in the left corner, the central rod is rod No. 7.

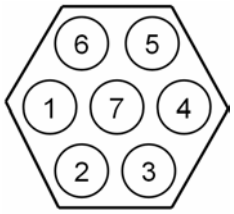

The main observations done on the cross sections can be summarised as follows:

- The cross section at elevation 160 mm shows the original structure of the bundle, since it was in cold water during the total duration of the experiment. In cross section at 210 mm the central rod shows significant ballooning and some can be seen on the other fuel rods between the pellet and cladding as well.
- At 360 mm elevation large accumulation of fuel debris can be seen. It is the elevation above of one spacer grid and the material collected here was originated from upper elevations. The original fuel rods at this elevation seem to be intact.
- The first cladding fragmentation can be observed at elevation of 410 mm where rod No. 1. has broken cladding. More severe fragmentation is indicated at elevation of 460 mm, while the 510 mm cross section shows less damaged structure.
- The upper elevations show some intact fuel rods that were relocated from the top part of the bundle after the fragmentation of the central section.
- The typical mechanism of loss of fuel integrity was the brittle failure of cladding tubes. Fig. 83 shows some full cross section cracks in the cladding.
- Long large ballooning of fuel rod no. 5. can be identified on cross section between 560-710 mm. The central rod showed large ballooning at higher elevations between 760-860 mm (Fig. 85).
- The oxide scale had layered and spalling character that is typical for the E110 type cladding (Fig. 84). The oxidation of cladding took place not only on the external surface, but after the burst on the internal surface as well (Fig. 86). The Zr shroud suffered similar oxidation, but the oxide scale was compact there (Fig. 87).

The oxide layer thickness was measured in several positions on each fuel rod and on the wall of shroud in each cross section. The oxide scale on the fuel rods had layered structure and the external oxide scales were spalling from the cladding (Fig. 84). The oxide scale on the shroud had more compact structure without layers (Fig. 87). The axial oxidation profiles are shown in Figures 88 and 89. The maximum oxide layer observed on the external surface of the shroud had 300 μm thickness at 660 mm elevation. On the internal surface of the shroud and on the external surface of the cladding tubes the oxide layer thickness was less, the maximum values appeared to be 230-240 μm. The oxidation profiles were similar on the internal surface of the shroud and the external surface of the tubes.

Since significant part of the external oxide scale fell down before fixation of the bundle, it was necessary to measure the thickness of the remaining metal phase of Zr (Table 13). It can help in the better estimation of the degree of oxidation. The metal layer thickness profile is shown in Fig. 90. During the evaluation of the metal layer thickness it must be considered that the decrease of tube wall thickness was a common result of two processes: ballooning and oxidation.

Elevation (mm)	Oxide layer on shroud		Oxide layer on cladding		Remaining metal layer (μm)
	external (μm)	internal (μm)	minimum (μm)	maximum (μm)	
160	12	12		10.3	
210	24.5	24		14.5	
260	162.3	58.6	19.9	40.4	
310	54	28.5	19.8	31.7	575
360	47.4	40	8.8	100.6	
410	146.2	47.4	120.1	142	454
460	128.8	122.5	24.5	270	382
510	241.9			136	311
560	224	130	160.4	194	221
610	215		91	274	252
660	300	233.2	135	234	242
710	107.5		107.5	214.2	240
760	274.3	207.1	22.9	240.9	352
810	227.6	171.5	40	158.1	466
860	193.6	173.1	76.6	86.1	514
910	139.9	53	49	92.5	525
960					

Table 13. Measured oxide and metal layers in the CODEX-CT-1 bundle

Elevation (mm)	External diameter (mm)						
	Rod No. 1	Rod No. 2	Rod No. 3	Rod No. 4	Rod No. 5	Rod No. 6	Rod No. 7
0	9.1	9.1	9.1	9.1	9.1	9.1	9.1
160	9.35	9.4	9.38	9.19	9.46	9.35	9.35
210	9.76	10.11	10.72	9.78	9.61	9.87	10.88
260	9.53	9.57	9.62	9.61	9.61	9.7	11.2
310	9.54	9.42	9.42	9.25	9.16	9.36	10.01
360	9.55	9.64	9.64	9.57	9.3	9.51	11.08
410	10.41	10.41	9.91	10.3	10.3	10.22	11.61
460	10.32	10.99	10.59	10.36	9.99	10.32	10.36
510	9.97	10.65	10.7	10.87	10.42	10.82	10.41
560	10.74	10.75	12.26	13.15	10.52	10.74	10.54
610	11.3	11.31	12.88	10.98	9.97	9.73	11.58
660	11.5	11.79	13.42	10.98	10.17	10.23	11.19
710	10.56	11.33	11.62	11.85	9.83	10.56	11.5
760	10.67	10.31	10.09	10.21	9.94	10.25	16
810	9.97	9.81	9.77	10.64	9.65	9.72	11.67
860	9.57	9.69	9.35	9.66	9.61	9.57	11.5
910	9.38	9.35	9.78	9.61	9.37	9.75	10.12
960	9.25	9.3	9.4	9.5	9.3	9.3	9.5
1000	9.1	9.1	9.1	9.1	9.1	9.1	9.1

Table 14. Measured external diameter of fuel rods

Long ballooned sections were observed in the post-test examinations. The diameter change was a common result of plastic deformation and oxidation, but the oxidation effect was much less in the diameter increase than that of ballooning. The ballooning profiles are shown in Figs. 91 and 92. The axial distribution of cladding diameter was determined using the final state of the bundle and considering the cladding sections in each elevation (Table 14). In case of intact cladding the diameter was determined as an average value for the given tube. The measured external diameter exceeded 16 mm.

8.5. SEM AND EDX ANALYSES OF SELECTED SAMPLES

Some samples were selected on the basis of the hydrogen measurements. Table 15 shows the elevation and the hydrogen content (in weight ppm) of the samples to be investigated.

Sample mark	Elevation (mm)	Hydrogen content (ppm)	Note
CT-1-910	910	4500 (shroud) and 6000 (cladding)	Piece of shroud and cladding
CT-1-810	810	4400	Piece of shroud
CT-1-360	360	4700	Al_2O_3 pellet with a piece of cladding
CT-1-360s	360	~ 8200	Piece of shroud
CT-1-210	210	~ 20000	Al_2O_3 pellet with piece of cladding
CT-1-110	110	0	Piece of shroud

Table 15. Some data of samples selected for SEM + EDX studies

From two elevations (360 mm and 210 mm) there were Al_2O_3 pellets together with pieces of the cladding. These samples were embedded and ground earlier, therefore they could be useful for SEM studies. They were put on the SEM sample holders by double sided carbon tape and sputtered with a thin carbon layer to decrease electrical charging. Shroud sample pieces were embedded into epoxy resin, ground and polished then sputtered with a thin carbon layer.

The morphological features and the elemental composition of the samples were studied by a JEOL Superprobe 733 electron microprobe equipped with an Oxford ISIS 200 type energy dispersive microanalyser (EDX). Some studies were performed by a Philips SEM 505 scanning electron microscope (SEM) and a LINK AN 10 55S type EDX system.

Figures 93 and 94 show BEI images taken from one piece of cladding and shroud on sample CT-1-910. There is a difference in the thicknesses of the oxide layers on the shroud: one has about 150-170 μm, and the other has 60-65 μm thickness. On the cladding the thickness of the oxide layer is about 50-55 μm. It seems that at higher hydrogen content only thinner oxide could be formed. More number of cracks can be seen at the oxide – metal interface of the cladding than for the shroud. EDX analysis of the sample showed 4.2 – 5.2

mass % oxygen content in the metallic parts and 16 – 18 mass % (close to the stochiometric ZrO_2 composition) on the oxides of the shroud and that of the cladding.

Figures 95 and 96 show BEI images of shroud sample taken from 810 mm elevation (sample CT-1-810). The oxide layer formed only at one side of the shroud has 190-260 μm thickness. Fine structure of the metallic part can also be observed on the enclosed images. At the oxide – metal interface several cracks (may be also hydrides) can be revealed. EDX analysis performed on the oxide and on the metal showed that in the oxide almost the stochiometric ZrO_2 was formed however small amounts of boron were also detected. On the metal oxygen content of 3.6 – 5.4 mass % was detected.

Figure 97 shows overviews of the Al_2O_3 pellet + cladding and that of the cladding taken from 360 mm elevation. On the left hand side image of the Figure 97 there is a small gap between the pellet and the cladding. On the right hand side image structure of the cladding and the outer oxide layer can be seen. The thickness of the oxide layer changed from about 40 up to 150 μm. This layer had columnar structure. Large-sized metal (probably α-zirconium) is the neighbouring of the oxide layer. EDX analysis of the cladding showed almost stochiometric ZrO_2 on the oxide layer, however there was small amounts of oxygen on the metallic part. Some quantitative EDX results are summarized in Table 16. Deviation of the elemental composition measured on the metallic part and also on the oxide layer can probably due to the presence of voids and cracks and also the inhomogeneous structure of the material.

Metallic part		Oxide part	
O (mass %)	Zr (mass %)	O (mass %)	Zr (mass %)
4	90.04	19.25	80.75
4.87	95.13	11.62	88.38
3.53	96.47	13.86	86.14
5.27	94.73	16.22	83.78
6.51	84.84	15.08	84.92
5.97	86.11	10.77	89.23
5.26	94.74	13.25	86.75
3.84	96.16	23.31	76.69
5.04	94.96	16.22	83.78
Average 4.9	92.58	15.51	84.49
Standard deviation 0.99	4.44	3.90	3.90

Table 16. Some quantitative EDX results for sample taken from 360 mm elevation

Figures 98 and 99 show BEI images of the shroud taken from 360 mm elevation (sample CT-1-360s). Thickness of the oxide layers is between 50 and 60 μm and at both sides needle crystals (probably also oxide) can be seen at the oxide – metal interface penetrating into the metal. Grain size of the shroud sample is ranging from about 65 μm to 310 μm. Fine structure inside the larger grains can also be revealed. EDX analysis performed

on the oxide showed almost stochiometric ZrO_2 composition; however few mass % of boron was also detected. On the metallic parts 2.8 – 3.2 mass % of oxygen was detected by EDX.

Figure 100 shows BEI images of the cladding taken from 210 mm elevation (sample CT-1-210). The left hand side image shows a lot of cracks and probably also hydrides with darker contrast than that of the matrix. Among the samples studied by SEM + EDX this sample had the highest amount of hydrogen. The right hand side image illustrates several tens of μm sized crystals (probably α-zirconium). The EDX analysis of different parts of the cladding shows relatively low oxygen content ranging from 3 to 8.7 mass %. Figure 101 shows an EDX spectrum typical for this cladding sample. It can be concluded from the EDX results, that the cladding was not oxidized heavily at this elevation.

SEM and EDX studies of shroud sample taken from 110 mm elevation (sample CT-1-110) showed only the normal surface of the alloy (see Figure 102) and generally very low oxygen (below 3 mass %). These findings are correlation with the experimental conditions. There is no oxide layer on the shroud. Only some remnants of the sample preparation can be seen.

9. EXPERIMENTAL DATABASE

The experimental data of the CODEX-CT-1 test were collected for code validation purposes into a database. The parameters are listed in Table 17 and plotted in Figs. 30-67 for the period of 0-27820 s. (Part of the preparatory work is also covered in the database before "0" time.)

The database is presented in a large ASCII type file. The first column of the matrix contains the time. The "0" experimental time was set at real time 10:00:00, 5th July 2007. Each variable listed in Table 17 is given in a separate column in the file. The order of variables is the same as listed in the table.

The preliminary test database has a similar structure, but the number of recorded variables was less (Table 18). The "0" experimental time corresponds to real time 07:27:43, 20th June 2007. The parameters are listed in Table 18 and plotted in Figs. 13-29.

Name	Unit	Definition
TFR136	°C	Fuel rod No. 1 temperature at 360 mm
TFR183	°C	Fuel rod No. 1 temperature at 830 mm
TFR229	°C	Fuel rod No. 2 temperature at 290 mm
TFR276	°C	Fuel rod No. 2 temperature at 760 mm
TFR322	°C	Fuel rod No. 3 temperature at 220 mm
TFR355	°C	Fuel rod No. 3 temperature at 550 mm
TFR415	°C	Fuel rod No. 4 temperature at 150 mm
TFR462	°C	Fuel rod No. 4 temperature at 620 mm
TFR550	°C	Fuel rod No. 5 temperature at 500 mm
TFR596	°C	Fuel rod No. 5 temperature at 960 mm
TFR690	°C	Fuel rod No. 6 temperature at 900 mm
TFR755	°C	Fuel rod No. 7 temperature at 550 mm
TSH27	°C	Shroud temperature at 270 mm
TSH70	°C	Shroud temperature at 700 mm
THR70	°C	Heater temperature at 700 mm
TG5	°C	Gap temperature at 50 mm
TG27	°C	Gap temperature at 270 mm
TG50	°C	Gap temperature at 500 mm
TG74	°C	Gap temperature at 740 mm

TG97	°C	Gap temperature at 970 mm
TCIN	°C	Coolant inlet temperature in the intlet junction
TCOUT	°C	Coolant outlet temperature in the outlet junction
PYROM	°C	Temperature measured by pyrometer
PFR1	bar	Fuel rod No.1 pressure
PFR2	bar	Fuel rod No.2 pressure
PFR3	bar	Fuel rod No. 3 pressure
PFR4	bar	Fuel rod No. 4 pressure
PFR5	bar	Fuel rod No. 5 pressure
PFR6	bar	Fuel rod No. 6 pressure
PFR7	bar	Fuel rod No.7 pressure
PSYS	bar	System pressure
LTS	cm	Water level in the test section
LXT	cm	Water level in the expansion tank
FLOW	g/s	Coolant flowrate
H2	l	Volume of released hydrogen from the cleaning tank model
TCD	-	Molar fraction of hydrogen
POWER	W	Electrical power

Table 17. List of measured parameters available in the CODEX-CT-1 database

Name	**Unit**	**Definition**
TG5	°C	Gap temperature at 50 mm
TG27	°C	Gap temperature at 270 mm
TG50	°C	Gap temperature at 500 mm
TG74	°C	Gap temperature at 740 mm
TG97	°C	Gap temperature at 970 mm
TSH27	°C	Temperature between the cladding tubes at 270 mm
THR90	°C	Heater temperature at 900 mm (position 1)
THR91	°C	Heater temperature at 900 mm (position 2)
TCIN	°C	Coolant inlet temperature in the inlet junction
TCOUT	°C	Coolant outlet temperature in the outlet junction

PSYS	bar	System pressure
LTS	cm	Water level in the test section
LXT	cm	Water level in the expansion tank
FLOW	g/s	Coolant flowrate
H2	l	Volume of released hydrogen from the cleaning tank model
TCD	-	Molar fraction of hydrogen
POWER	W	Electrical power

Table 18. List of measured parameters available in the CODEX-CT pretest database

The database includes also the pictures of post-test examination. There are 437 pictures in 17 subdirectories. The subdirectories are named after the elevation of cross section.

Each subdirectory includes the following pictures:

- View of the bundle.
  - The names of the files are N-0.bmp,
    - where N is the number of cross section.

- View of each fuel rod at the given elevation.
  - The names of the files are: N-R.bmp,
    - where N is the number of cross section and
    - R is the number of rod.
  - The magnification in these pictures was 6.5x.

- Close view of cladding and shroud segments.
  - The names of the files are N-R-MX.bmp,
    - where N is the number of cross section,
    - M indicates magnification with the following values: M=2-5 means 2.5x, M=10 means 10x, M=16 means 16x,
    - R is the number of rod, R=0 is the shroud,
    - X=A,B,C,Ap.... shows that there are several pictures from the same cladding.

10. SUMMARY AND CONCLUSIONS

Fuel assembly damage took place in the cleaning tank under specific conditions during the Paks-2 incident. The fuel was oxidised in large stagnant steam volume that had high hydrogen content. The fragmentation of brittle fuel happened during the quenching of heavily oxidised assemblies. This incident was beyond the LOCA type accidents, for the oxidation took place for a very long time.

The main conditions of the incident were reproduced in the CODEX-CT-1 experiment. After the test the fuel bundle rods showed similar view to the samples observed at the Paks NPP after the incident. The upper part of the rods was almost fully oxidized, while the bottom part – cooled by water during the experiment – remained intact. The middle and upper sections were broken into several pieces. The material was very brittle, further fragmentation took place during the handling of fuel rods. The post-test examination indicated very high hydrogen content (several thousands ppm) in the Zr components (cladding and shroud). Many similarities were found between the damaged Paks-2 fuel and the rods tested in the CODEX-CT-1 experiment. This fact allowed us to draw conclusions on the similarities between measured test parameters and the unknown parameters of the incident.

The simulation of the cleaning tank incident provided detailed information on the probable scenario of the real incident. The data will be used for model development purposes to improve the predictive capabilities of fuel behaviour codes.

ACKNOWLEDGMENTS

The CODEX-CT-1 experiment was performed in the framework of the Economic Competitiveness Operational Programme of Hungary (contract number GVOP-3.1.1.-2004-05-0020/3.0) with the financial support of the National Office for Research and Technology (NKTH).

REFERENCES

[1] Perez-Feró, E, Vasáros, L., Győri, Cs., Windberg, P., Hózer, Z., Horváth, M. (2005): 'Effects of oxidation and hydrogen uptake of E110 cladding oxidized in hydrogen rich steam atmosphere', *QUENCH-11 Workshop*, October 2005, Karlsruhe.

[2] Hózer, Z., Maróti, L., Windberg, P., Matus, L., Nagy, I., Gyenes, Gy., Horváth, M., Pintér, A., Balaskó, M., Czitrovszky., A., Jani, P., Nagy, A., Prokopiev, O., Tóth, B. (2006). 'Behaviour of VVER fuel rods tested under severe accident conditions in the CODEX facility', *Nuclear Technology*, vol.154, pp. 302-317.

[3] Hózer, Z., Windberg, P., Nagy, I., Maróti, L., Matus, L., Horváth, M., Pintér, A, Balaskó, M., Czitrovszky, A., Jani P. (2003) 'Interaction of failed fuel rods under air ingress conditions', *Nuclear Technology*, vol. 141, pp. 244-256

[4] C.R. Wilke: 'A viscosity equation for gas mixtures', *J. Chem. Phys*. vol. 18. 617 (1950)

[5] L. Maróti: 'Chemical Interaction between VVER Core Components under Accidental Conditions', *Nucl. Eng. Des.*, vol. 172, p. 73 (1997).

[6] Pintér Csordás A, Matus L, Czitrovszky A, Jani P, Maróti L, Hózer Z, Windberg P, Hummel R: 'Investigation of aerosols released at high temperature from nuclear core models', *J. Nucl. Materials*, vol 282, Iss 2-3, pp. 205-215

[7] Trambauer K, Haste T J, Adroguer B, Hózer Z, Magallon D, Zurita A: In-Vessel Core Degradation Code Validation Matrix, Update 1996-1999, NEA/CSNI/R(2000)21

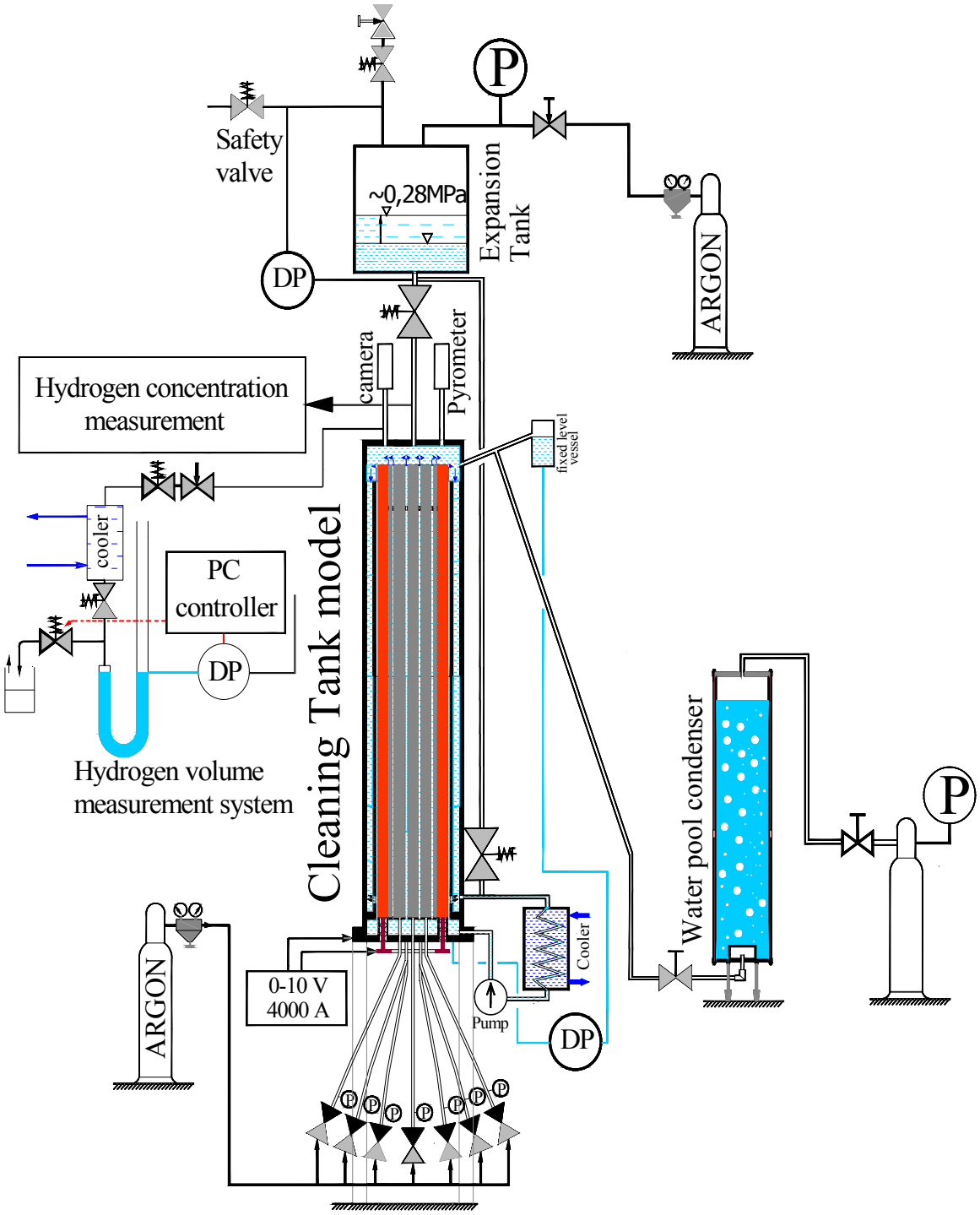

Fig. 1. Scheme and main components of the CODEX-CT facility

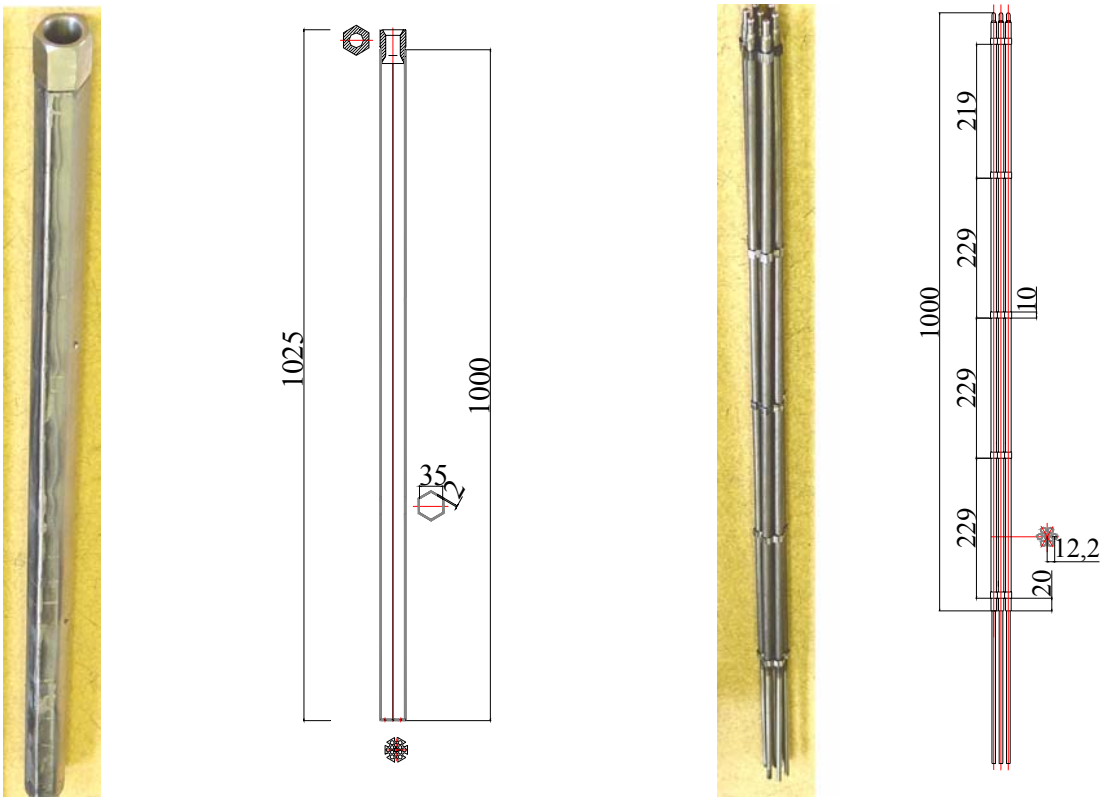

Fig. 2. Design and view of the shroud (left) and bundle (right)

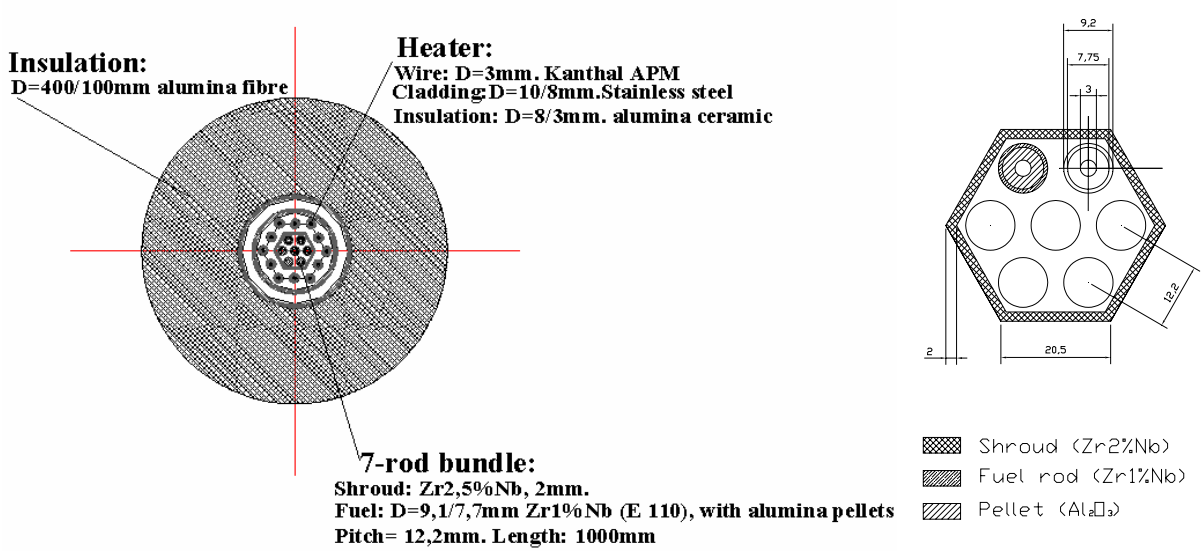

Fig. 3. Cross section of the test section of the facility

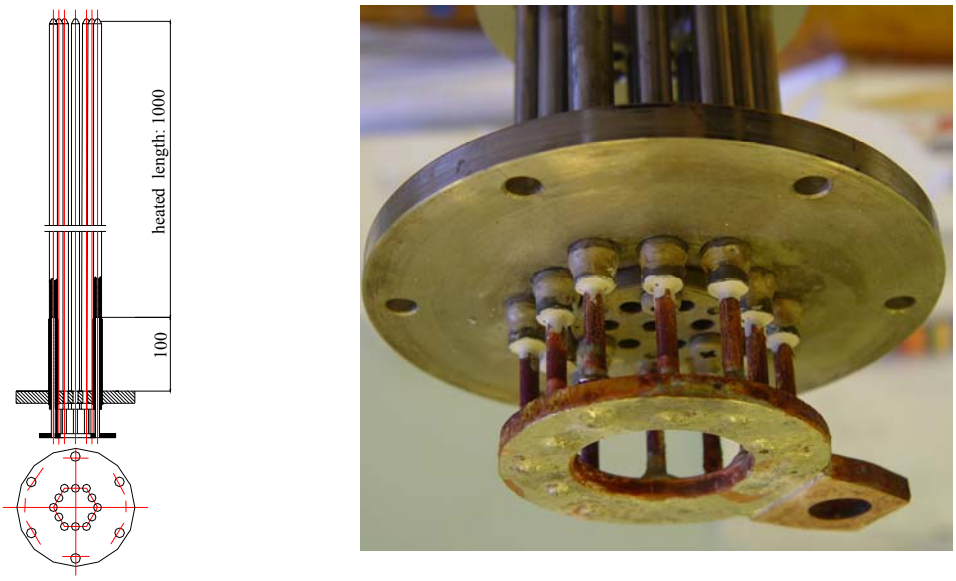

Fig. 4. Scheme (left) and view (right) of the heaters

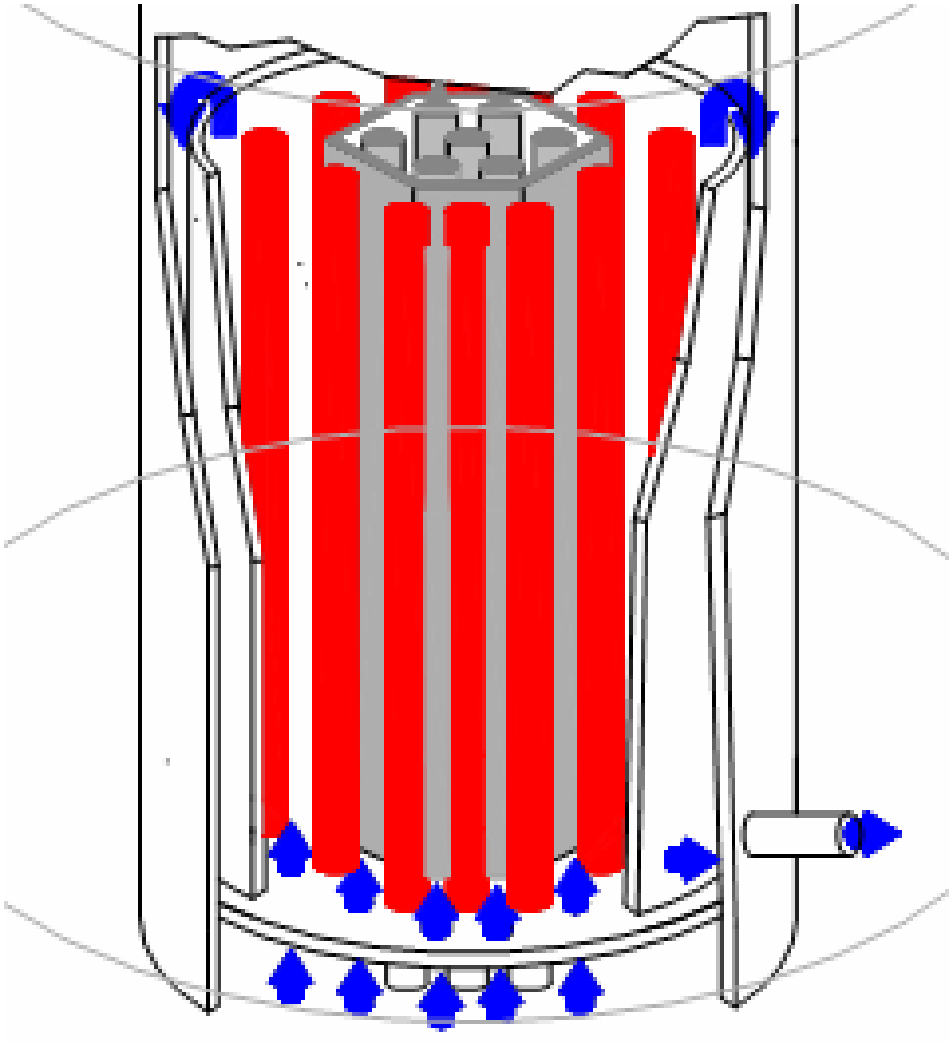

Fig. 5. Flow path in the test section of the CODEX-CT

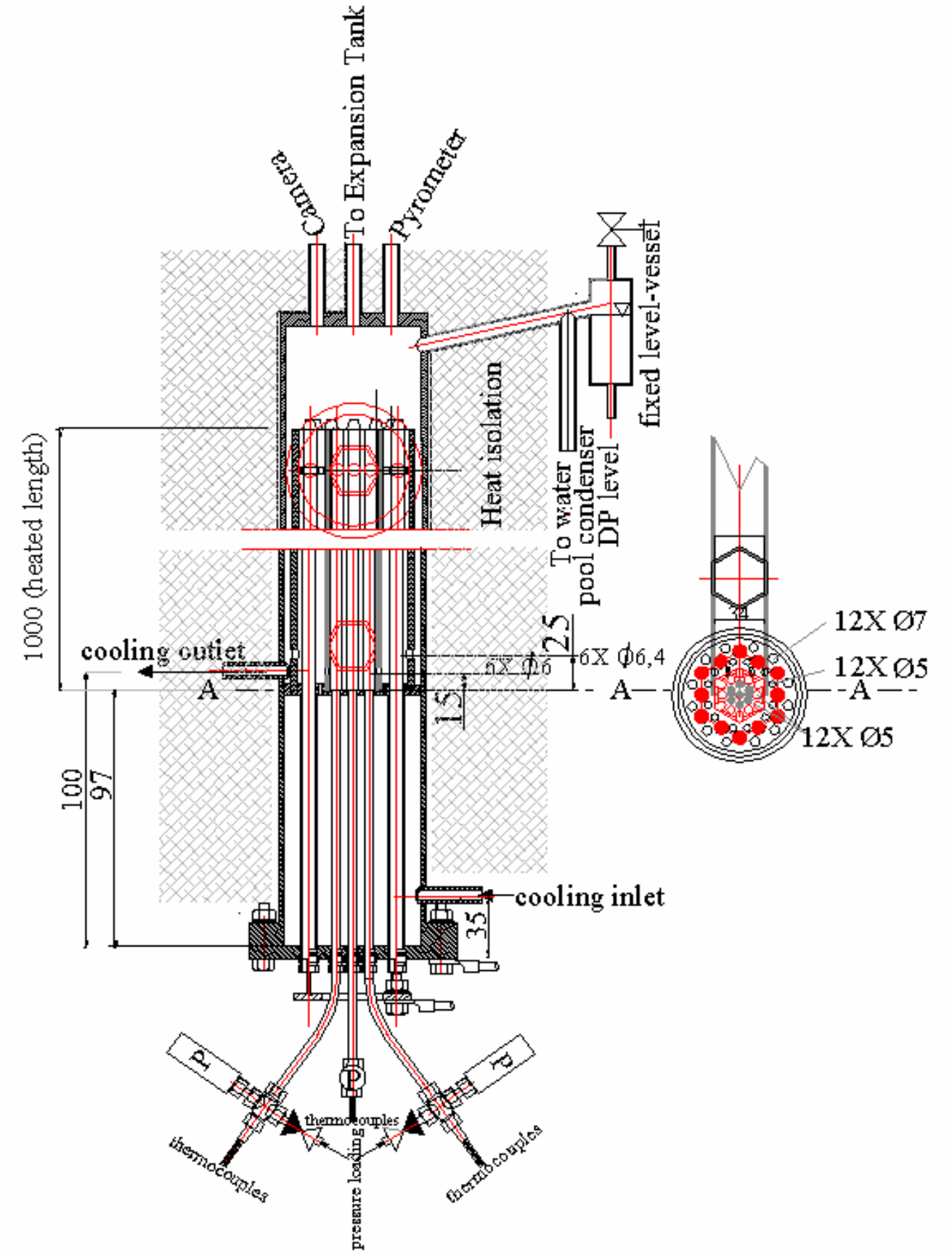

Fig. 6. Scheme of the CODEX-CT cleaning tank model

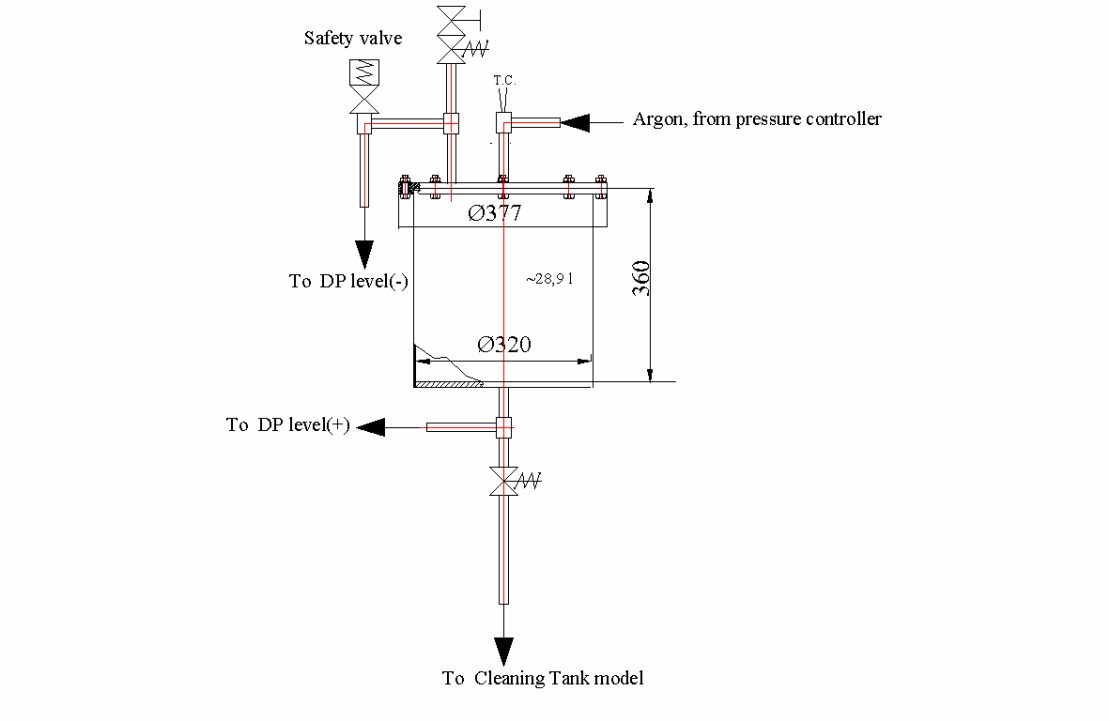

Fig. 7. Scheme of the expansion tank

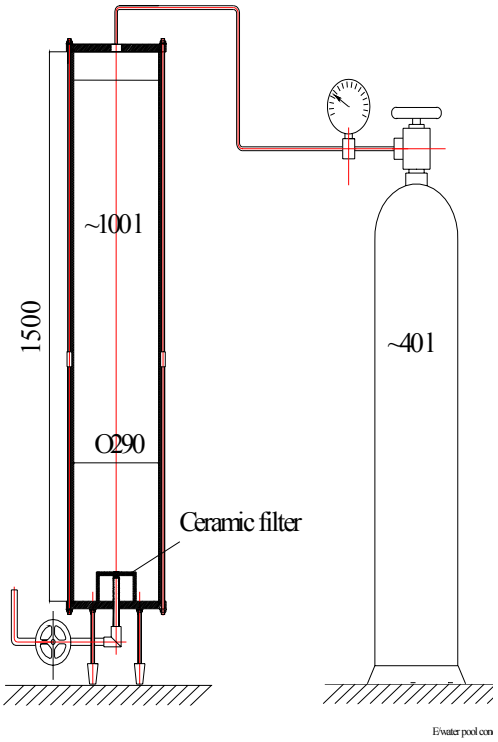

Fig. 8. Scheme of the condenser tank

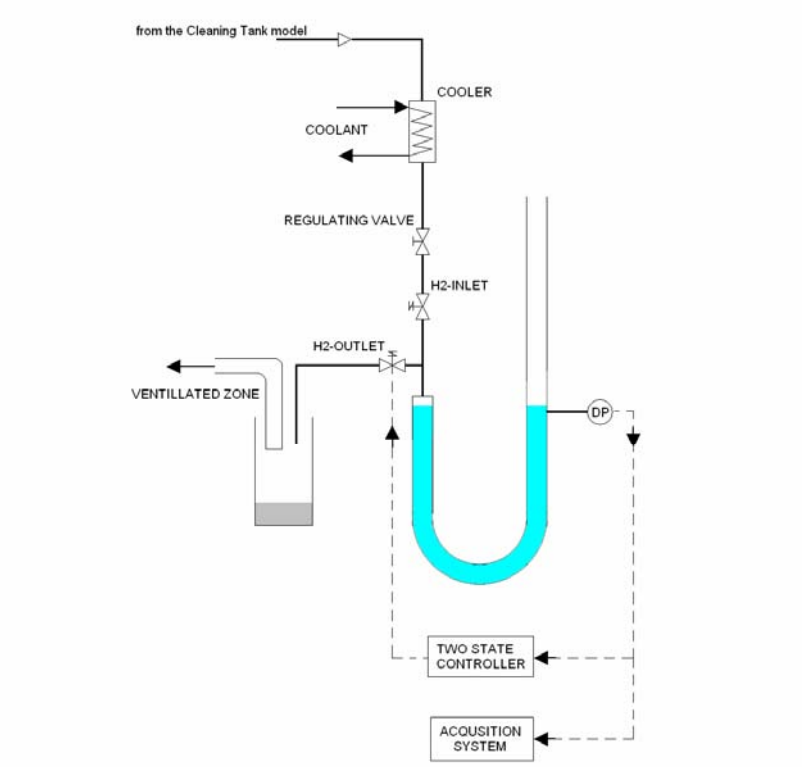

Fig. 9. Hydrogen flowrate measurement system

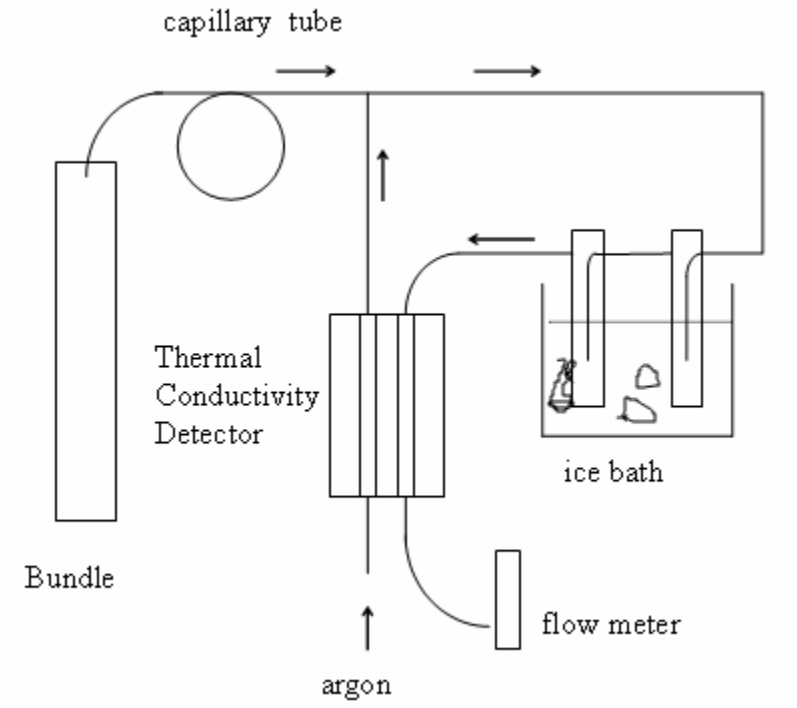

Fig. 10. Scheme of hydrogen concentration measurement

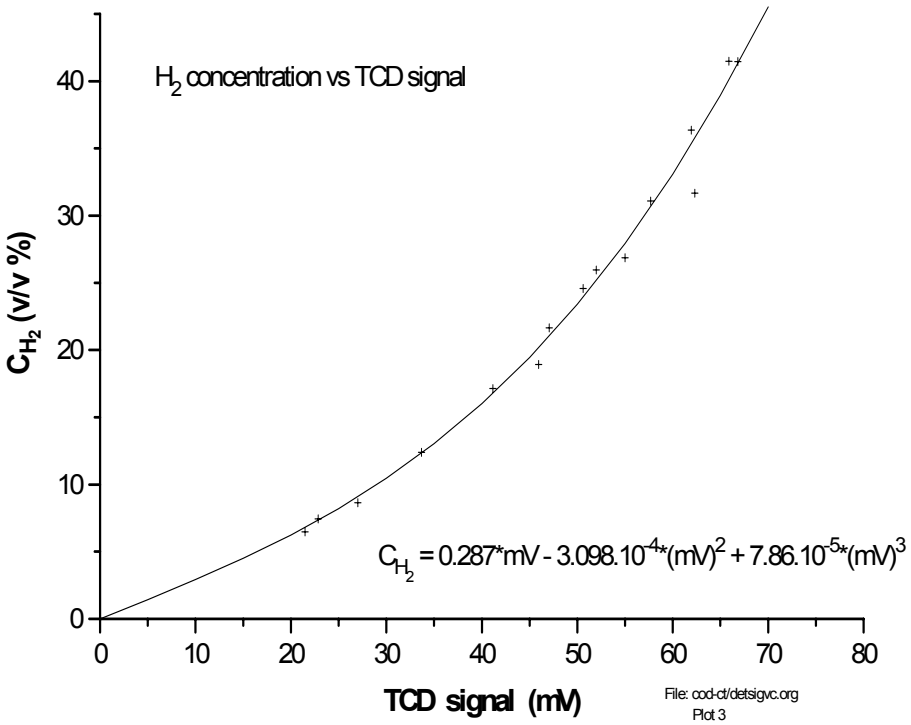

Fig. 11. Calibration curve, H_2 concentration in function of TCD signal

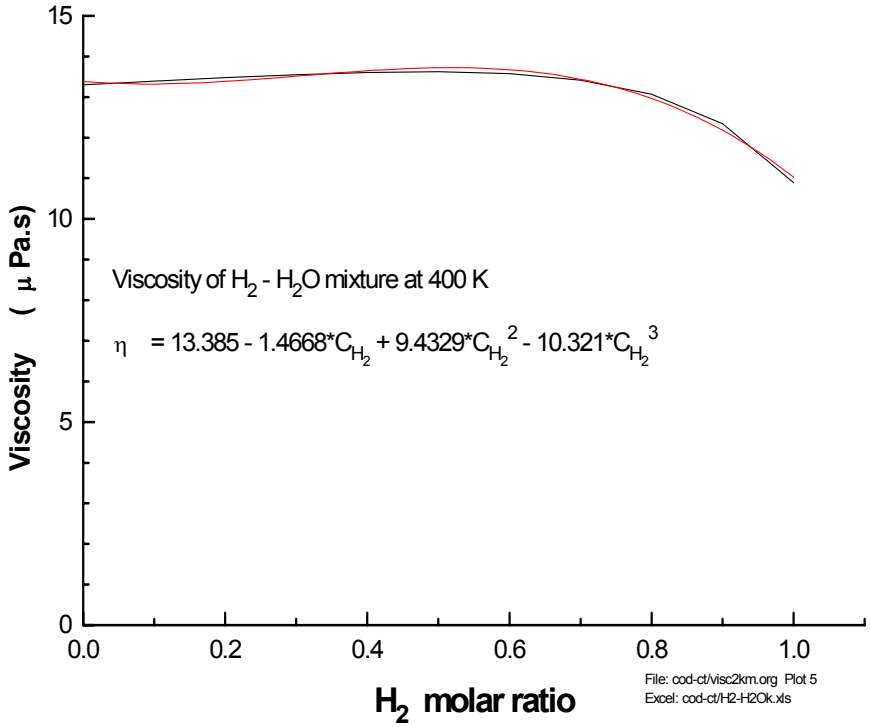

Fig. 12. Viscosity of H_2 - H_20 gas mixture at 400 K
(solid line calculated by [1], dotted line fitted curve)

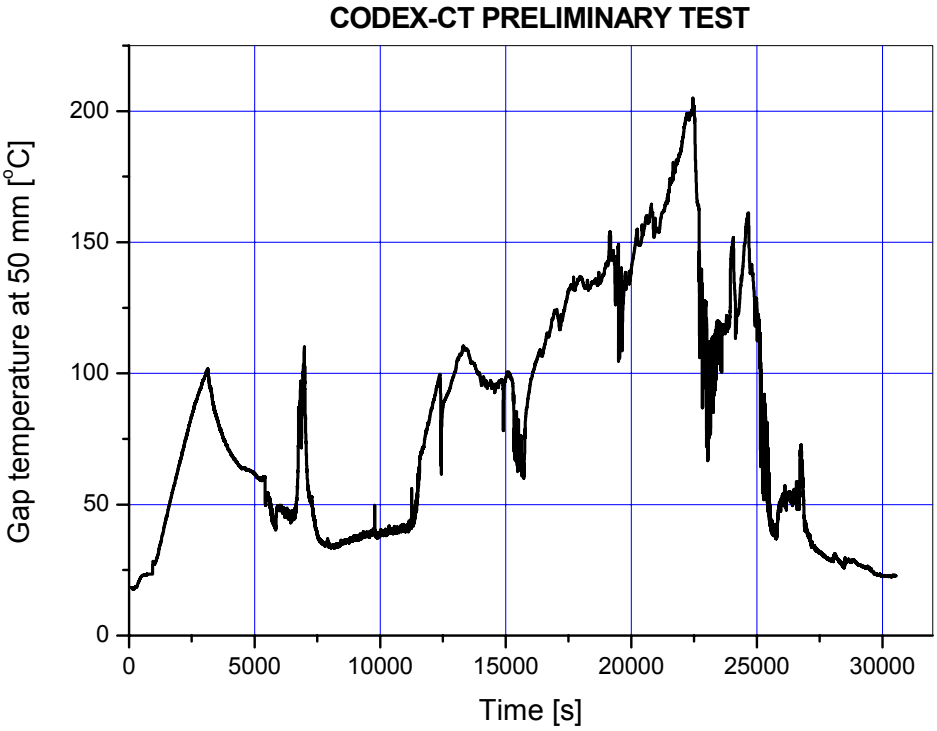

Fig. 13. TG5(pretest): Gap temperature at 50 mm

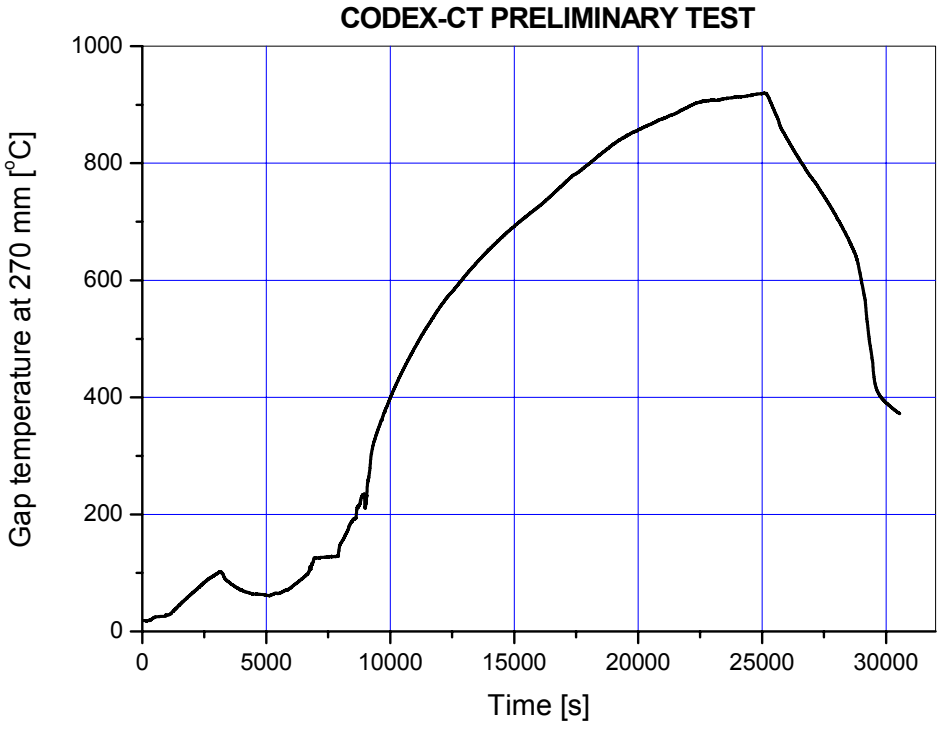

Fig. 14. TG27(pretest):Gap temperature at 270 mm

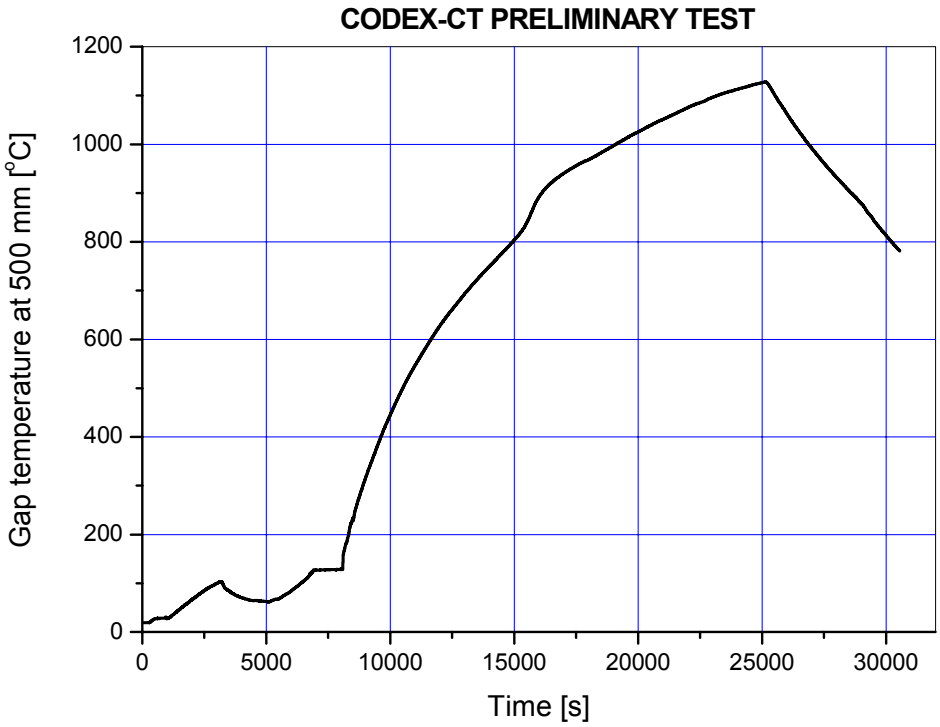

Fig. 15. TG50(pretest): Gap temperature at 500 mm

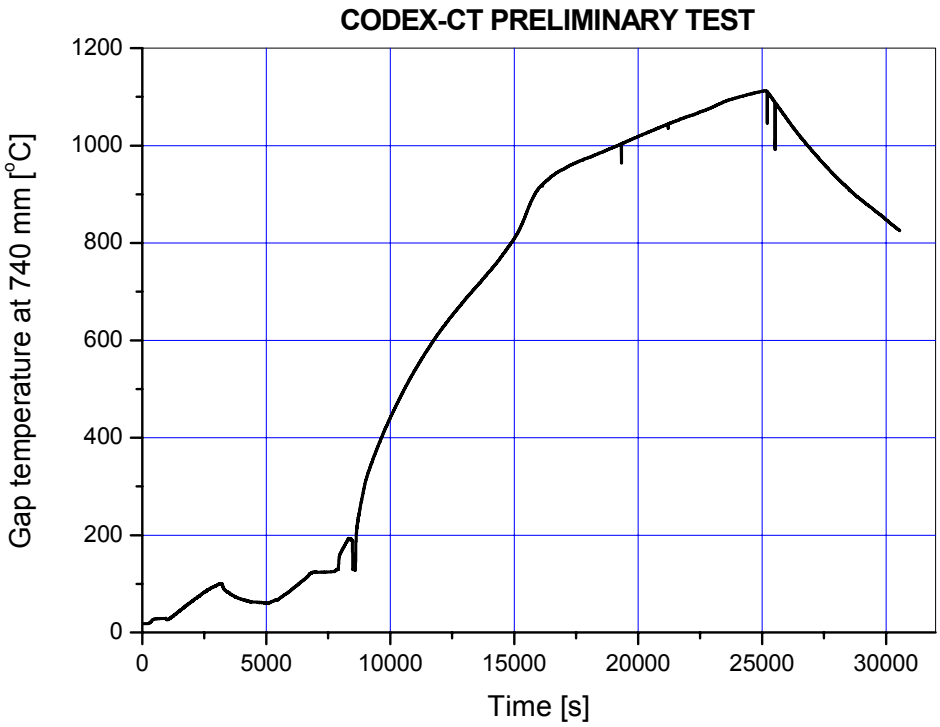

Fig. 16. TG74(pretest): Gap temperature at 740 mm

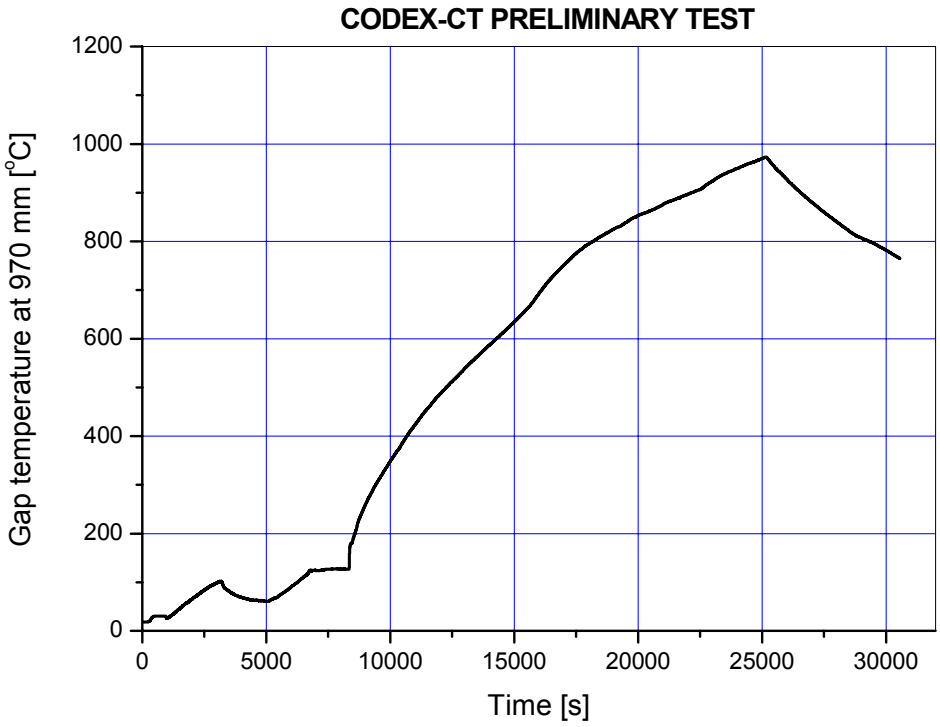

Fig. 17. TG97(pretest): Gap temperature at 970 mm

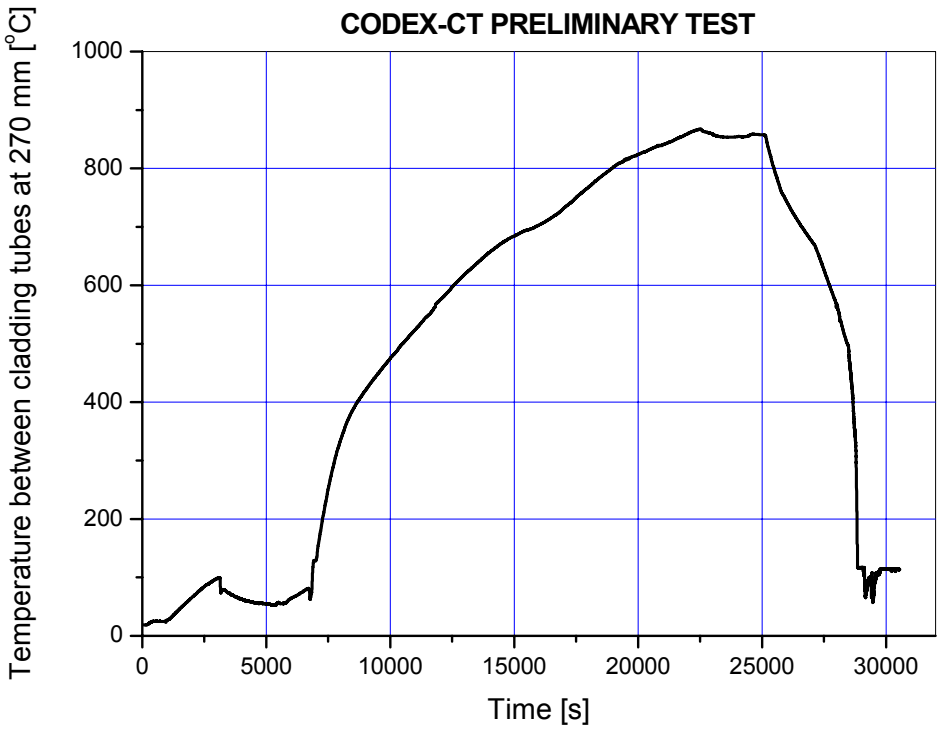

Fig. 18. TSH27(pretest): Temperature between cladding tubes at 270 mm

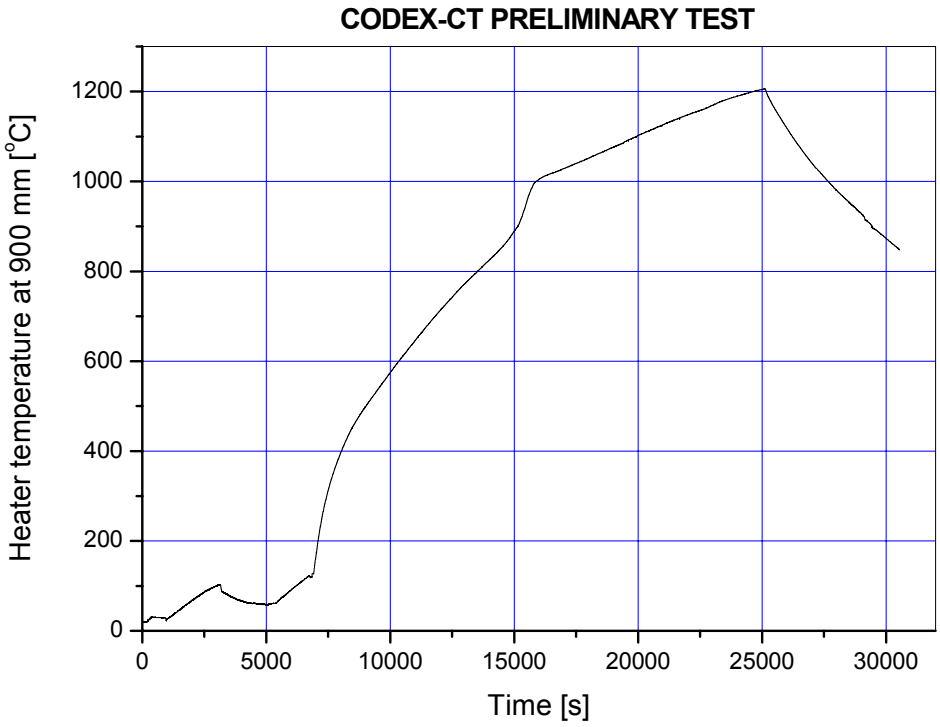

Fig. 19. THR90(pretest): Heater temperature at 900 mm (position 1)

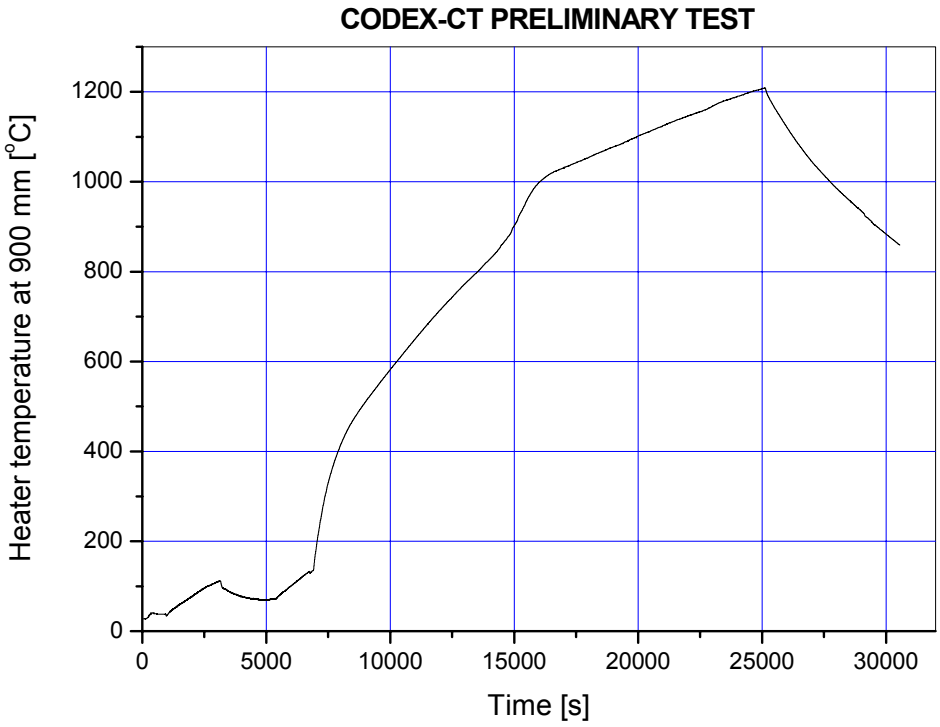

Fig. 20. THR91(pretest): Heater temperature at 900 mm (position 2)

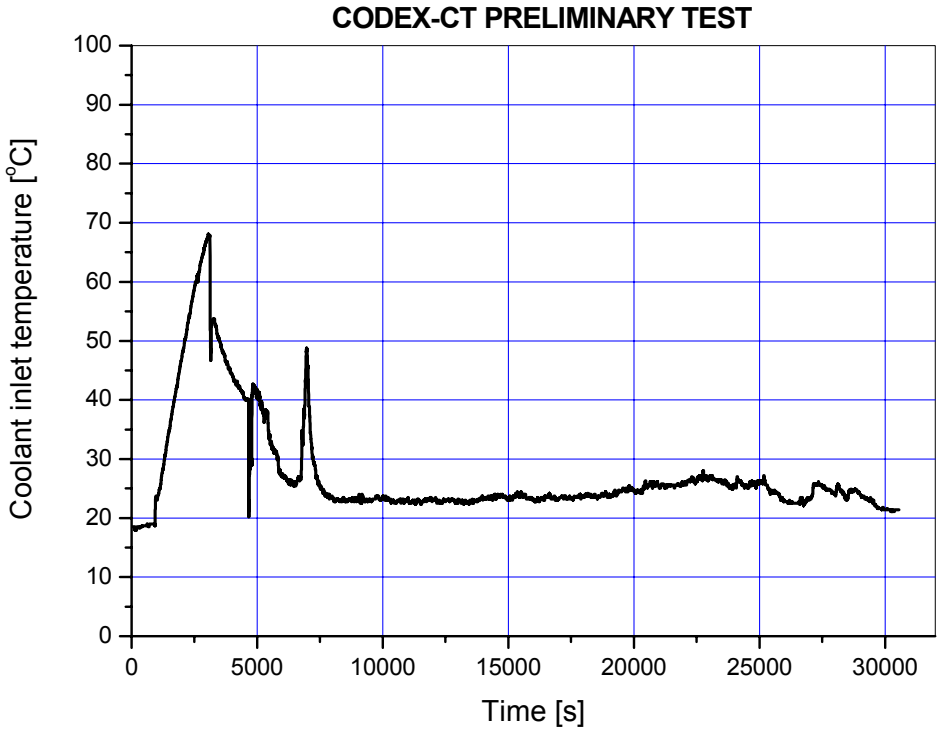

Fig. 21. TCIN(pretest): Coolant inlet temperature in the inlet junction

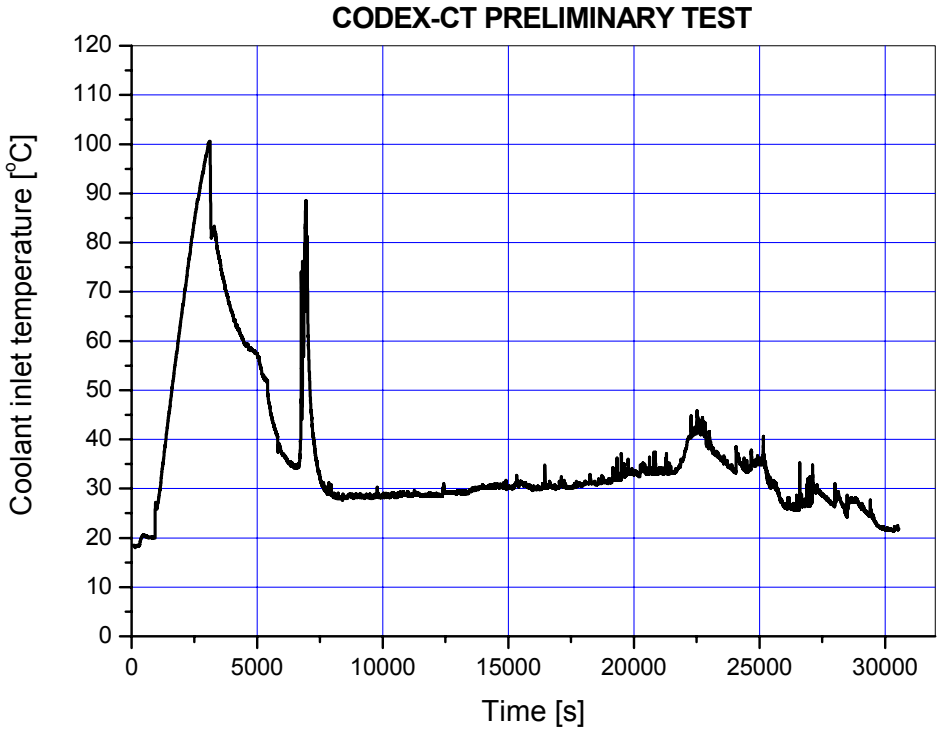

Fig. 22. TCOUT(pretest): Coolant outlet temperature in the outlet junction

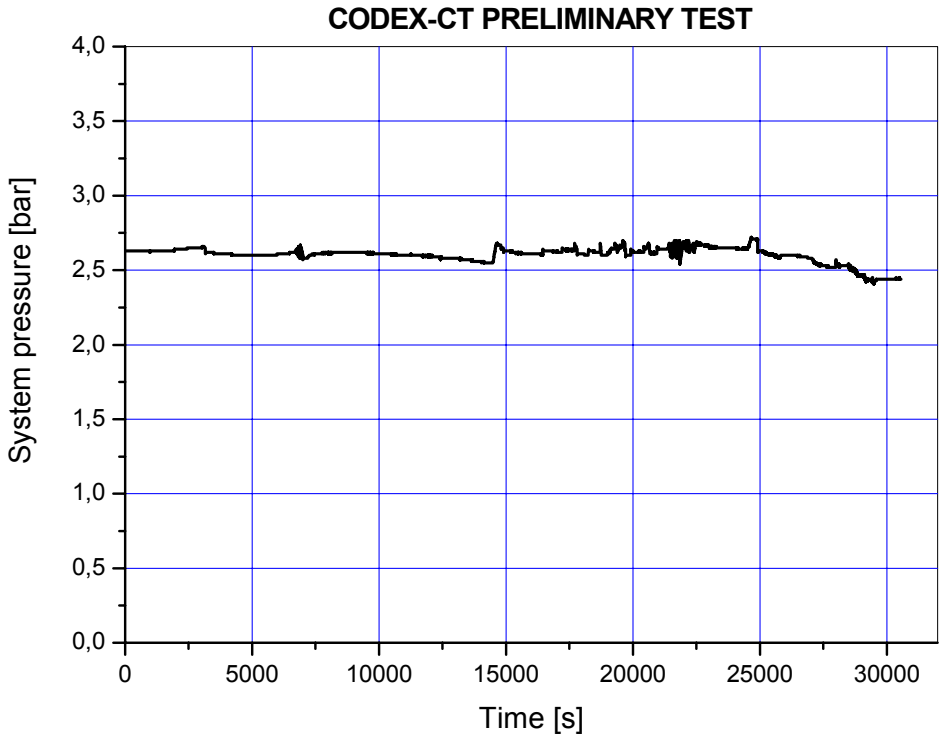

Fig. 23. PSYS(pretest): System pressure

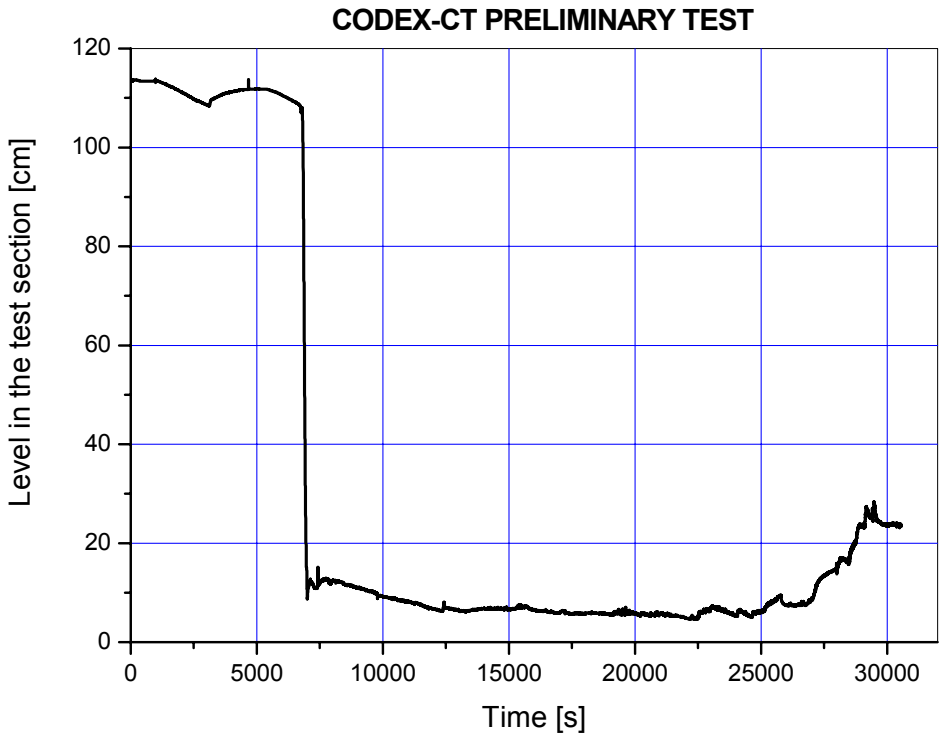

Fig. 24. LTS(pretest): Water level in the test section

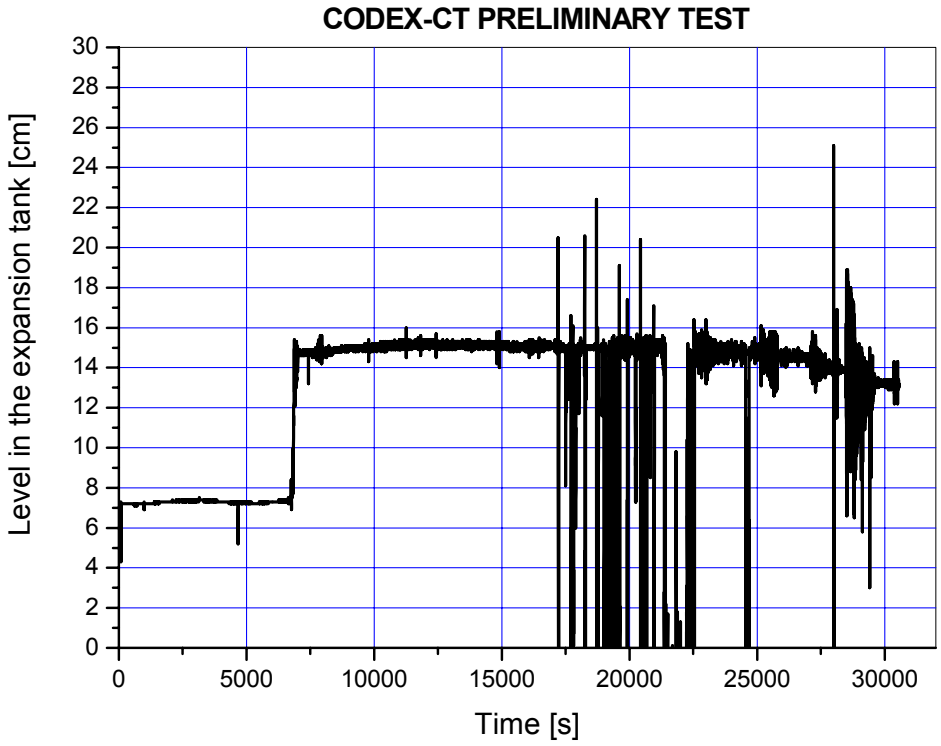

Fig. 25. LXT(pretest): Water level in the expansion tank

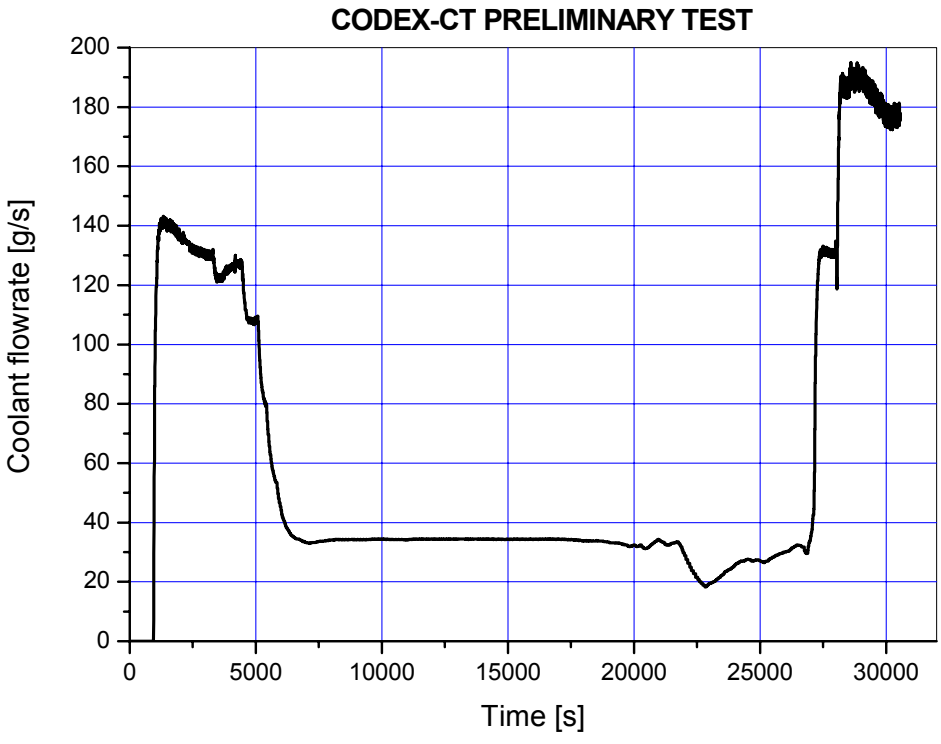

Fig. 26. FLOW(pretest): Coolant flowrate

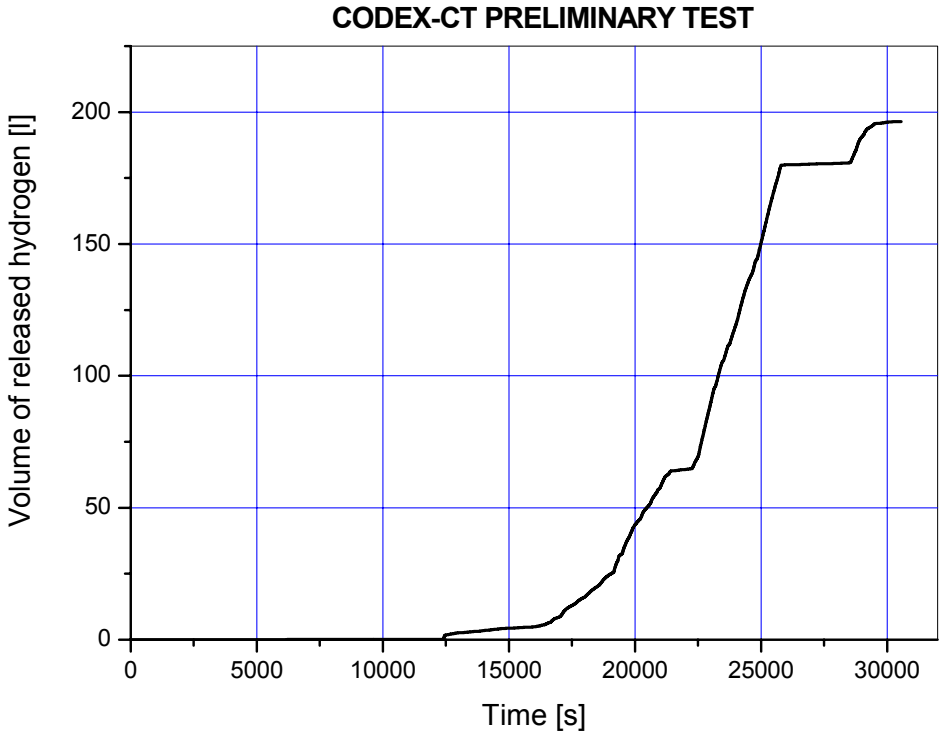

Fig. 27. H2(pretest): Volume of released hydrogen from the cleaning tank model

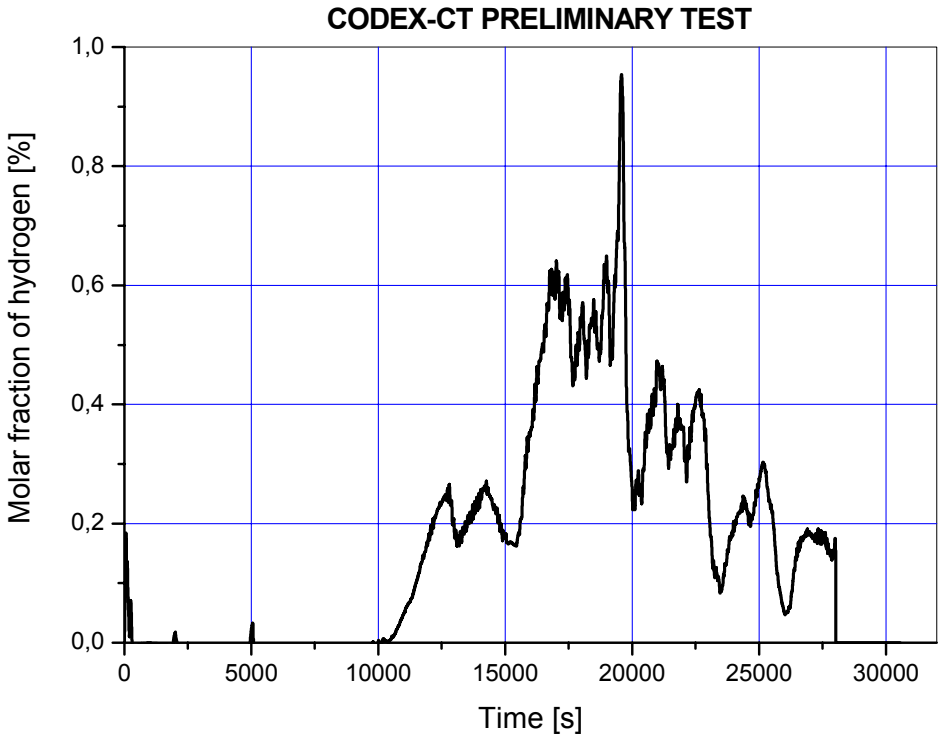

Fig. 28. TCD(pretest): Hydrogen concentration

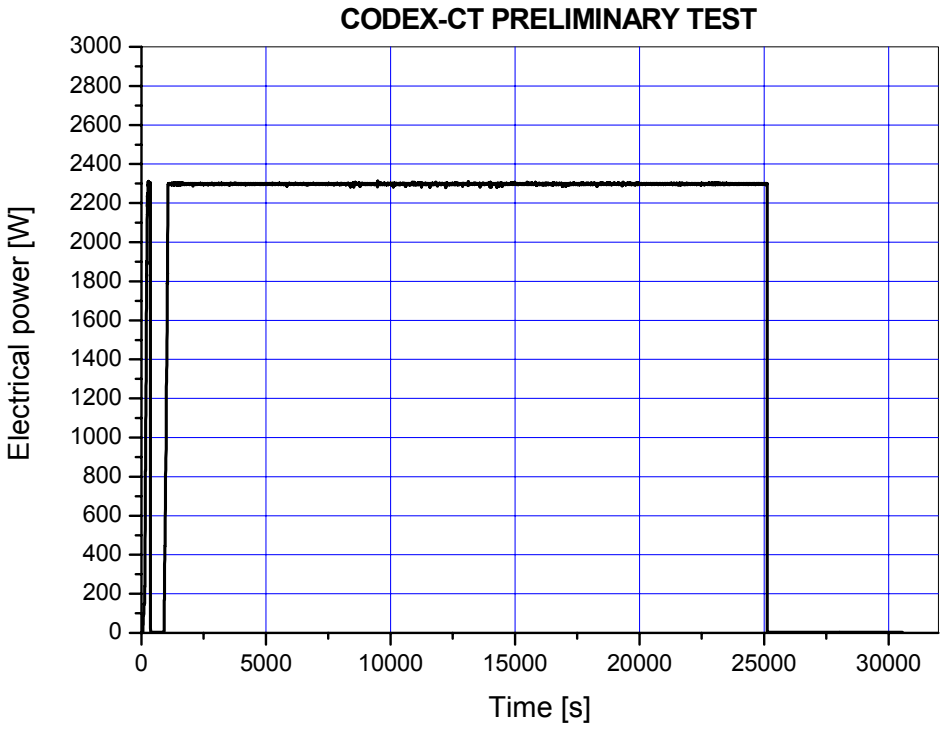

Fig. 29. POWER(pretest): Electrical power

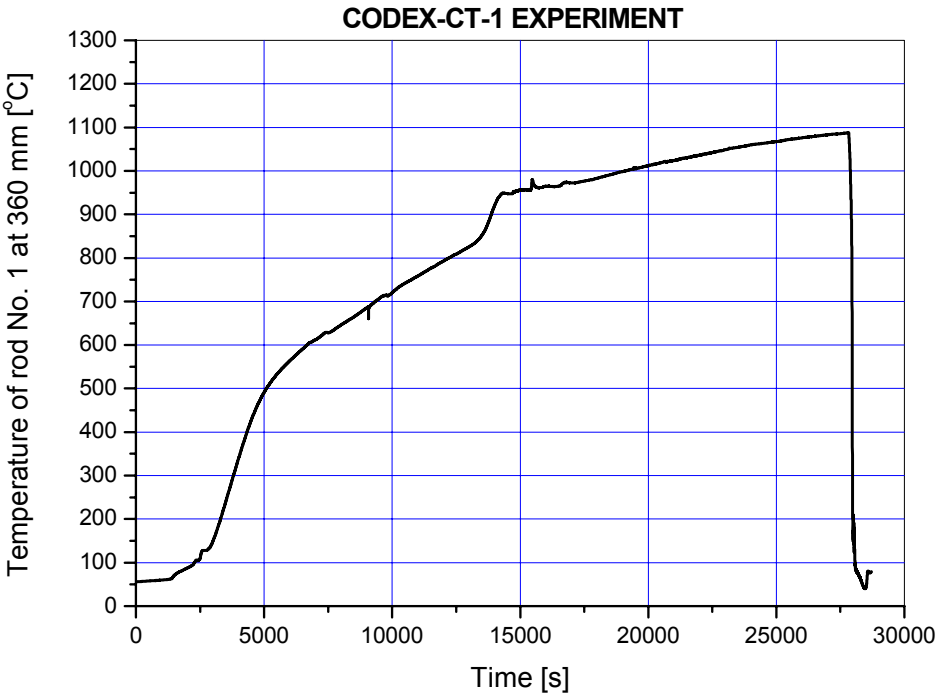

Fig. 30. TFR136: Temperature of fuel rod No. 1 at 360 mm elevation

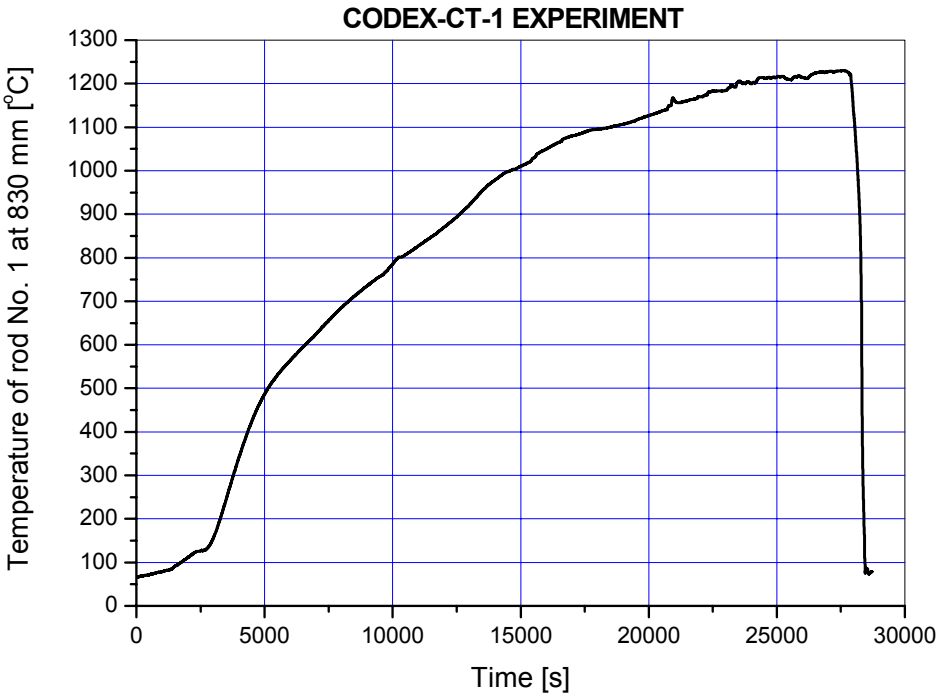

Fig. 31. TFR183: Temperature of fuel rod No. 1 at 830 mm elevation

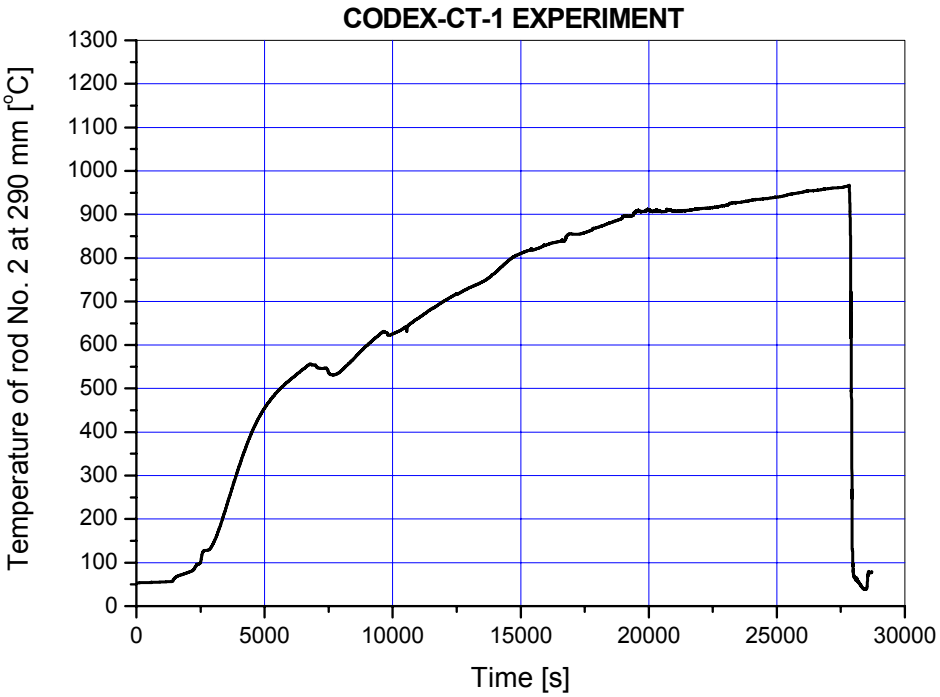

Fig. 32. TFR229: Temperature of fuel rod No. 2 at 290 mm elevation

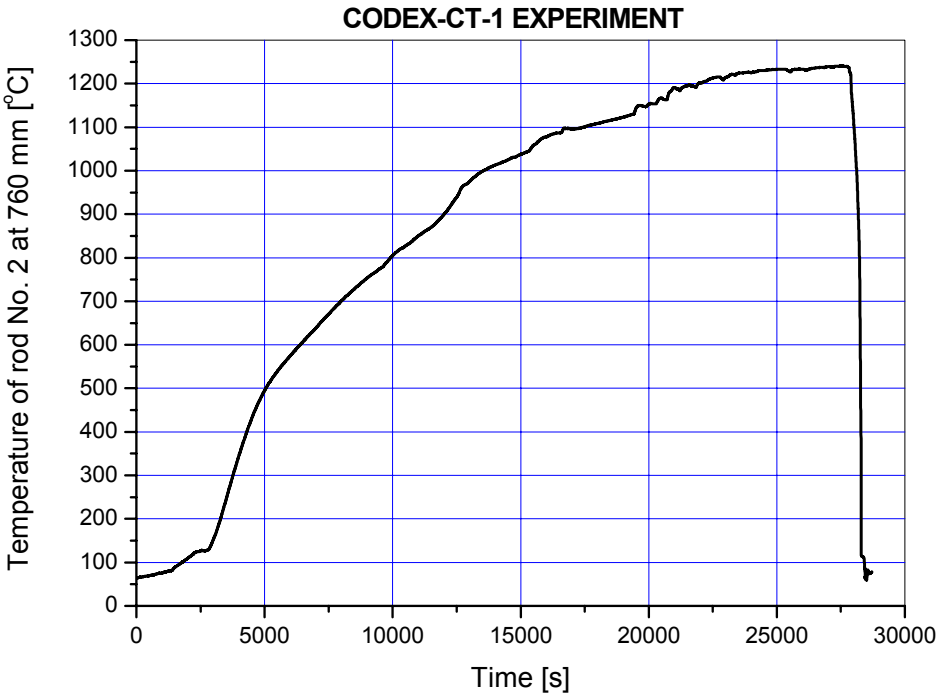

Fig. 33. TFR276: Temperature of fuel rod No. 2 at 760 mm elevation

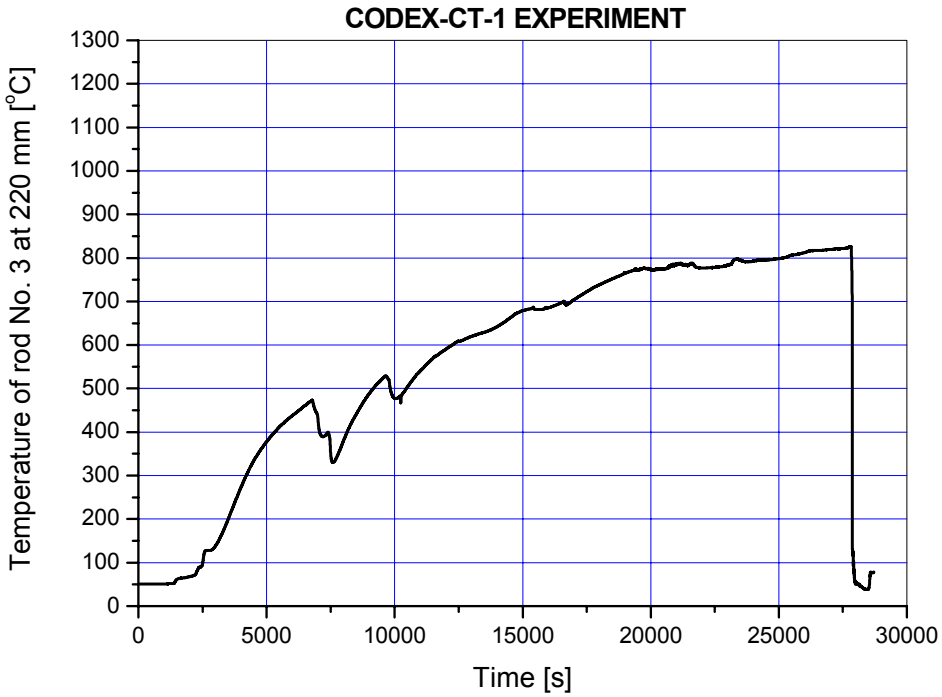

Fig. 34. TFR322: Temperature of fuel rod No. 3 at 220 mm elevation

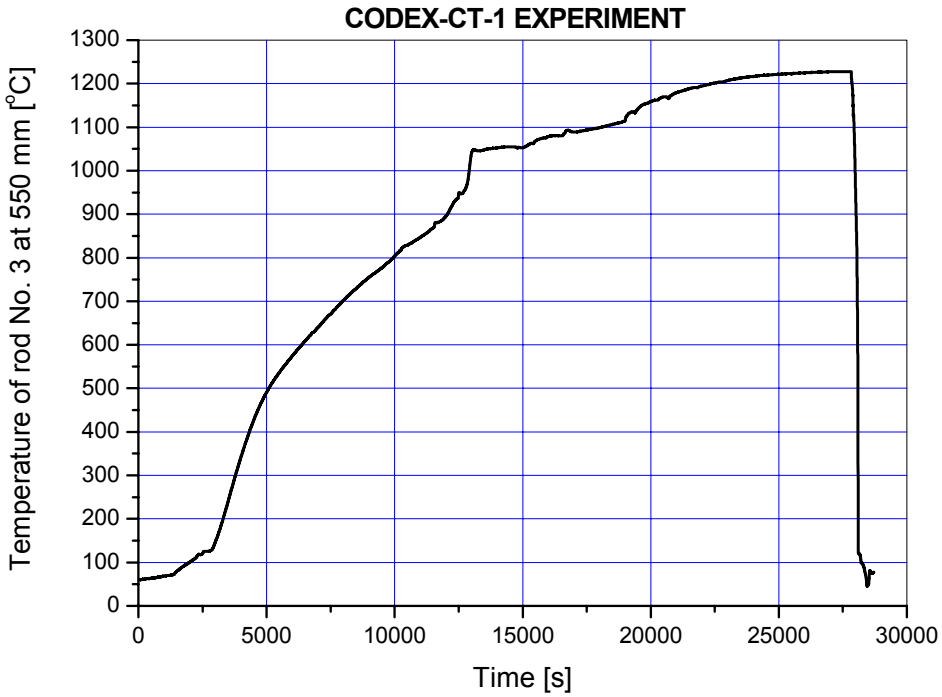

Fig. 35. TFR355: Temperature of fuel rod No. 3 at 550 mm elevation

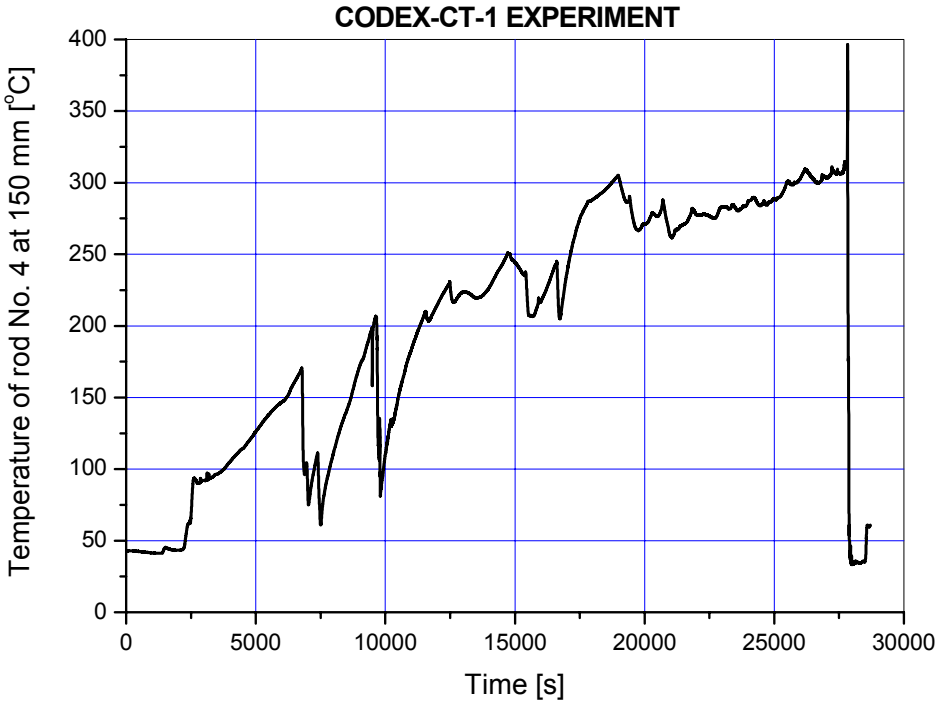

Fig. 36. TFR415: Temperature of fuel rod No. 4 at 150 mm elevation

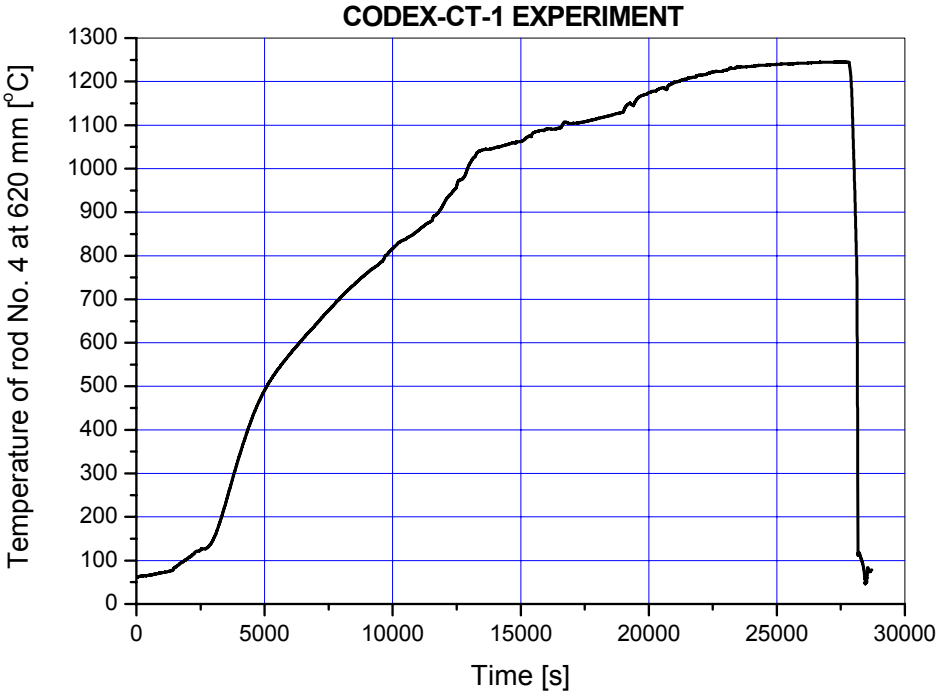

Fig. 37. TFR462: Temperature of fuel rod No. 4 at 620 mm elevation

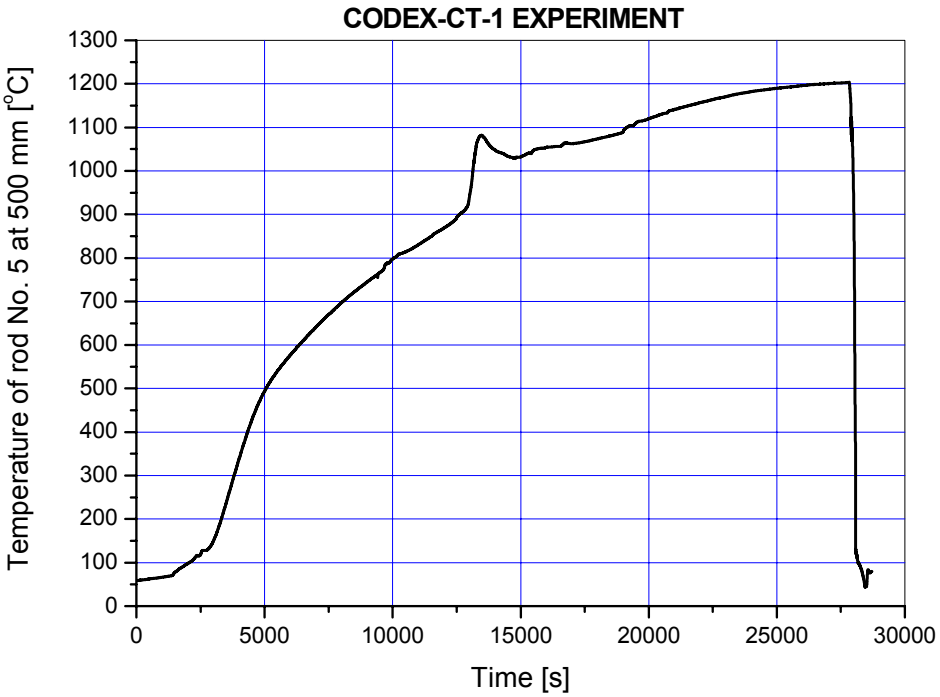

Fig. 38. TFR550: Temperature of fuel rod No. 5 at 500 mm elevation

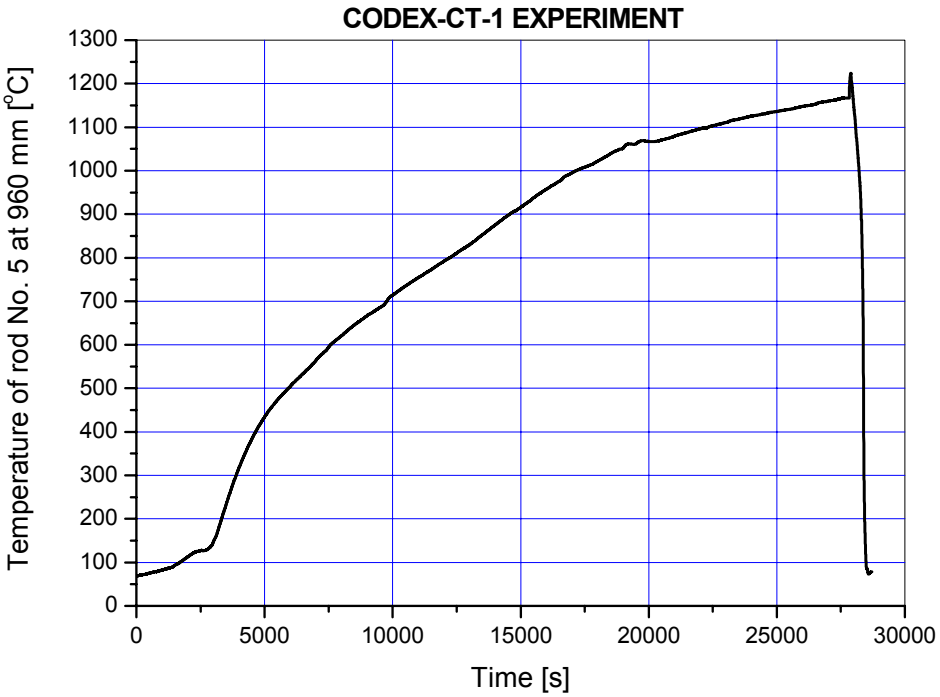

Fig. 39. TFR596: Temperature of fuel rod No. 5 at 960 mm elevation

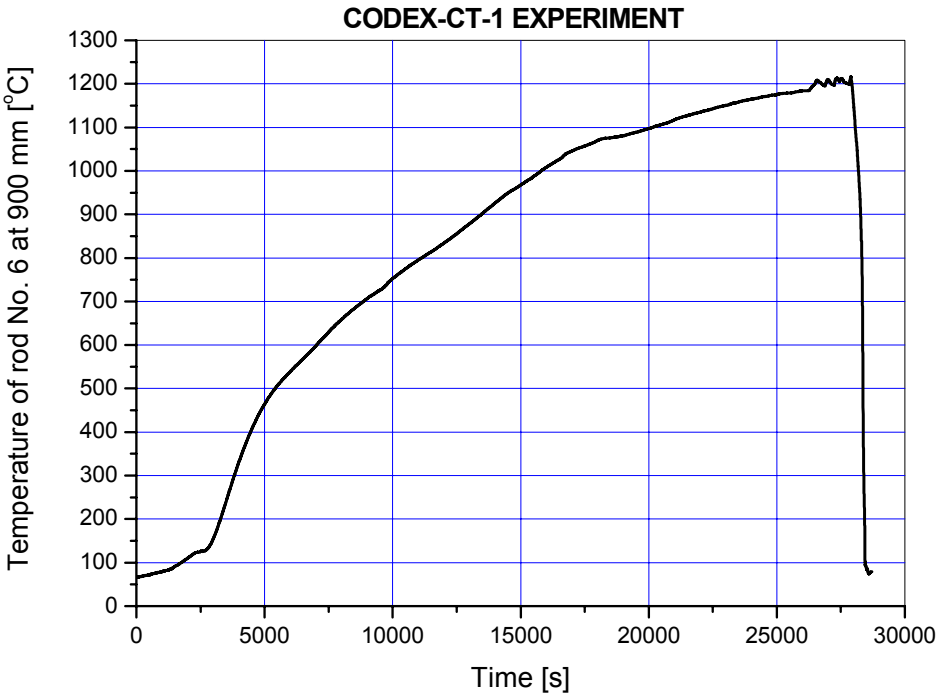

Fig. 40. TFR690: Temperature of fuel rod No. 6 at 900 mm elevation

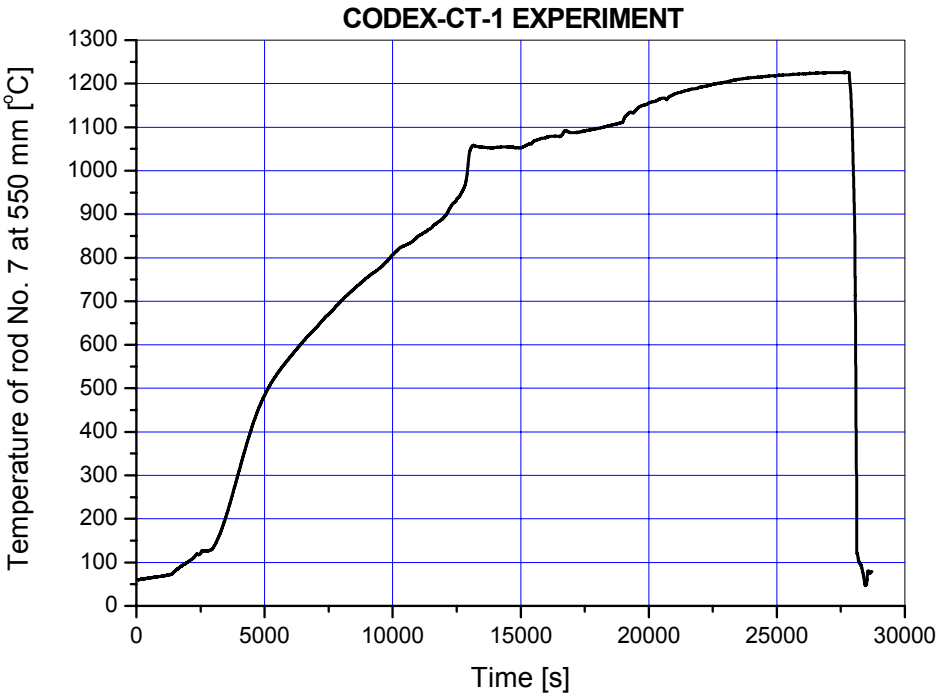

Fig. 41. TFR755: Temperature of fuel rod No. 7 at 550 mm elevation

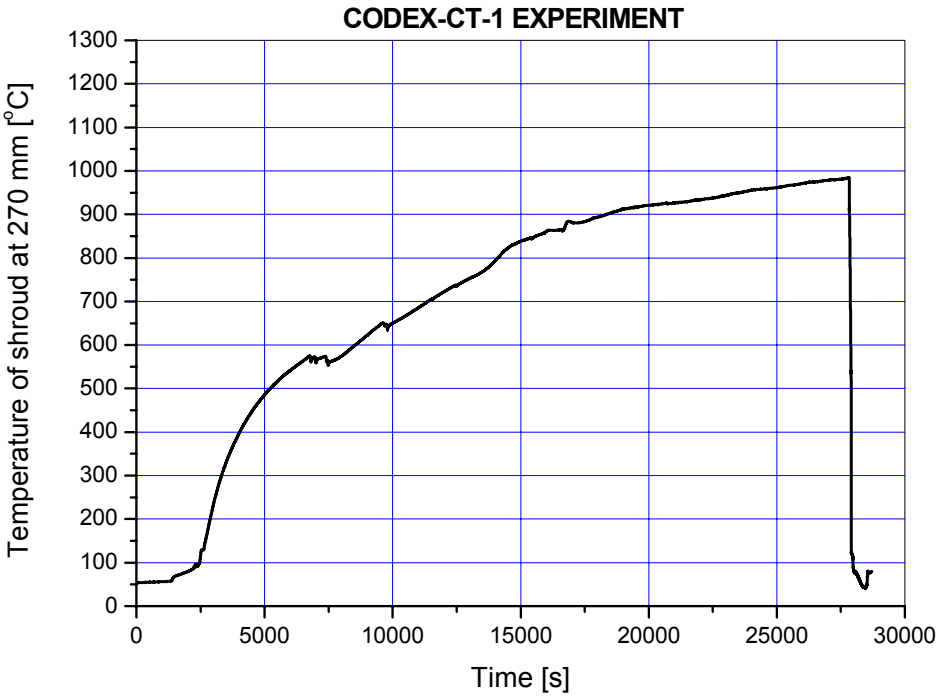

Fig. 42. TSH27: Temperature of shroud at 270 mm elevation

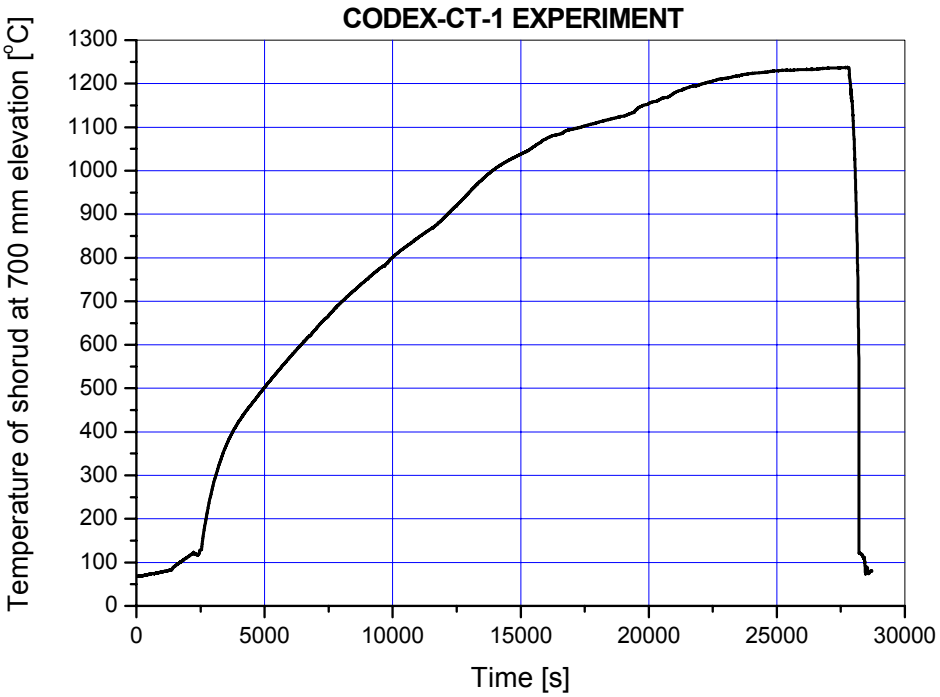

Fig. 43. TSH70: Temperature of shroud at 700 mm elevation

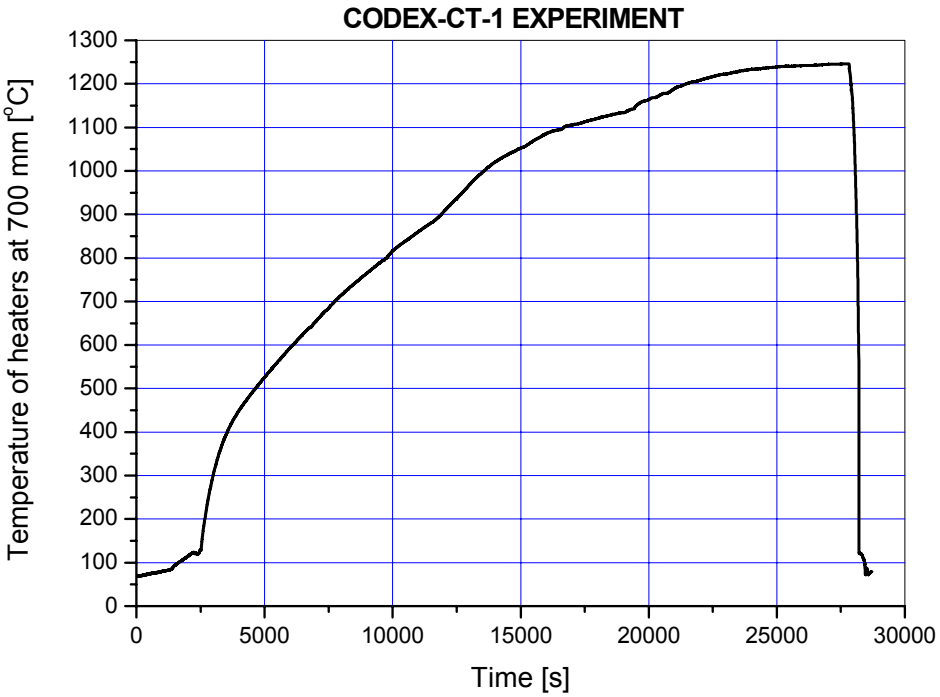

Fig. 44. THR70: Temperature of heaters at 700 mm elevation

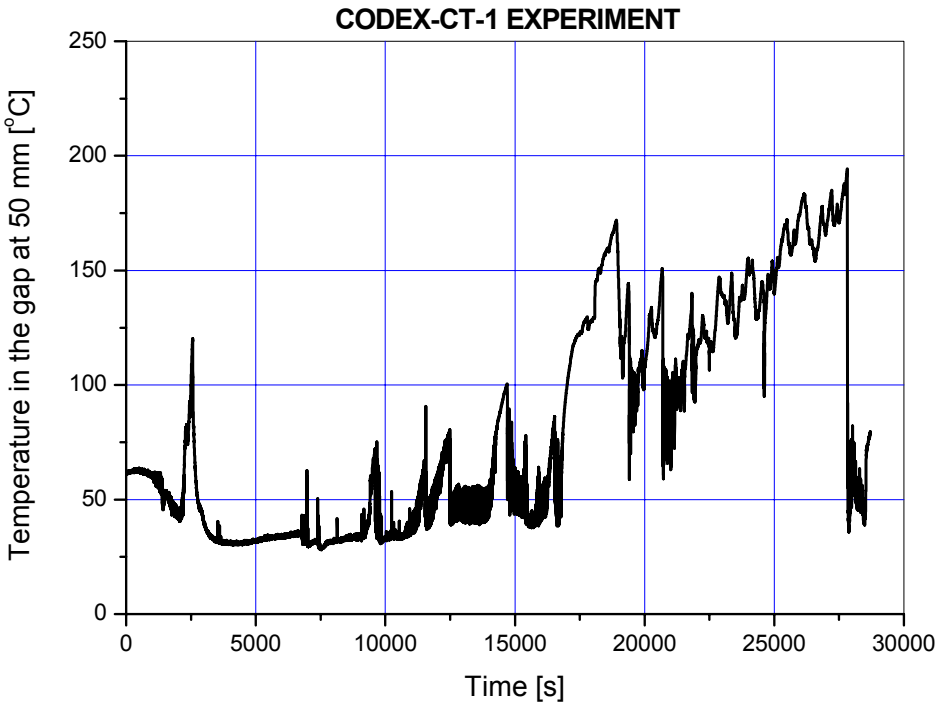

Fig. 45. TG5: Temperature in the gap at 50 mm elevation

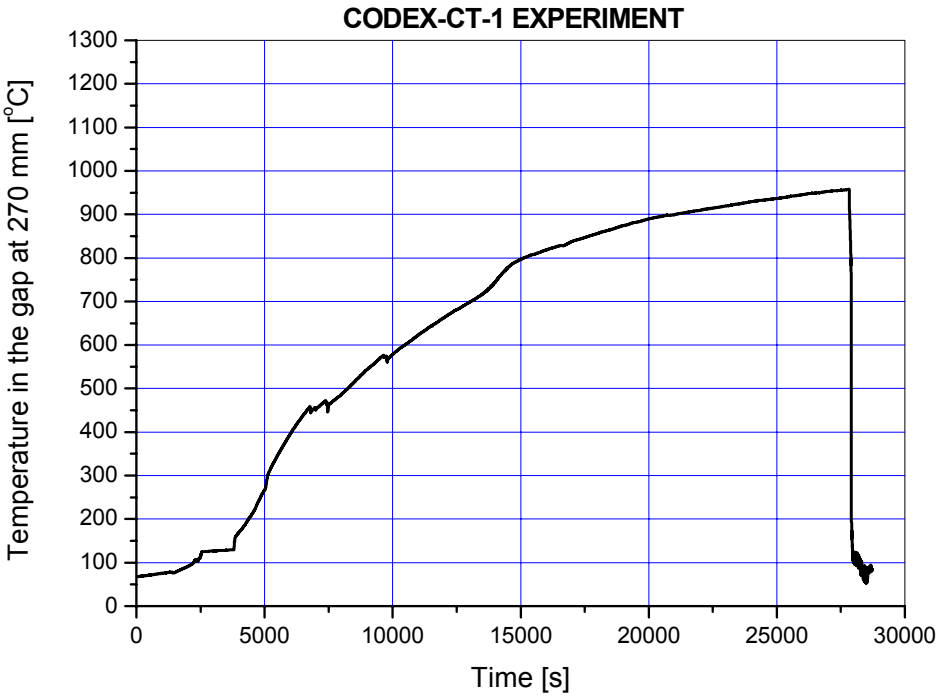

Fig. 46. TG27: Temperature in the gap at 270 mm elevation

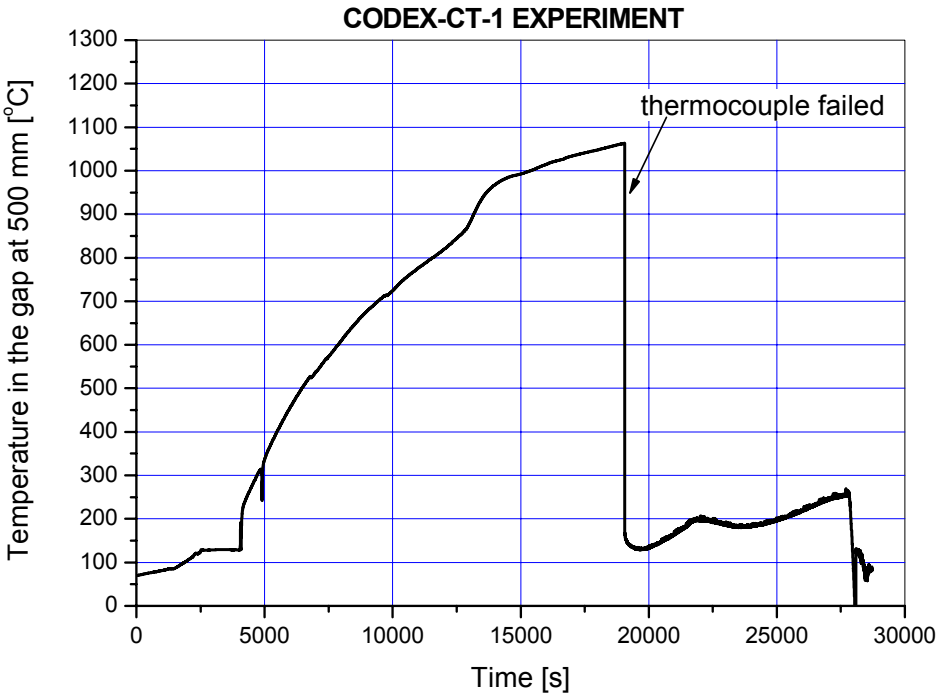

Fig. 47. TG50: Temperature in the gap at 500 mm elevation

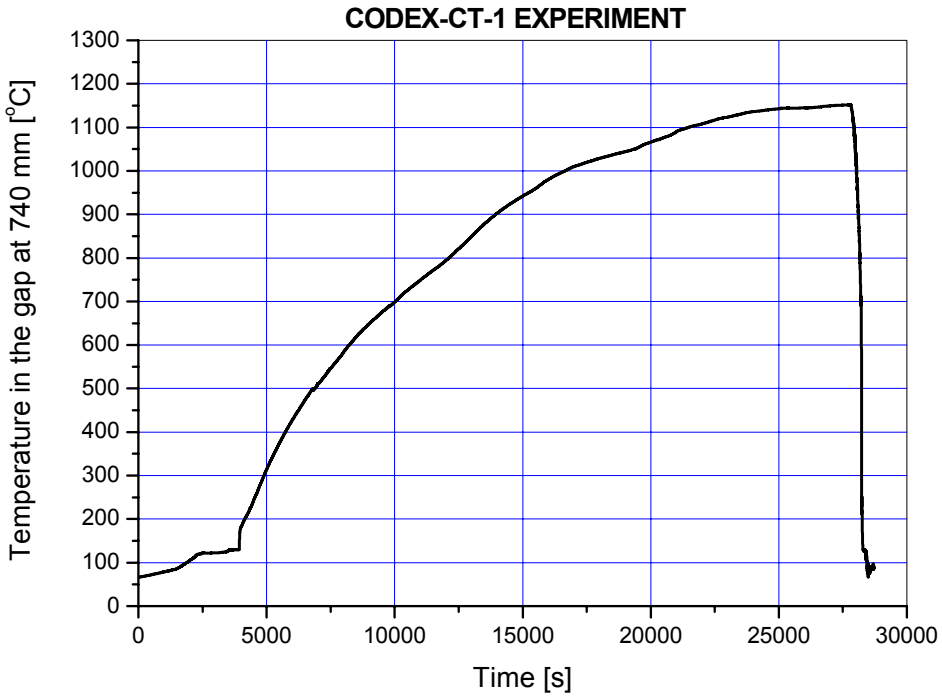

Fig. 48. TG74: Temperature in the gap at 740 mm elevation

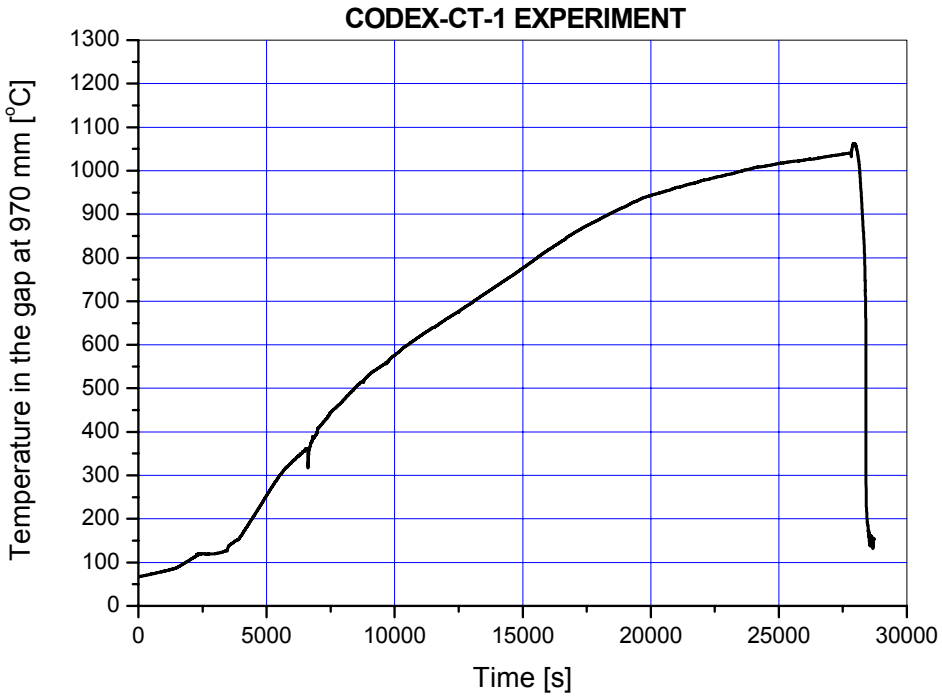

Fig. 49. TG97: Temperature in the gap at 970 mm elevation

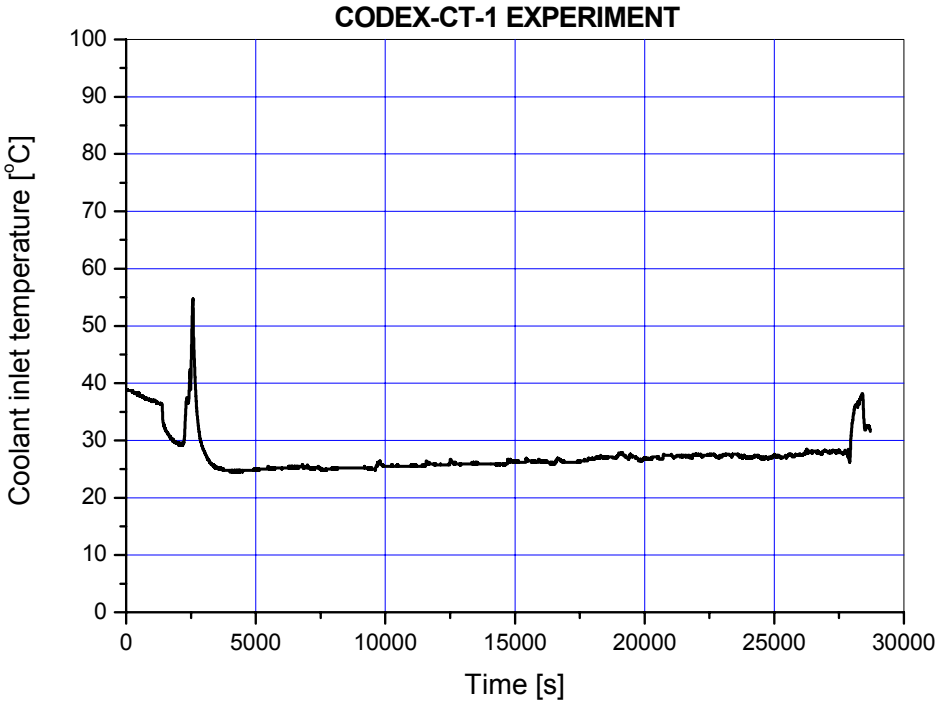

Fig. 50. TCIN: Coolant inlet temperature

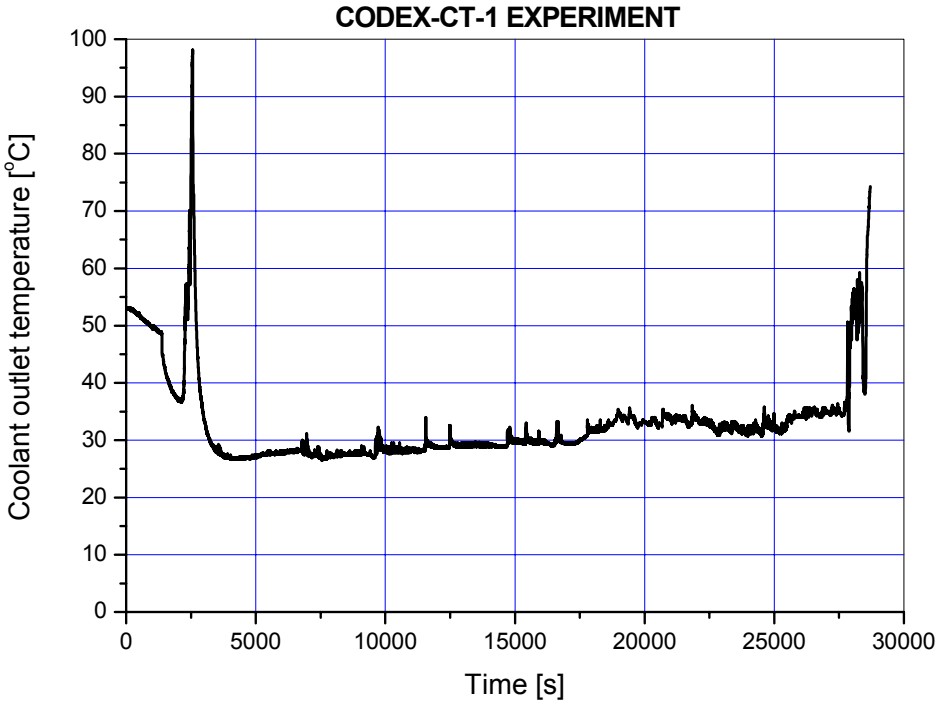

Fig. 51. TCOUT: Coolant outlet temperature

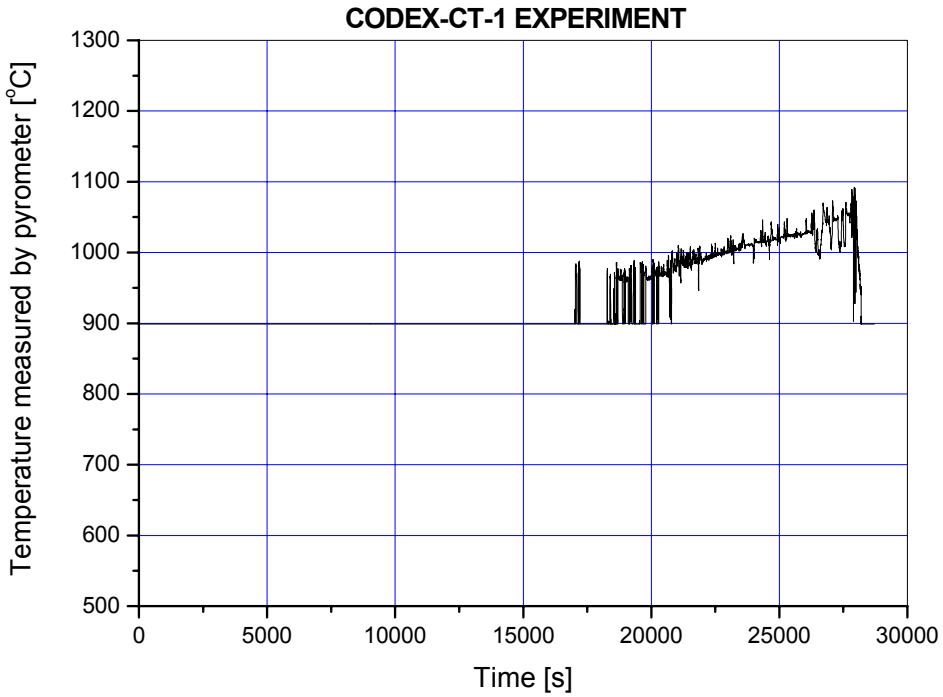

Fig. 52. PYROM: Temperature measured by pyrometer at the top of the bundle

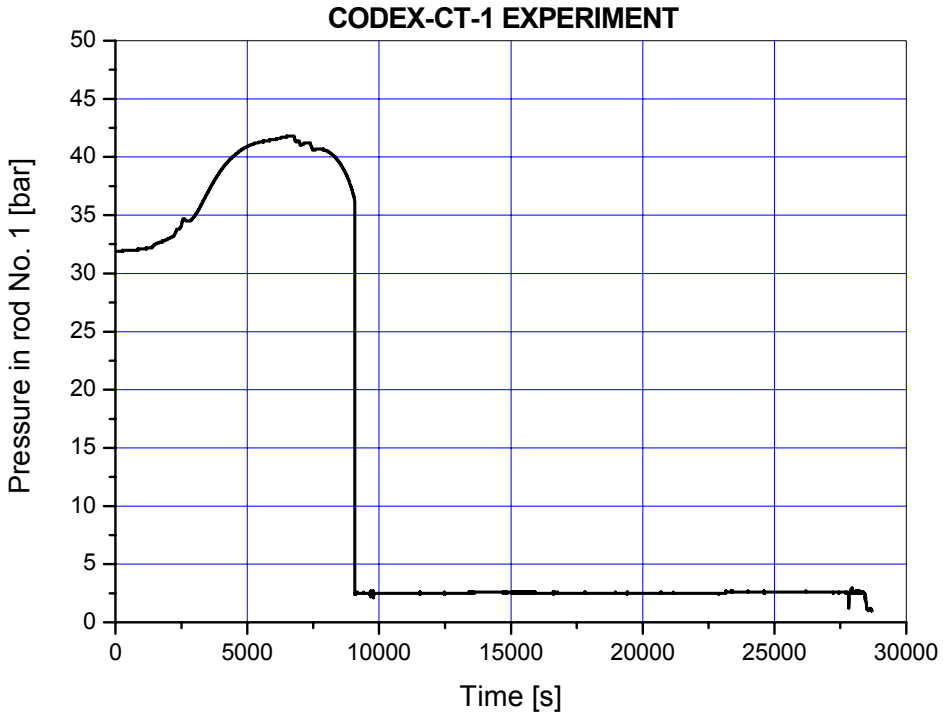

Fig. 53. PFR1: Pressure in fuel rod No. 1

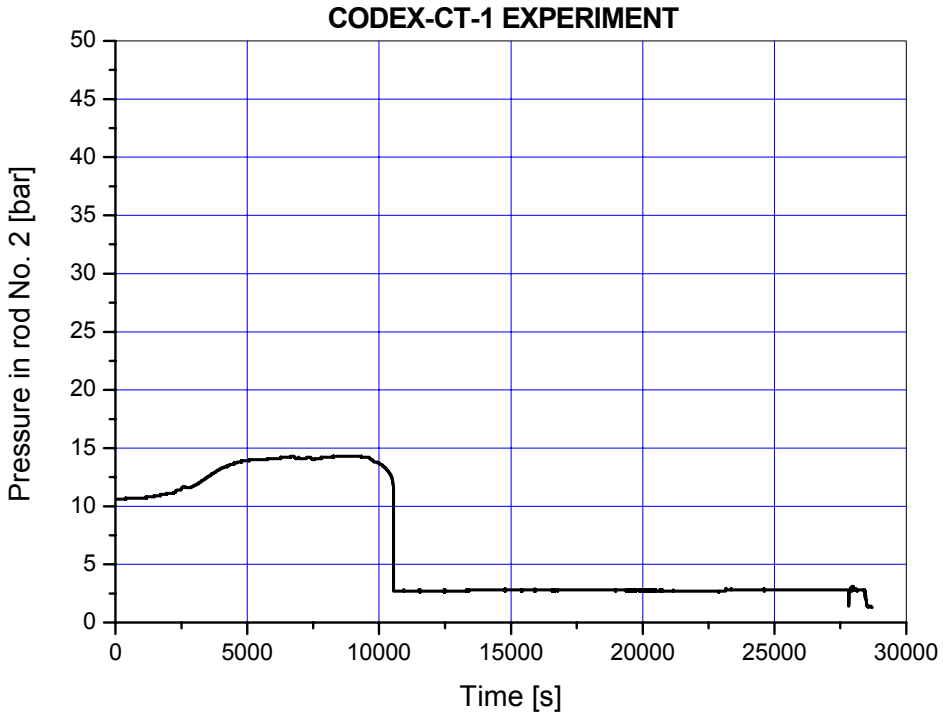

Fig. 54. PFR2: Pressure in fuel rod No. 2

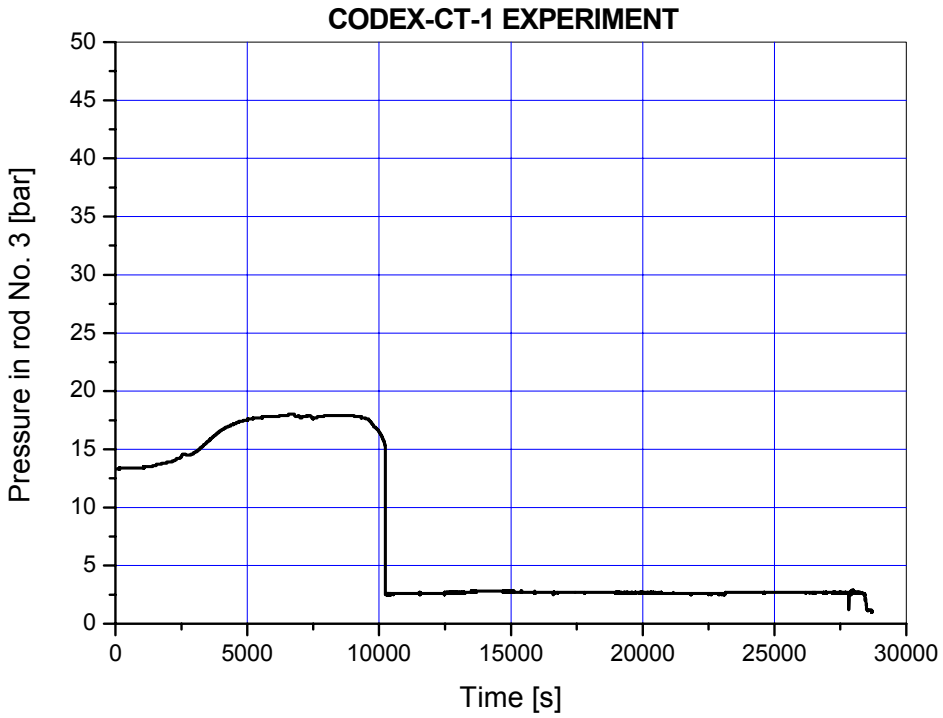

Fig. 55. PFR3: Pressure in fuel rod No. 3

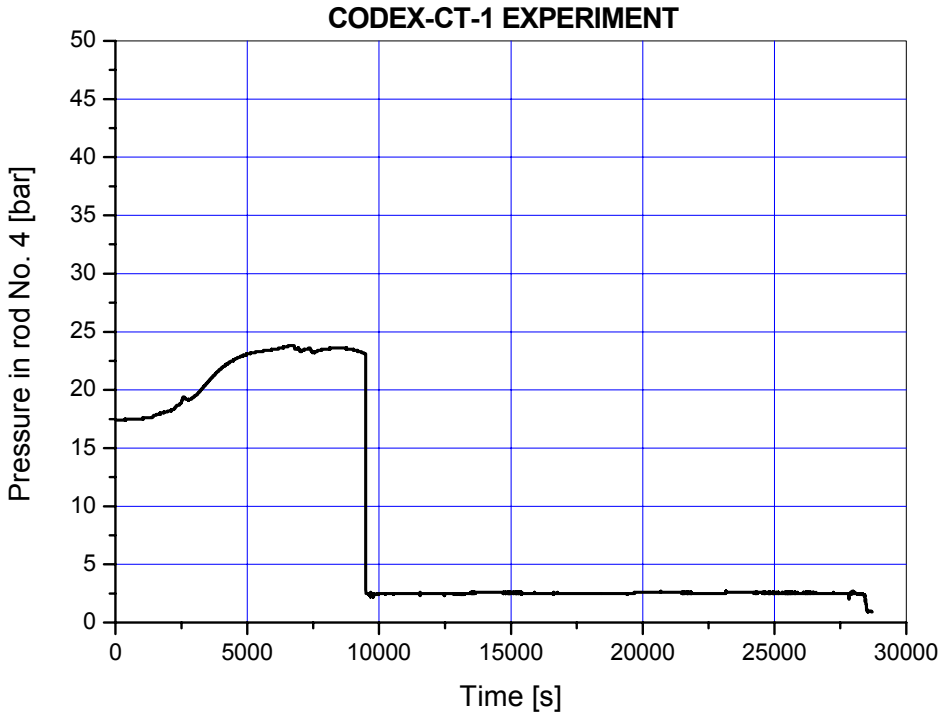

Fig. 56. PFR4: Pressure in fuel rod No. 4

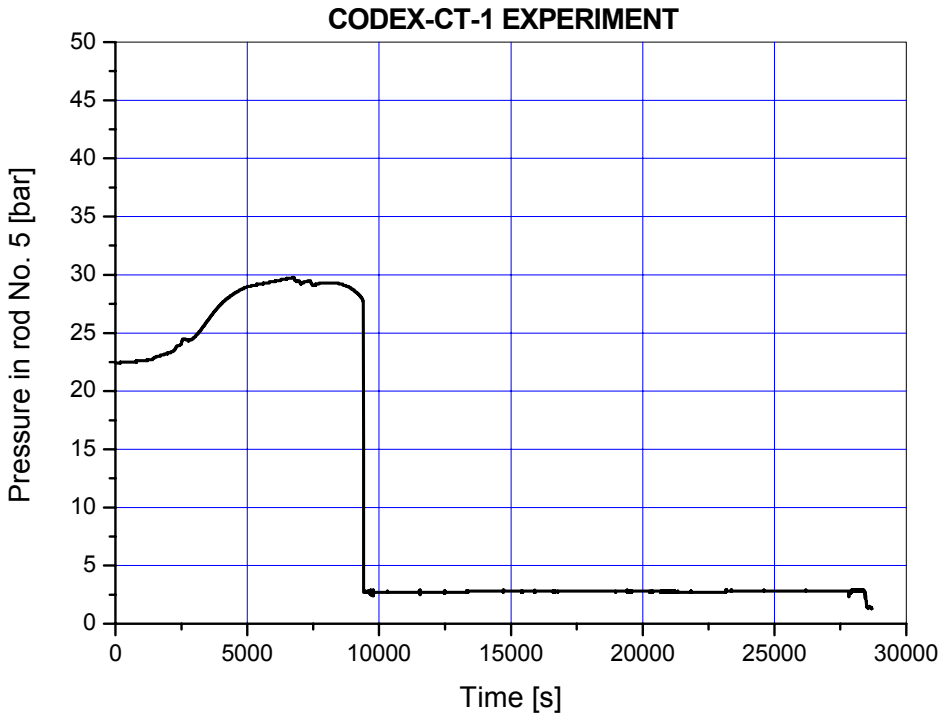

Fig. 57. PFR5: Pressure in fuel rod No. 5

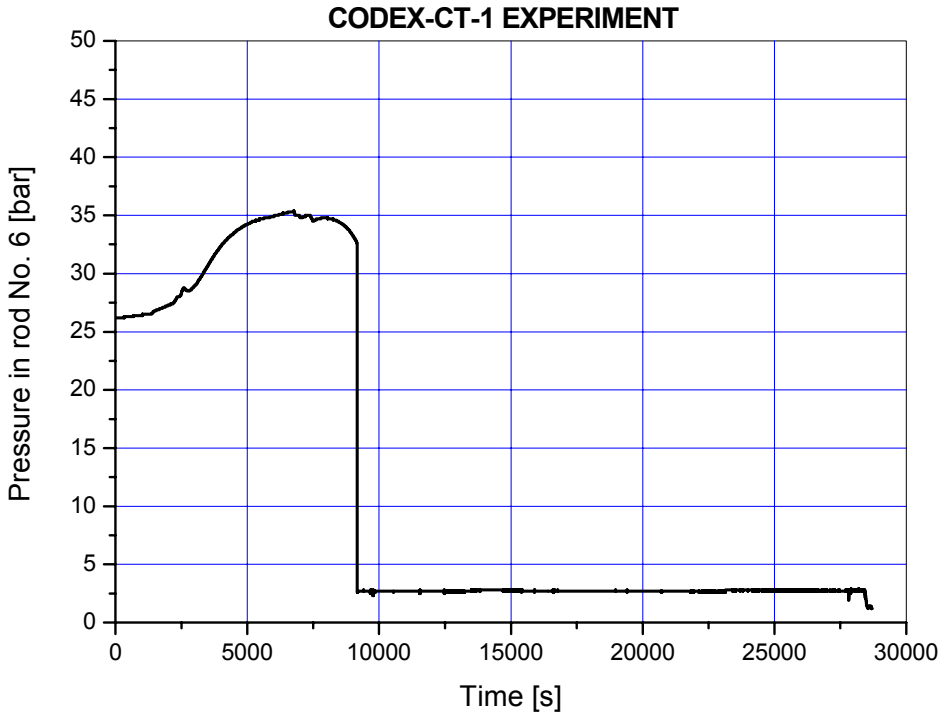

Fig. 58. PFR6: Pressure in fuel rod No. 6

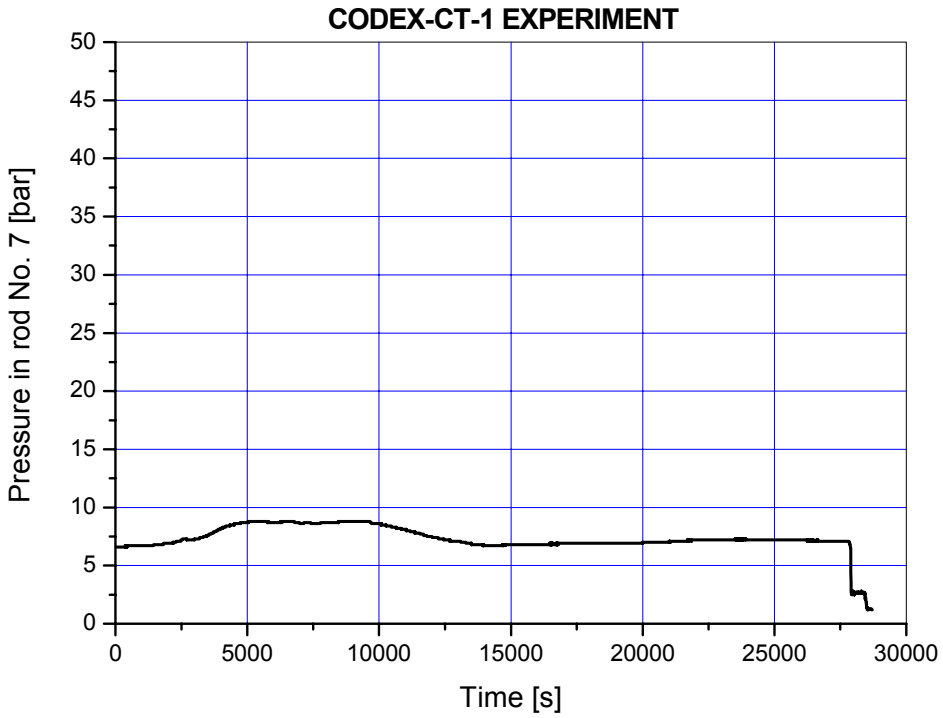

Fig. 59. PFR7: Pressure in fuel rod No. 7

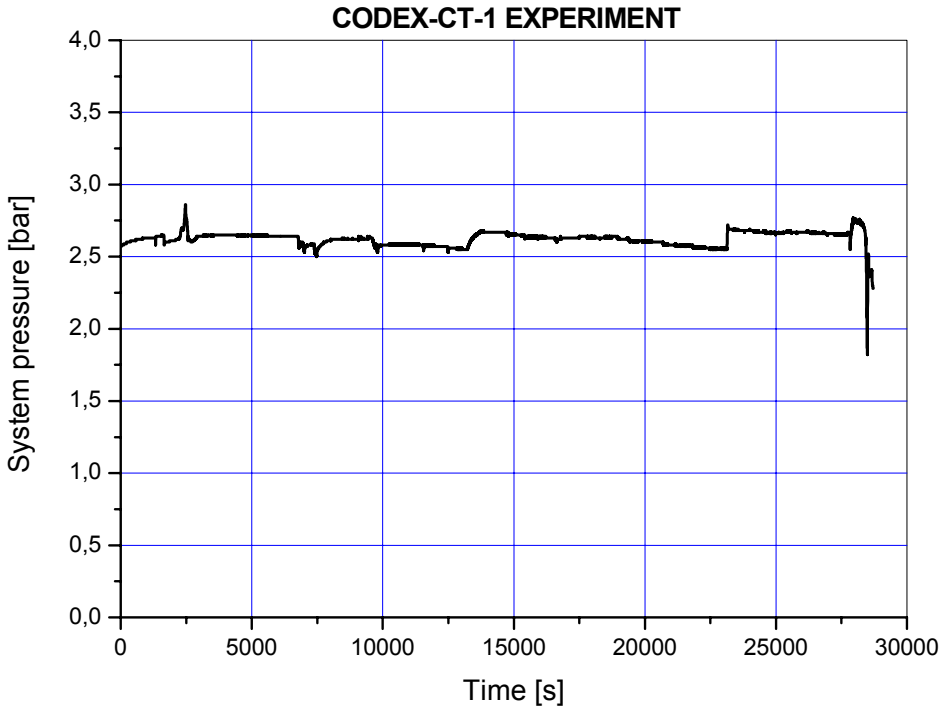

Fig. 60. PSYS: System pressure

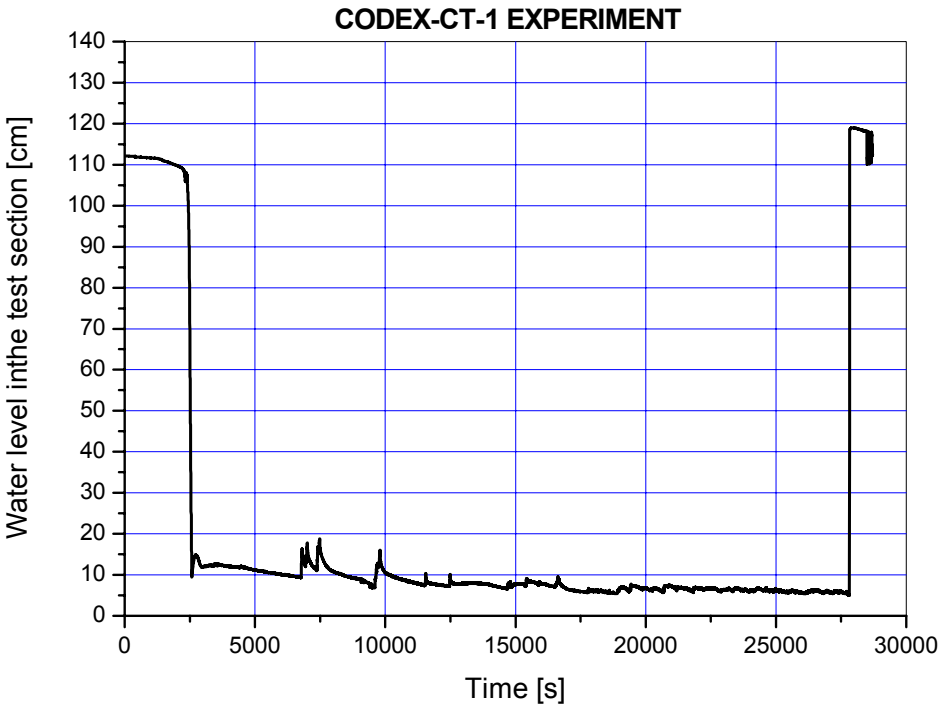

Fig. 61. LTS: Water level in the test section

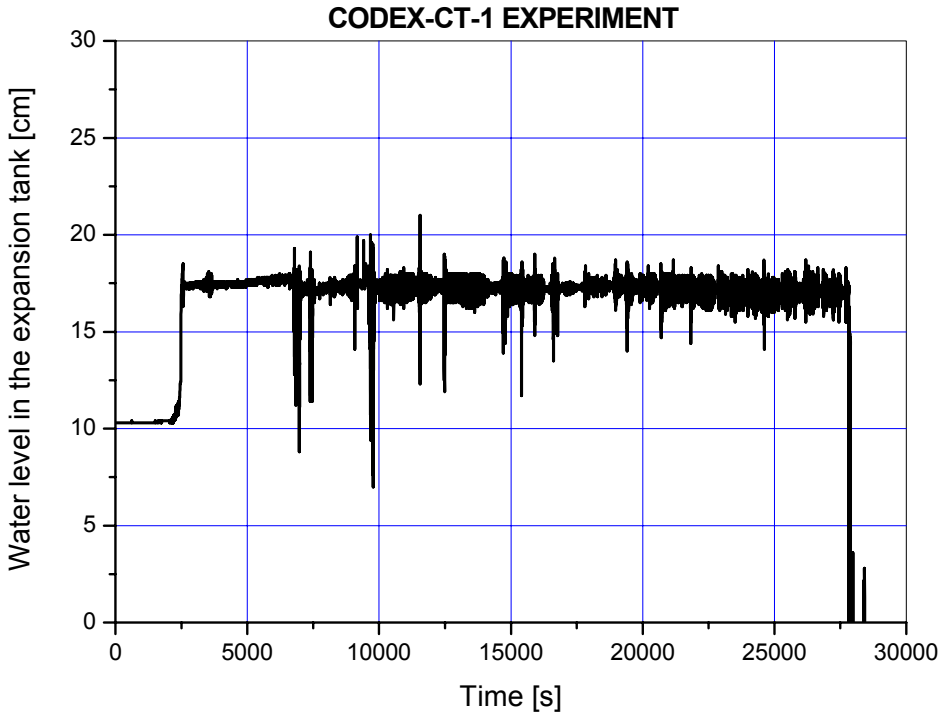

Fig. 62. LXT: Water level in the expansion tank

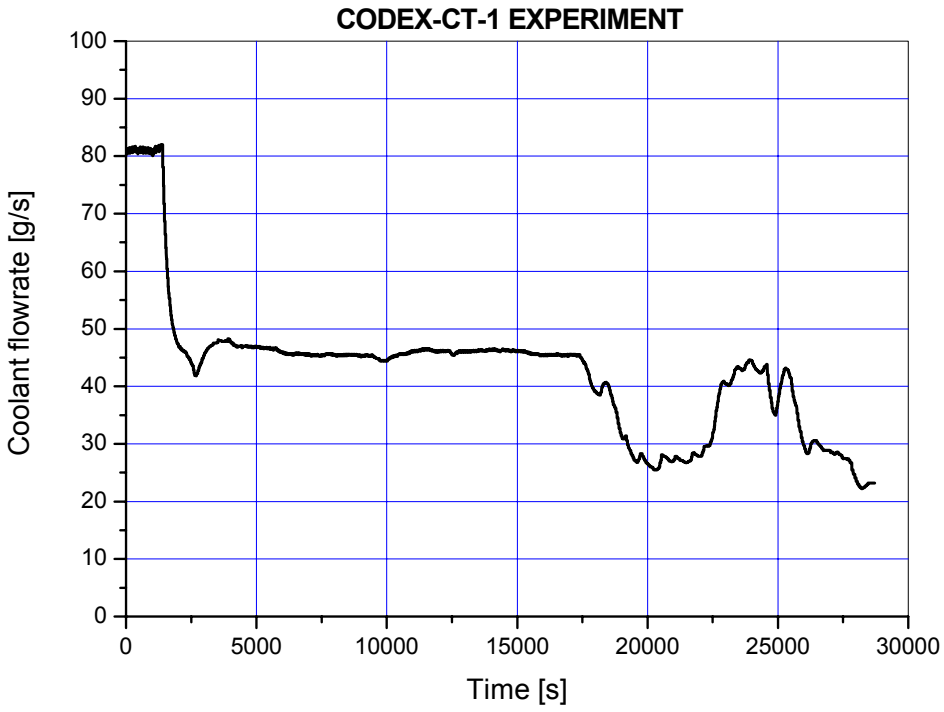

Fig. 63. FLOW: Coolant flowrate

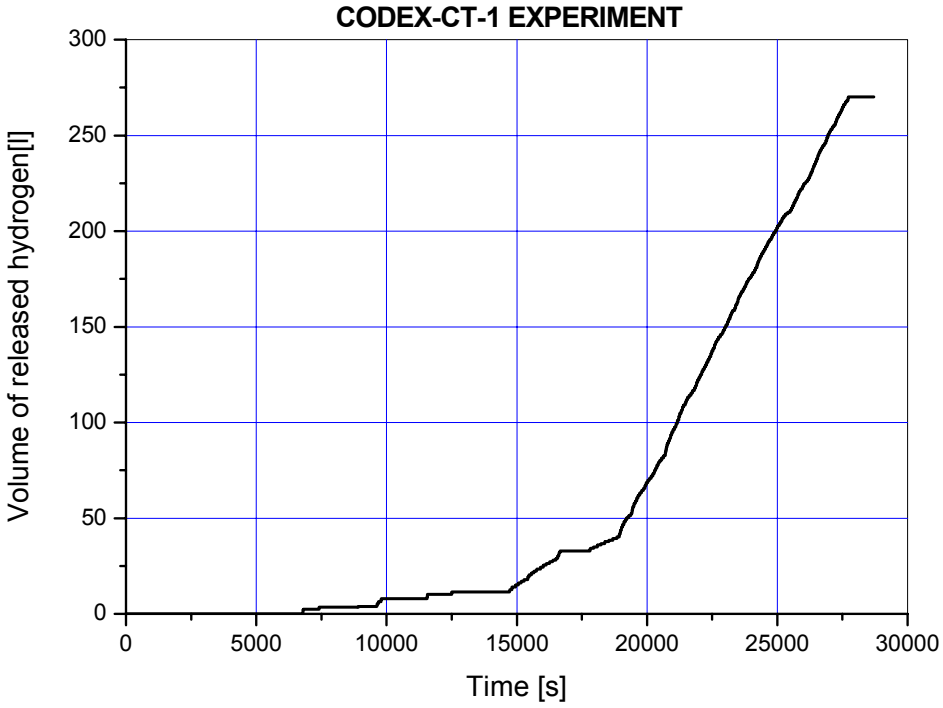

Fig. 64. H2: Volume of hydrogen released from the cleaning tank model

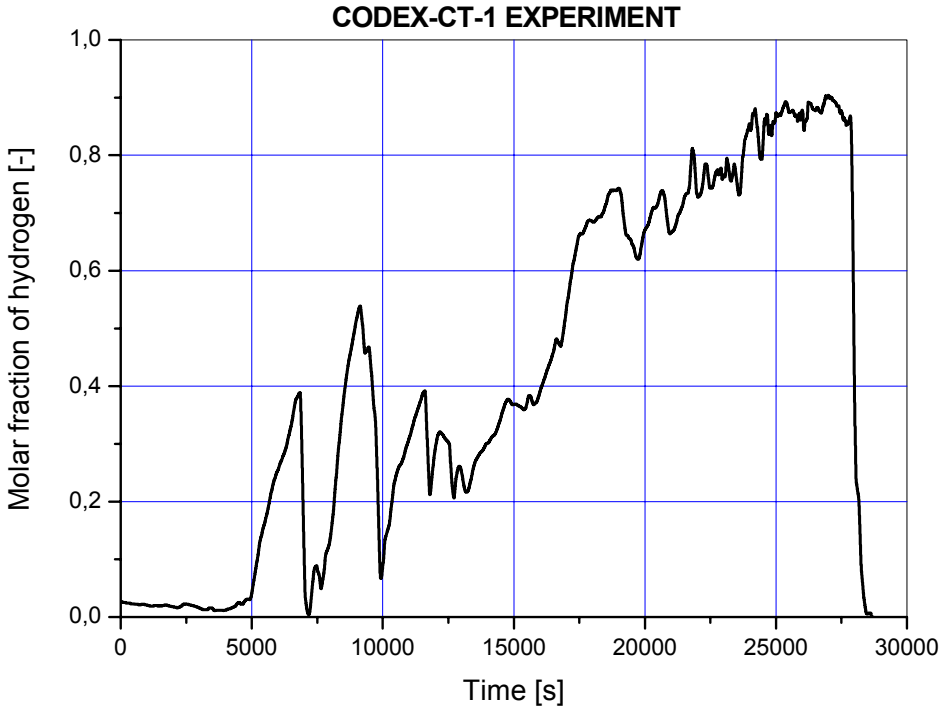

Fig. 65. TCD: Hydrogen concentration in the cleaning tank

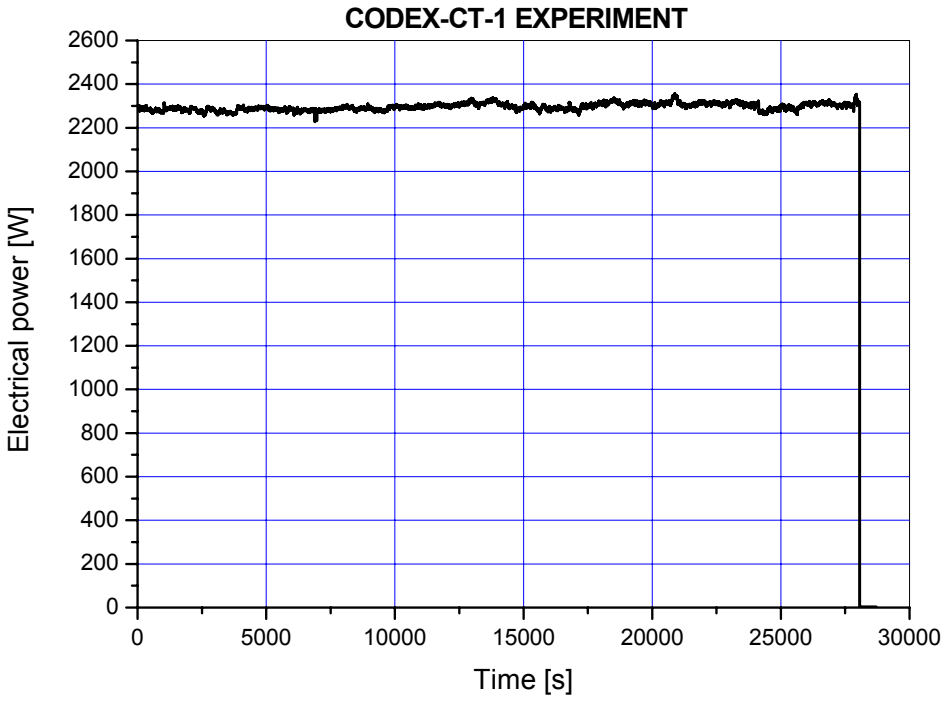

Fig. 66. POWER: Electrical power

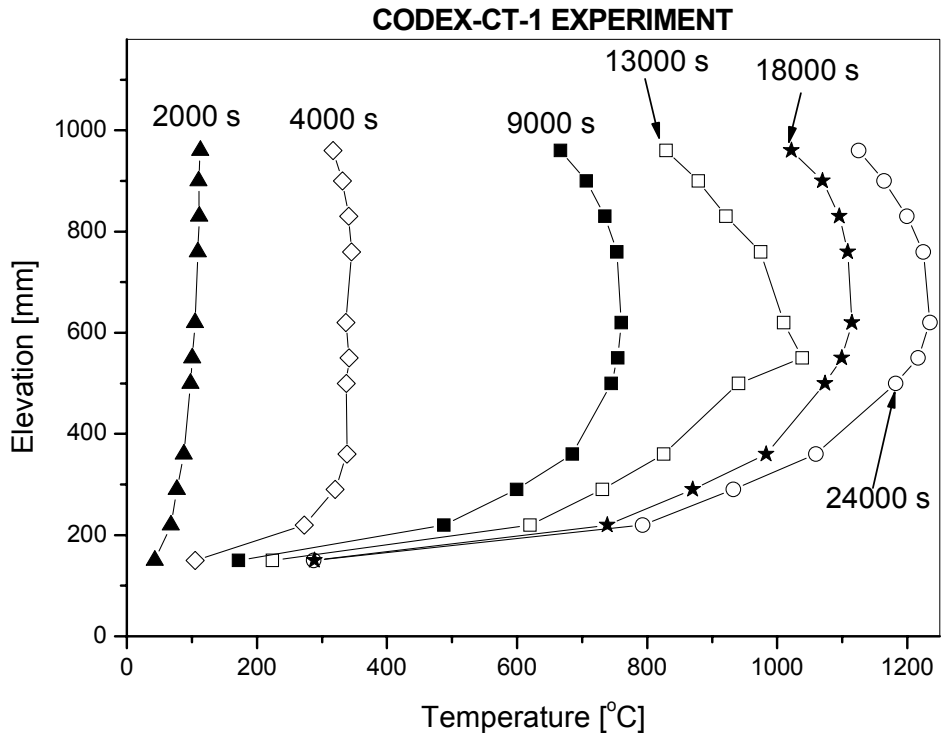

Fig. 67. Temperature profile in the CODEX-CT-1 test

Fig. 68. View of Zr cladding and shroud plates after the CODEX-CT preliminary test

Fig. 69. View of the broken cladding tubes CODEX-CT preliminary test

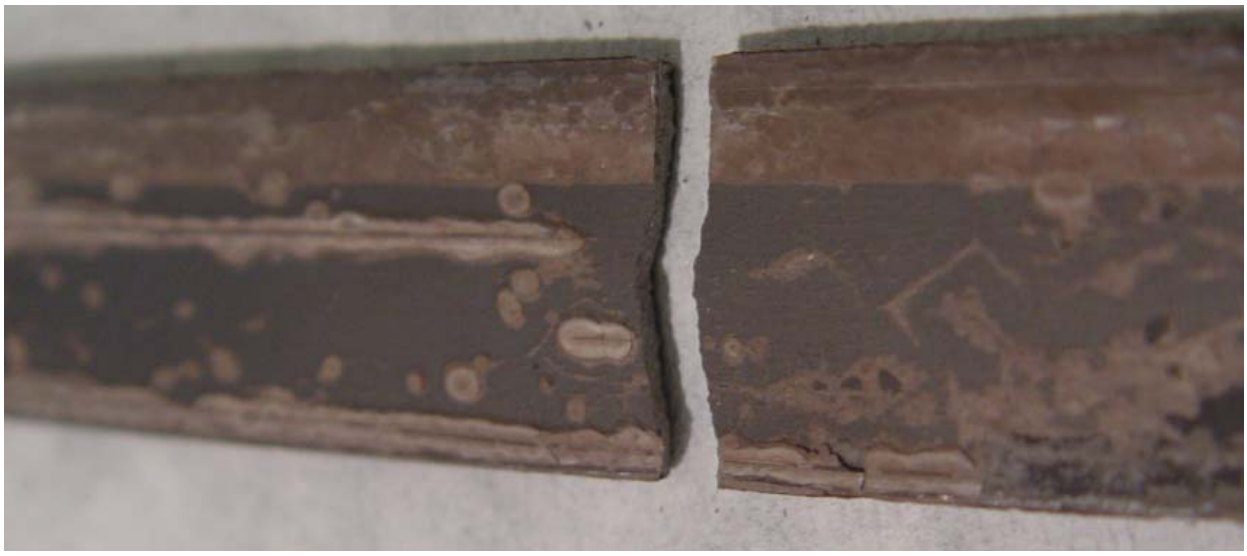

Fig. 70. View of the broken shroud plate CODEX-CT preliminary test

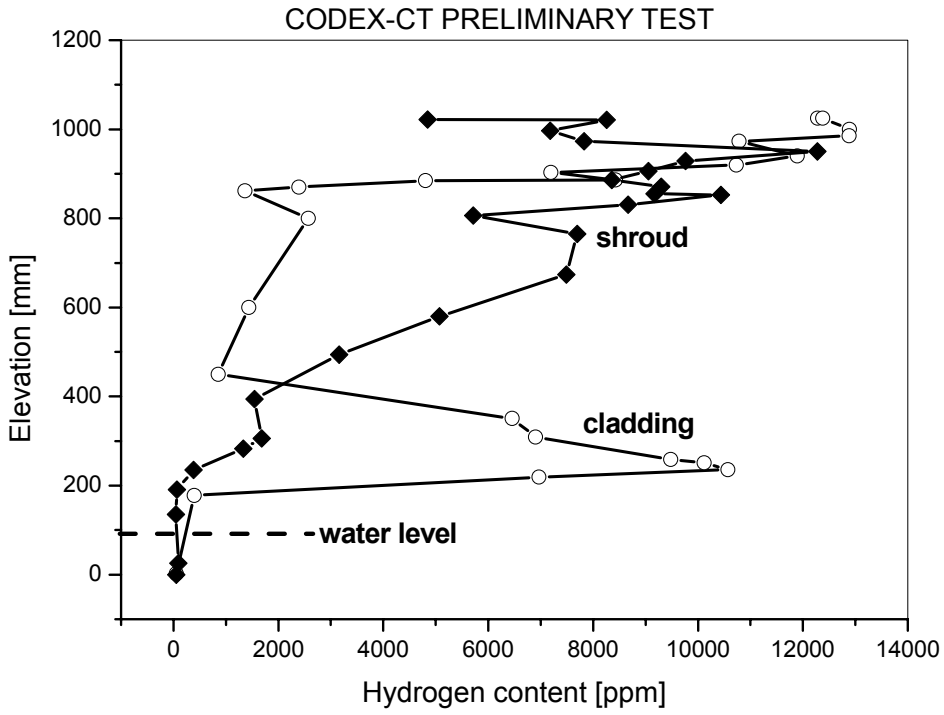

Fig. 71. Hydrogen content in the cladding tubes and shroud plates of the preliminary test

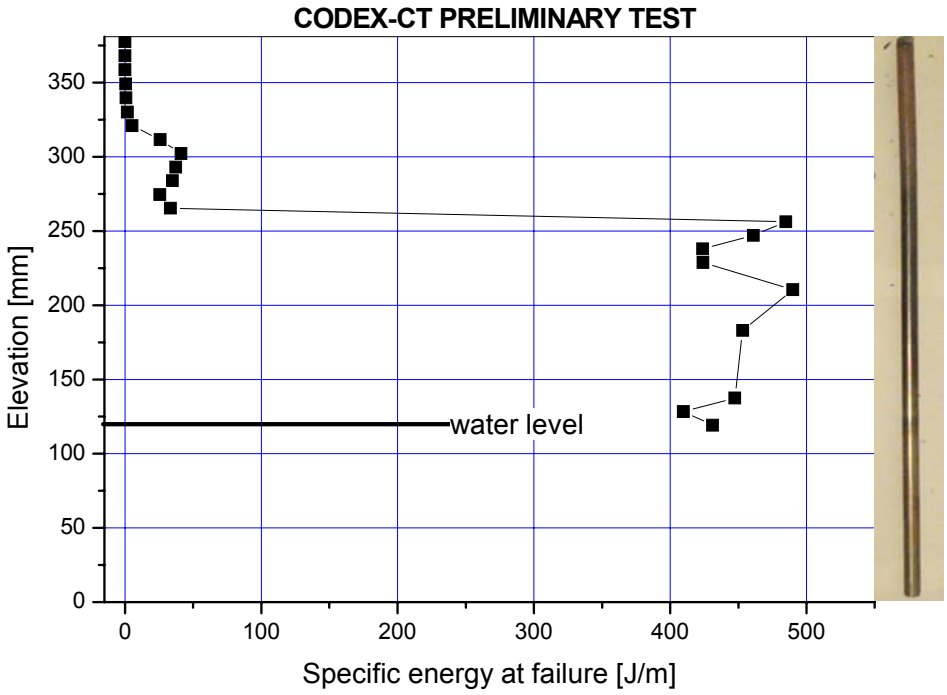

Fig. 72. Specific energy at failure for rod No. 2 of preliminary test

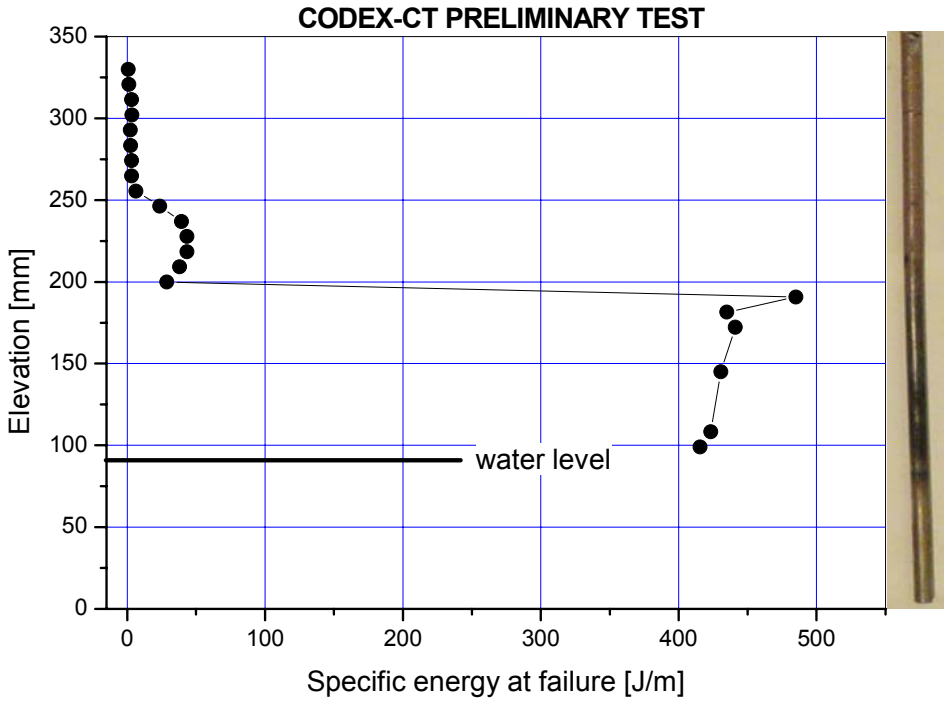

Fig. 73. Specific energy at failure for rod No. 6 of preliminary test

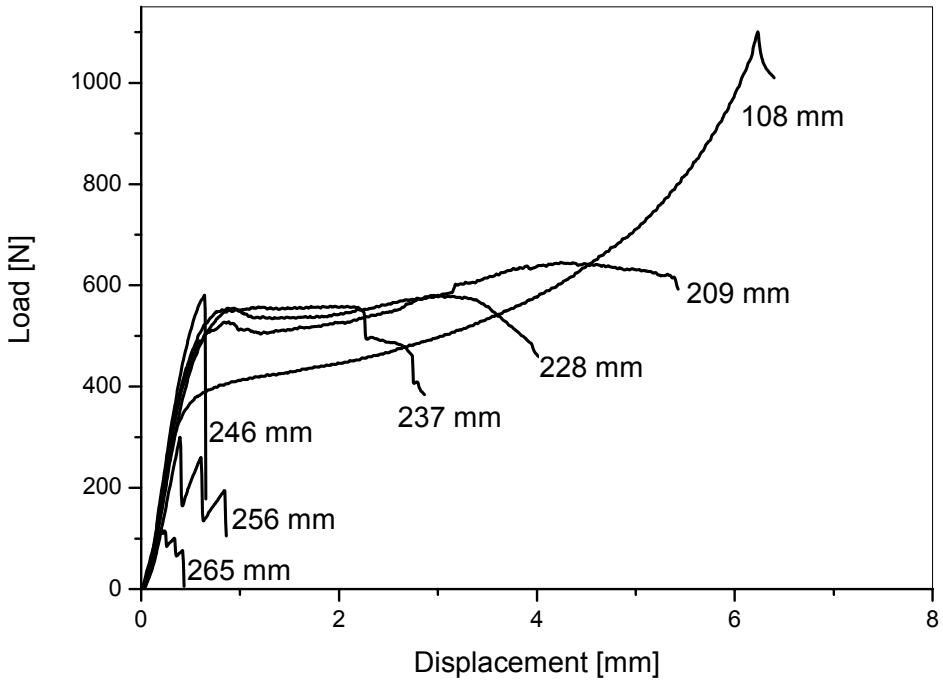

Fig. 74. Load-displacement curves of rings cut from rod No. 6 of preliminary test

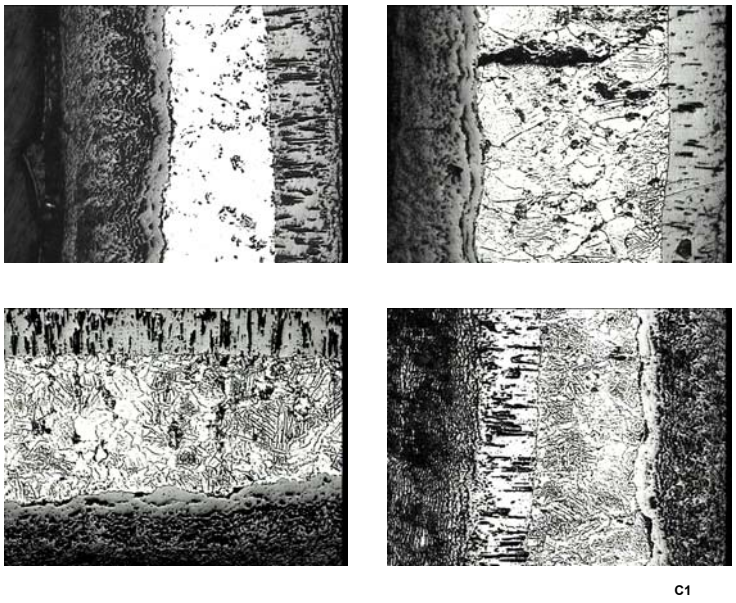

Fig. 75. Cross sections of cladding tubes of the preliminary test (central section)

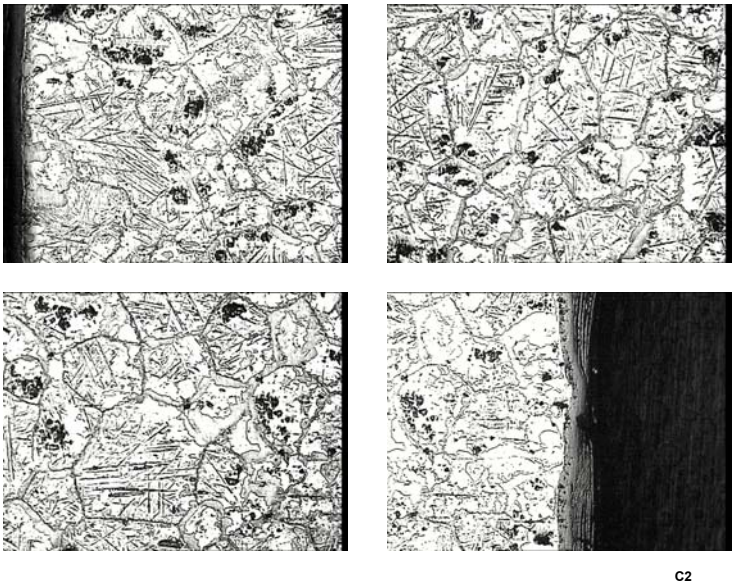

Fig. 76. Cross sections of the shroud of the preliminary test (650 mm elevation)

Fig. 77. Cross sections of cladding tubes of the preliminary test (upper section)

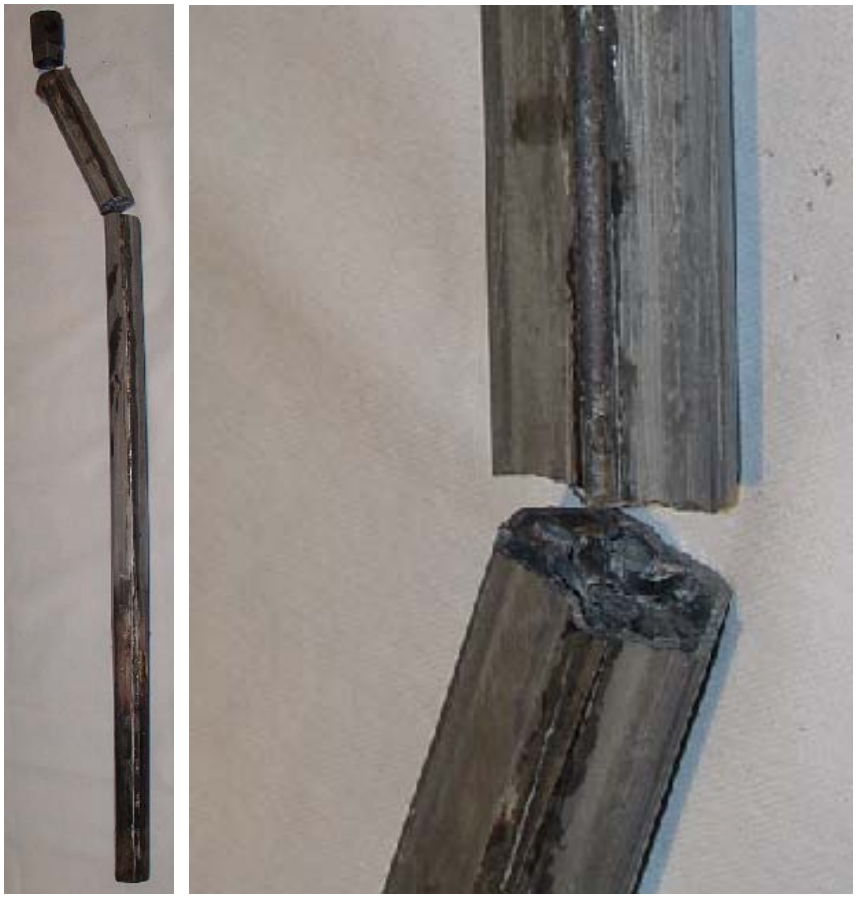

Fig. 78. View of the CODEX-CT-1 bundle after the experiment (left) and close view of the broken cross section (right)

Fig. 79. X-Ray radiographic examination of the CODEX-CT-1 bundle
(the bundle is inside of the horizontal plastic tube in the exposure position)

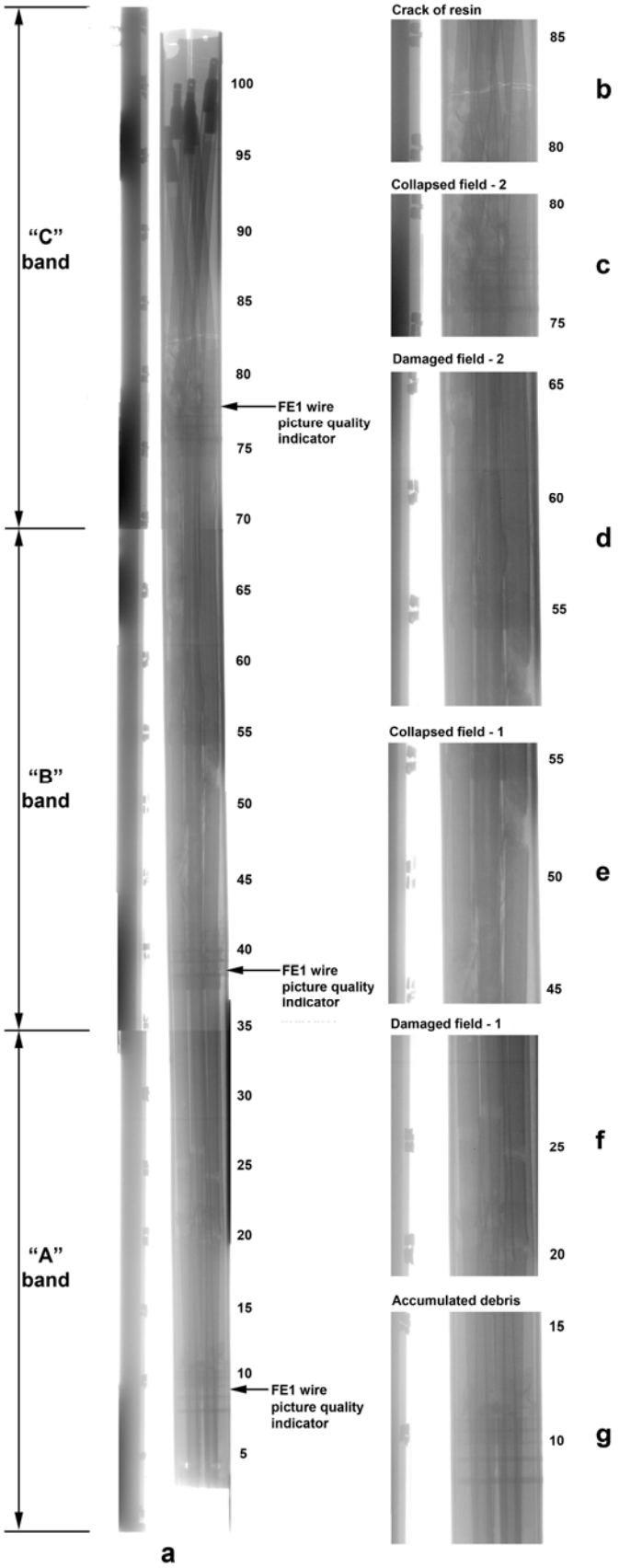

Fig. 80. X-ray radiography of the CODEX-CT-1 bundle

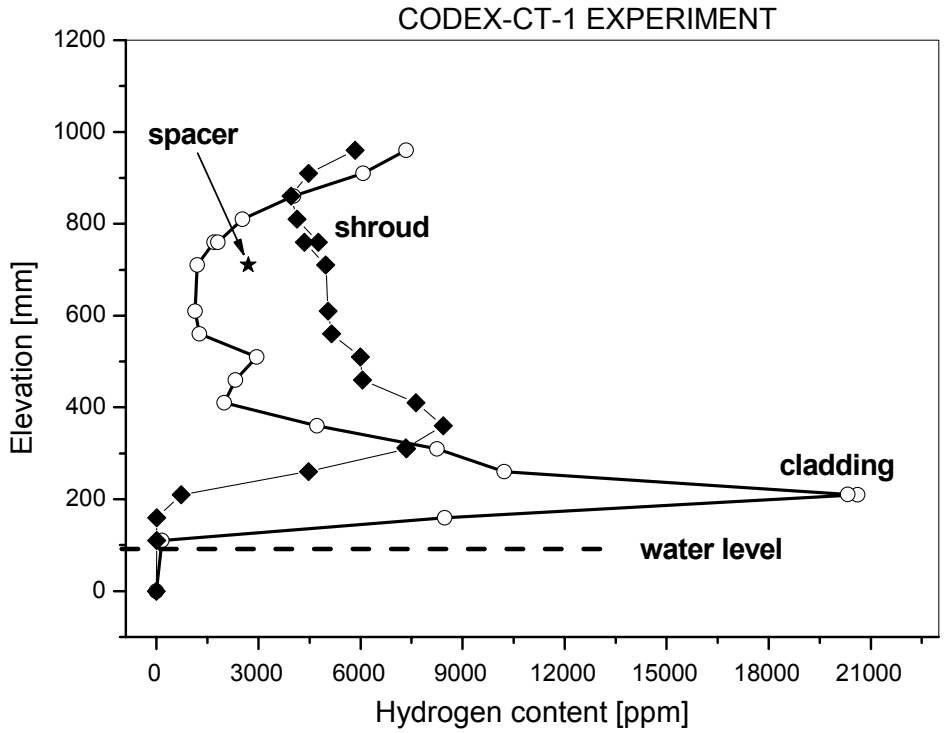

Fig. 81. Hydrogen content in the cladding and shroud of the CODEX-CT-1 experiment

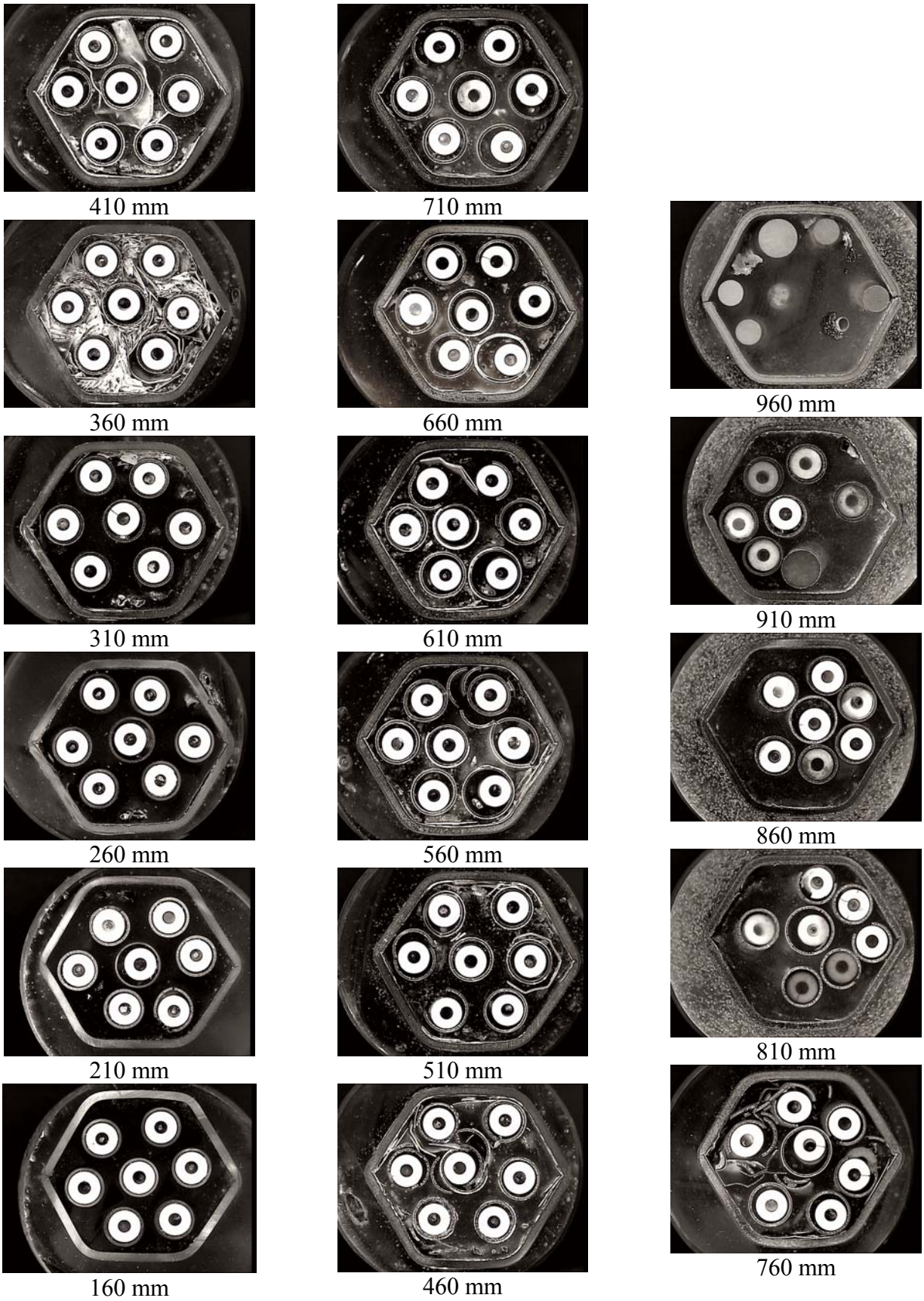

Fig. 82. Cross sections of the CODEX-CT-1 bundle

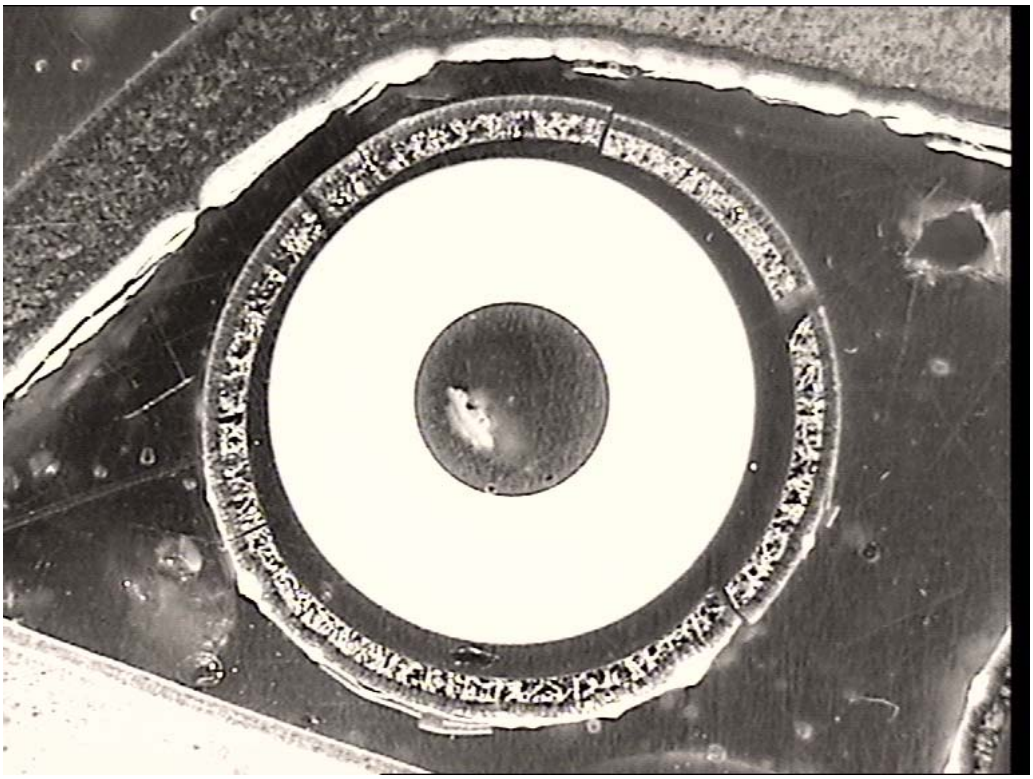

Fig. 83. Rod No. 5 at 460 mm elevation with cracked and fragmented cladding

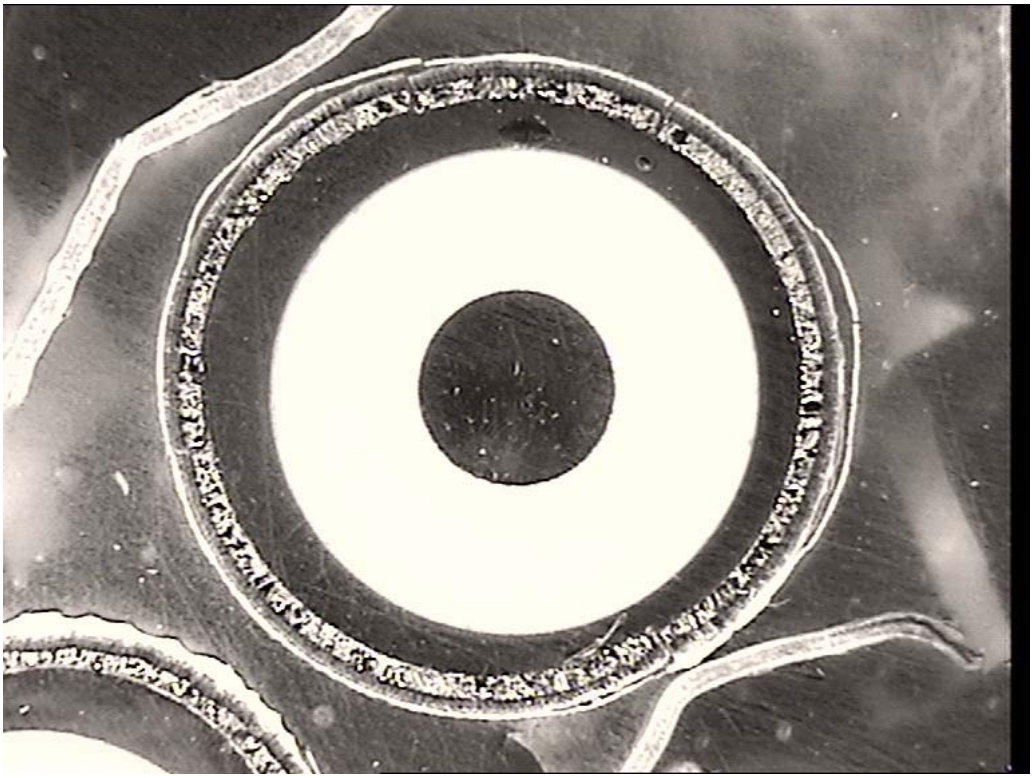

Fig. 84. Rod 7 at 460 mm elevation showing spalling external oxide scale

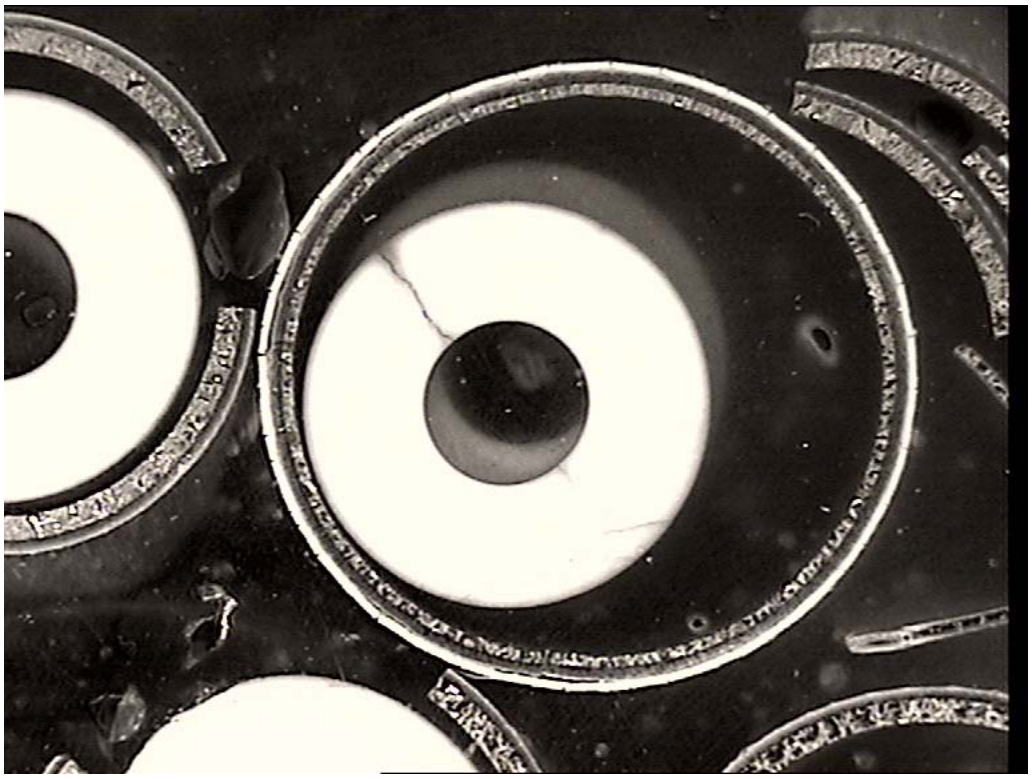

Fig. 85. Rod No. 7 at 760 mm elevation showing very large ballooned cladding

Fig. 86. Rod No. 1 at 710 mm elevation with external (top) and internal (bottom) oxide scales

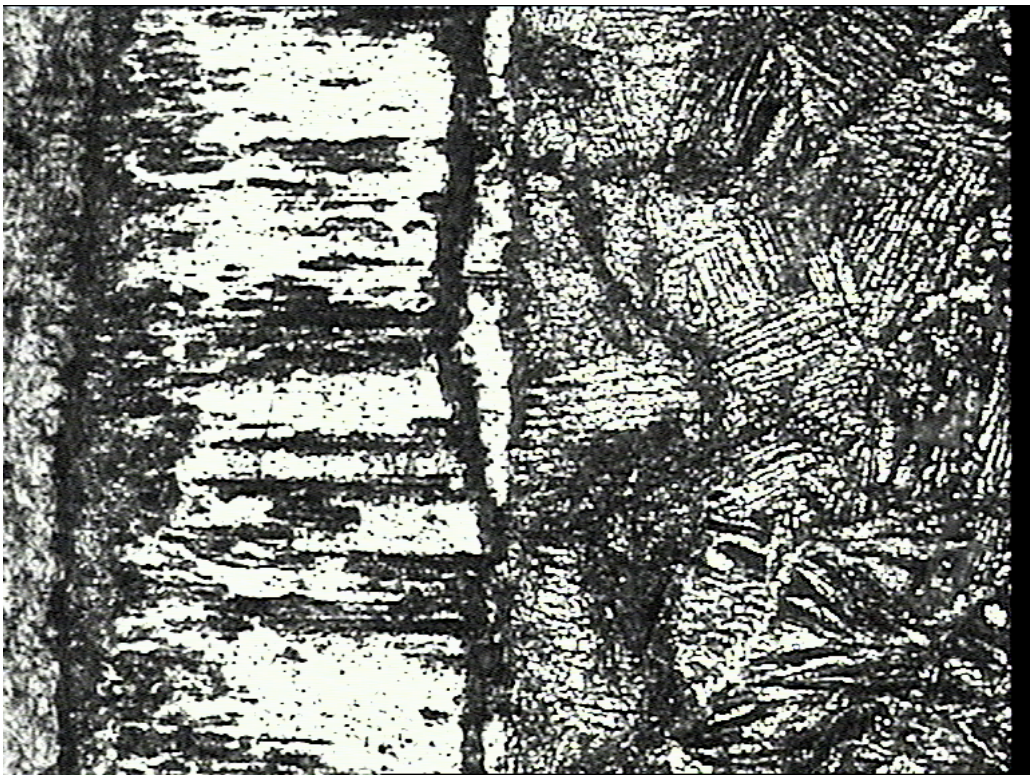

Fig. 87. Oxide scale on the shroud at 810 mm elevation

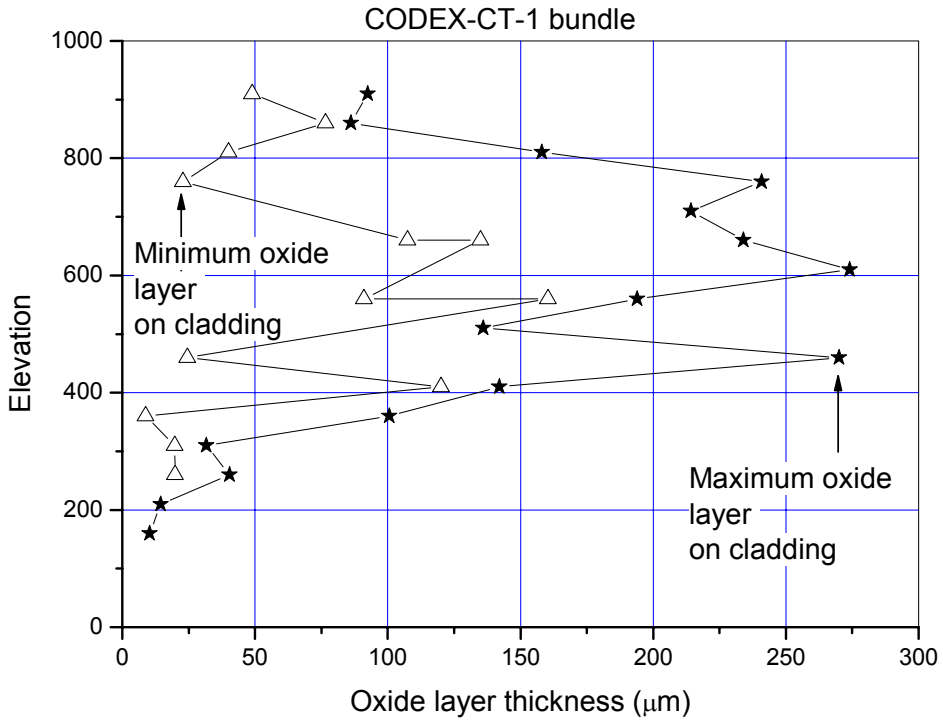

Fig. 88. External oxide layer thickness on cladding tubes

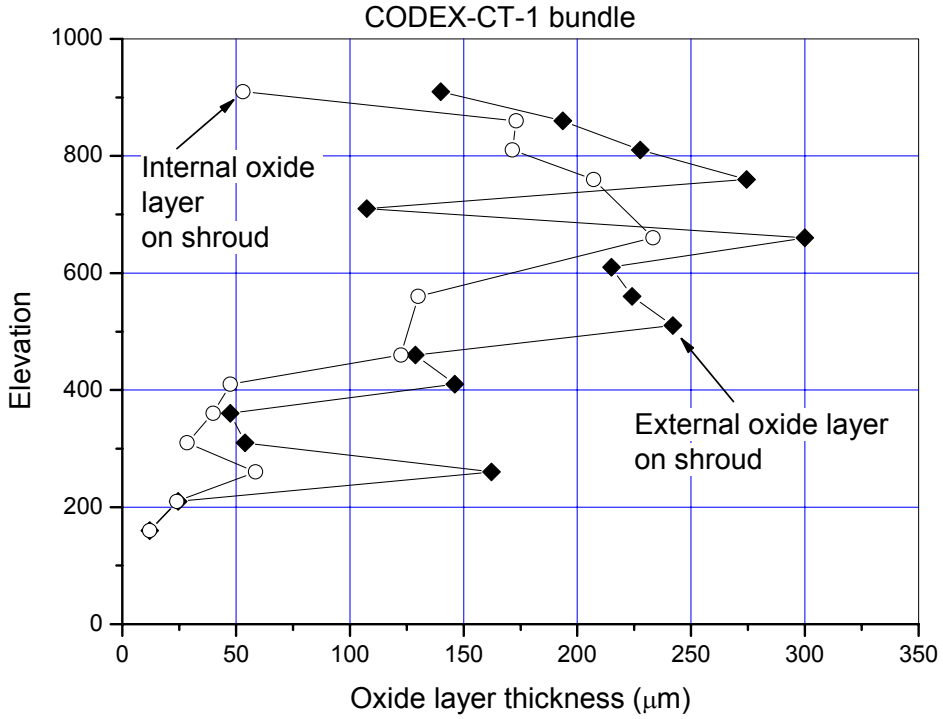

Fig. 89. Oxide layer thickness on shroud

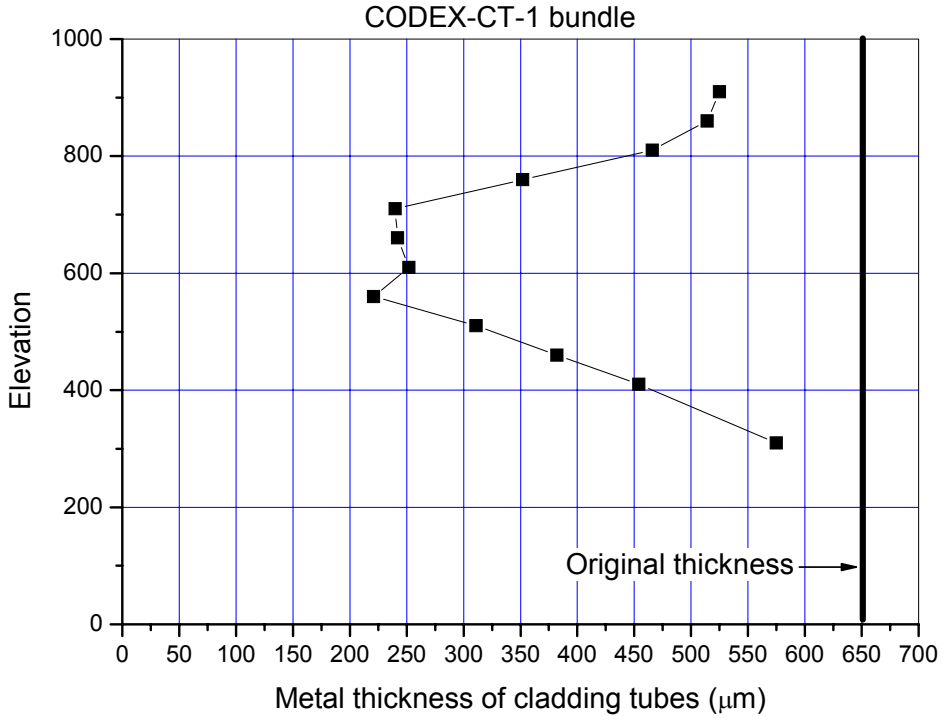

Fig. 90. Remaining metal layer thickness in the cladding tubes

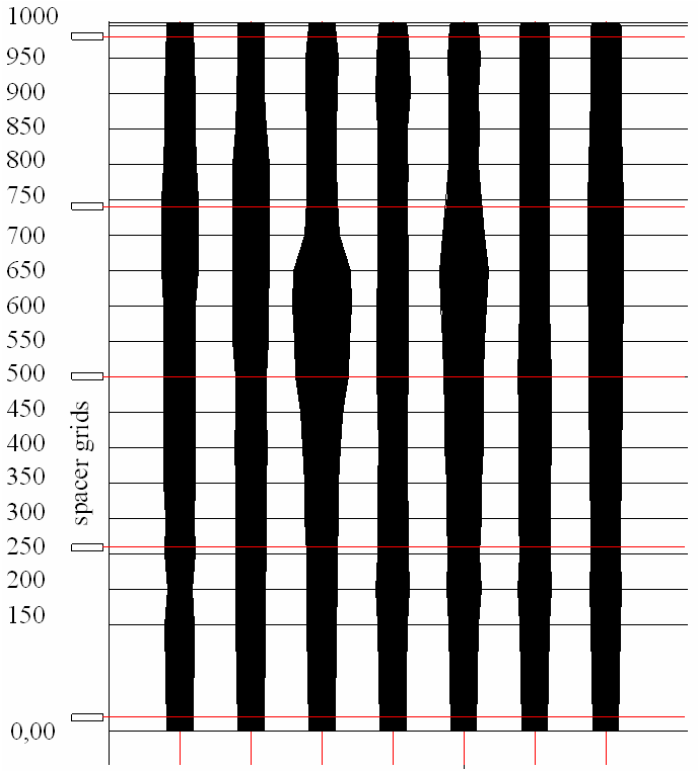

Fig. 91. Ballooning of fuel rods (based on metallographic examination)

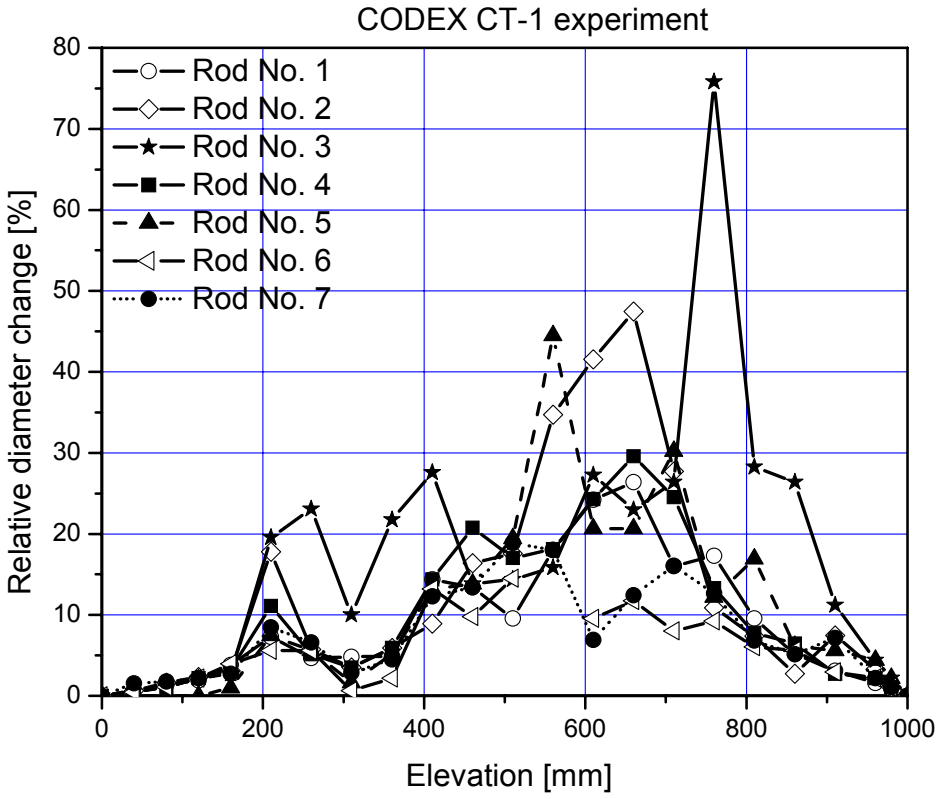

Fig. 92. Relative diameter change profile of fuel rods

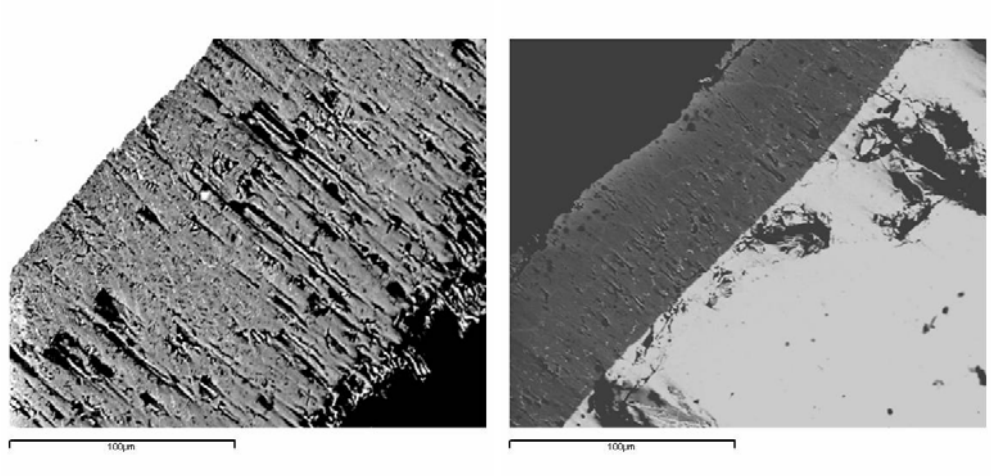

Fig. 93. BEI images from the two oxide layers (thicker and thinner) on the shroud
Note: The sample was rotated

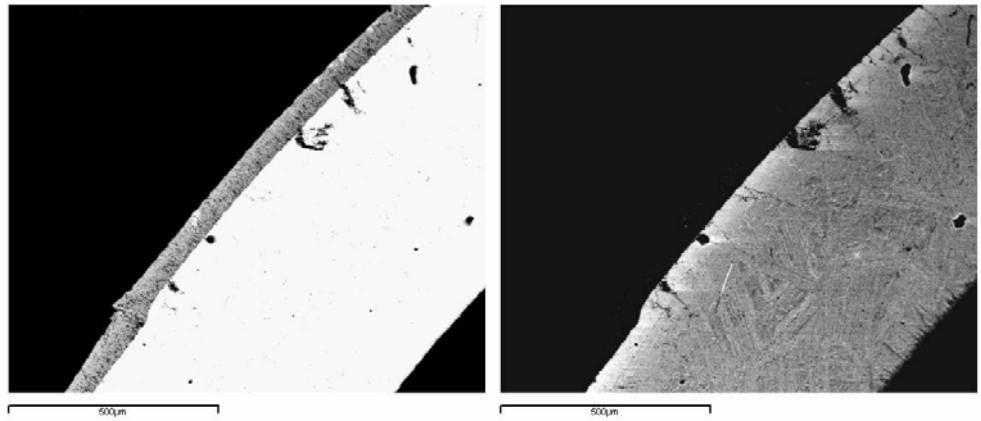

Fig. 94. BEI images of the cladding and the shroud in sample CT-1-910

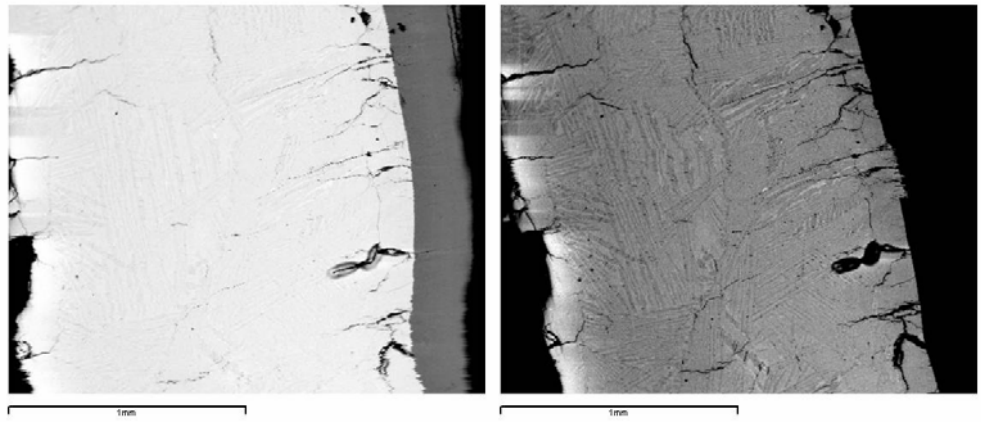

Fig. 95. BEI images taken from sample CT-1-810

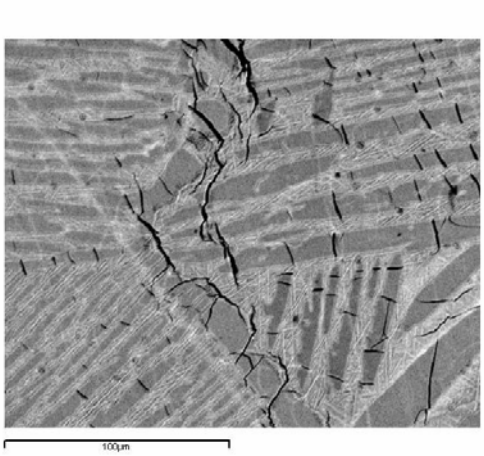

Fig. 96. BEI image taken from sample CT-1-810

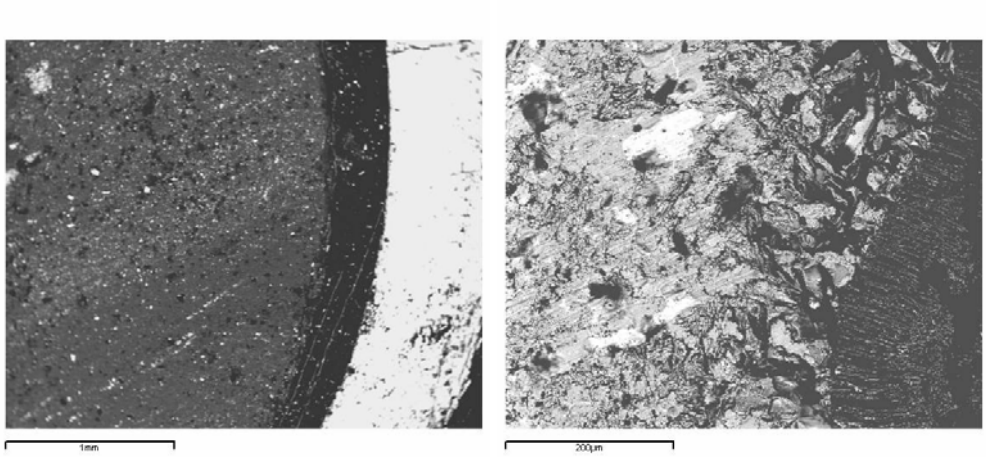

Fig. 97. BEI images of sample CT-1-360

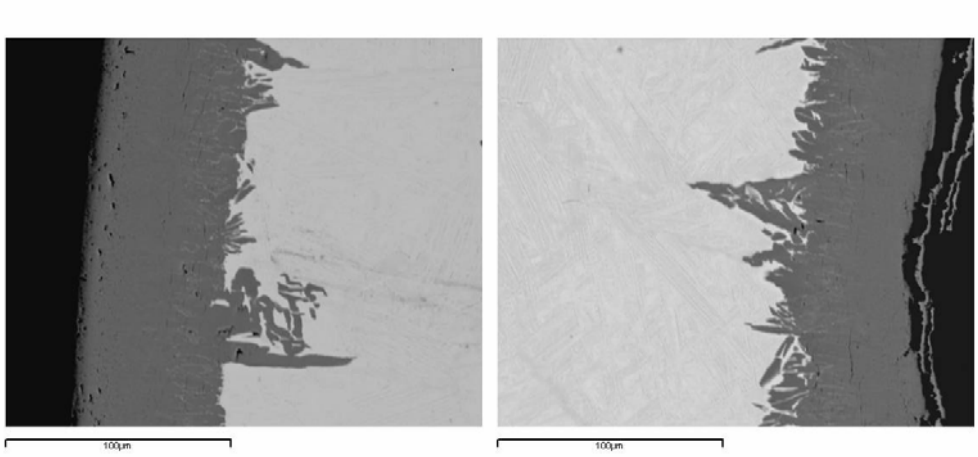

Fig. 98. BEI images from both oxide layers formed on the shroud taken from 360 mm elevation

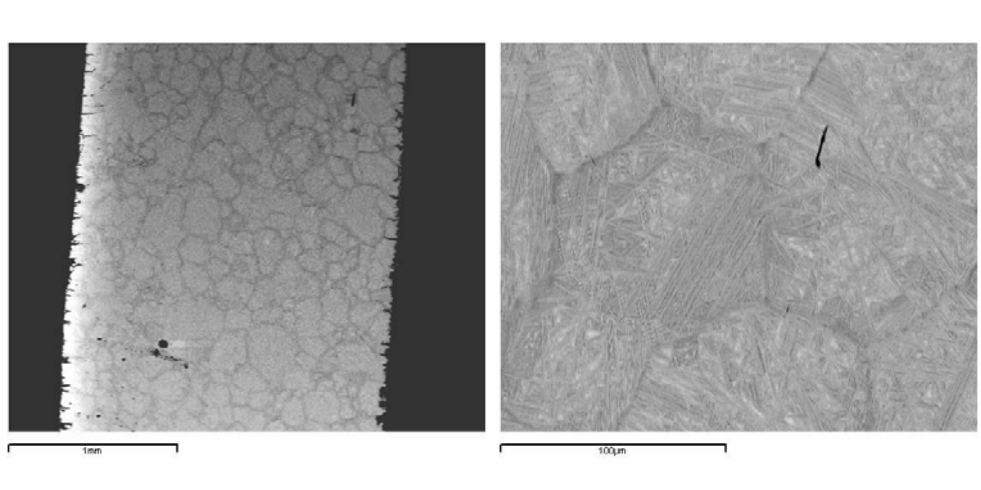

Fig. 99. BEI images taken from sample CT-1-360s

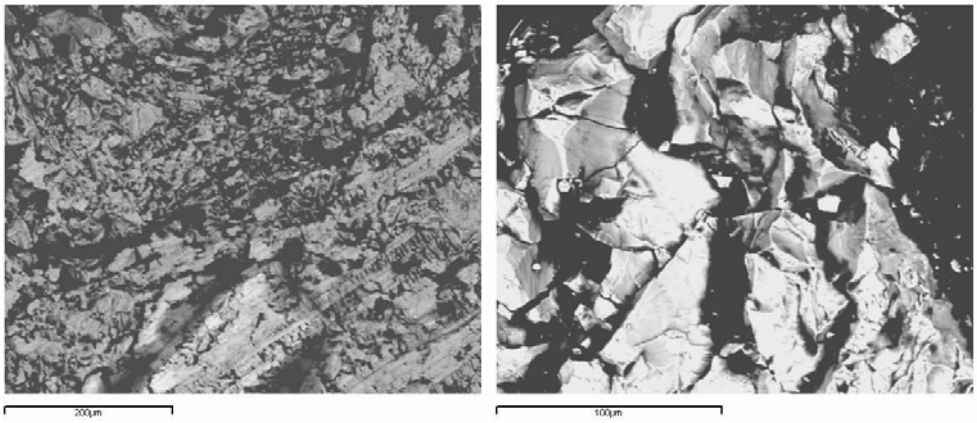

Fig. 100. BEI images of the cladding material in sample CT-1-210

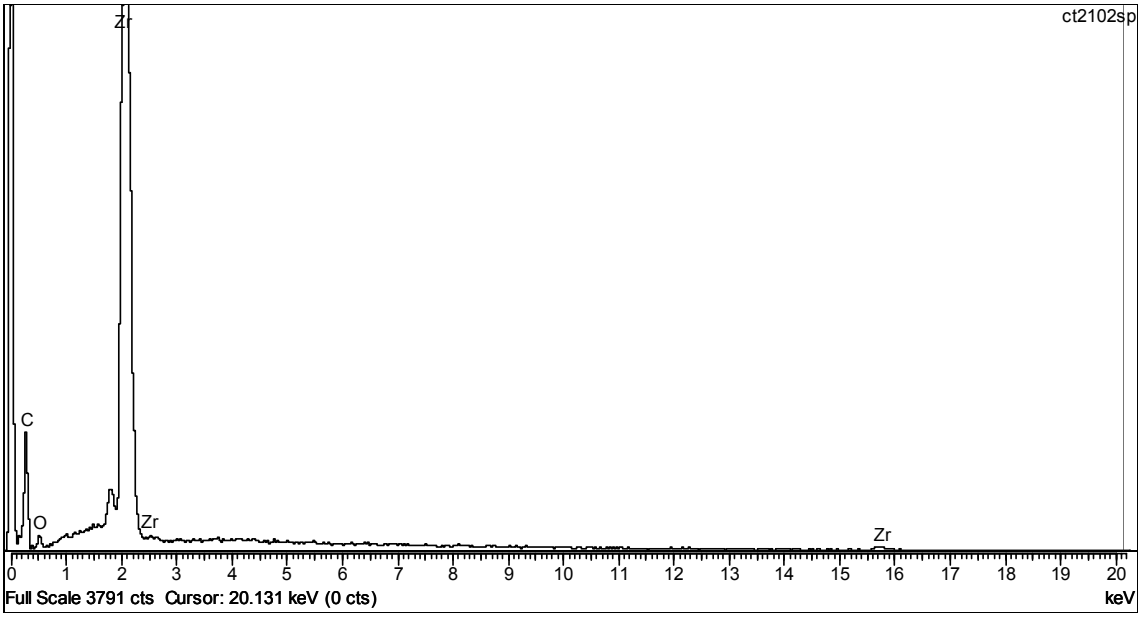

Fig. 101. EDX spectrum taken from sample CT-1-210

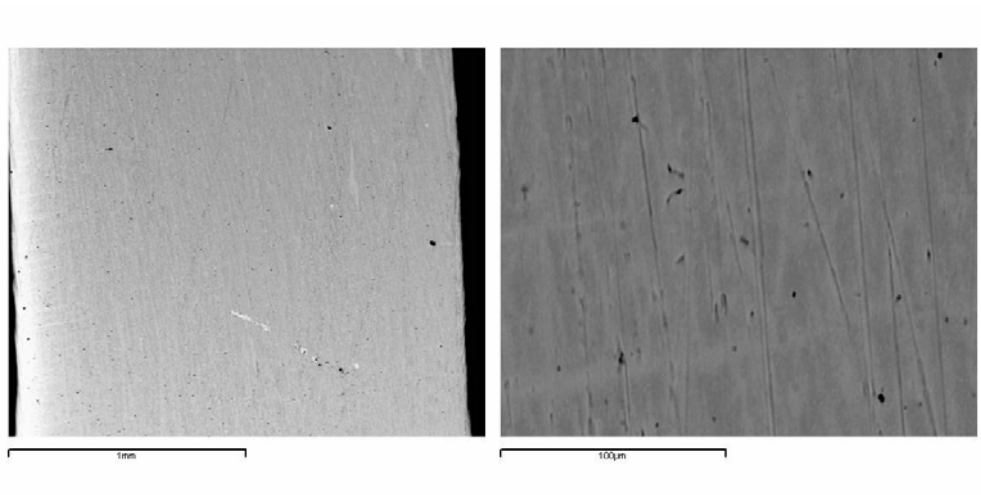

Fig. 102. BEI images of the shroud taken from 110 mm elevation